

## ABSTRACT

YOUNGBLOOD, WILLIAM JUSTIN.

SYNTHESIS OF PHTHALOCYANINES FOR USE IN ELECTRONIC MATERIALS.

(Under the Direction of Dr. Jonathan S. Lindsey.)

This dissertation describes the synthesis of phthalocyanines having specialized structures that provide for electrochemical studies of their fundamental properties and/or for direct preparation of phthalocyanine-based electronic materials. Much of the synthetic effort herein is directed toward the development of a particular class of phthalocyanine, herein referred to as benzimidazoporphyrazines. Benzimidazoporphyrazines are desirable substitutes for typical phthalocyanines in applications requiring phthalocyanine-based materials. The value of benzimidazoporphyrazines is derived from their geometry, which provides four substitution positions at peripheral carbon atoms that lie along the N-N axes of the macrocycles. The modular construction of pigment arrays that include phthalocyanines may be greatly facilitated with the use of benzimidazoporphyrazines. The history of research in benzimidazoporphyrazines is brief, and has not heretofore provided access to benzimidazoporphyrazines bearing substituents that may serve as synthetic handles for modification of the pigments after their formation. This report details the development of synthetic methodology to prepare benzimidazoporphyrazines that bear useful synthetic handles. The synthesis of a set of such pigments is also described. Additionally, the new pigments (and one pigment array) are studied with regard to structural confirmation, as well as by photochemical and electrochemical means.

**SYNTHESIS OF PHTHALOCYANINES FOR USE IN ELECTRONIC MATERIALS**

by

**WILLIAM JUSTIN YOUNGBLOOD**

A dissertation submitted to the Graduate Faculty of

North Carolina State University

In partial fulfillment of the requirements

For the Degree of Doctor of Philosophy

**DEPARTMENT OF CHEMISTRY**

Raleigh, North Carolina

2005

**APPROVED BY:**



Jonathan S. Lindsey  
Chair of Advisor Committee



Daniel L. Feldheim



Daniel L. Comins



Edmond F. Bowden

## BIOGRAPHY

Justin Youngblood was born on an Air Force base in west Texas in October of 1972. His childhood was spent primarily in eastern North Carolina, and the suburbs of Atlanta, Georgia. After graduating from Milton High School in Alpharetta, Georgia, he attended Washington and Lee University in Lexington, Virginia, where he studied chemistry and literature. After receiving a Bachelor of Science in 1994, he served in the United States Peace Corps as a volunteer stationed in the Kingdom of Swaziland. After 12 weeks of in-country training, he served for one year as a high school science teacher at a remote secondary school, and afterward for another year as an advisor in urban environmental management in the town of Nhlangano (population ~8000 in 1996). In 1996 he attended the IUPAC meeting of Chemistry and the Environment, held at the University of Witswatersrand in Johannesburg, South Africa, where he was inspired to pursue a career as a chemist working toward discoveries that would improve the world's environment. After returning to the U.S. in early 1997, he moved to San Francisco, California, where he found work in the biotechnology industry, primarily as an enzymologist at Axys Pharmaceuticals, and conducted career research to choose a foundation for a scientific career. In 1999, he moved to Raleigh, North Carolina, to obtain a Ph.D. in Chemistry from North Carolina State University.

## **ACKNOWLEDGEMENTS**

I would like to thank Dr. Jonathan S. Lindsey for the opportunity to work in his research group, for financial support, helpful discussion, and for the guidance he provided towards the conduct of good research. I would like to thank the group members of the Lindsey Research group for helpful and enjoyable discussions on matters both scientific and mundane. In particular I thank Dr. James Dixon and Dr. Han-Je Kim, for being good colleagues and better friends. I thank Dr. Patchanita Thamyongkit and Dr. Kisari Padmaja for providing samples of a compound used in my research. I thank Dr. David Bocian and members of his research group, especially Lingyun Wei, for performing analyses of compounds described in this report on my behalf with and without my participation. I am grateful for the moral support I received from my family. Lastly, this work was financially supported for three years by a GAANN-ELMAT Fellowship (General Assistance in Areas of National Need) from the U.S. Department of Education, and by a grant to Prof. Jonathan S. Lindsey from the Division of Chemical Sciences, Office of Basic Energy Sciences, Office of Energy Research, U.S. Department of Energy.

## TABLE OF CONTENTS

	Page
List of Charts	vii
List of Equations	viii
List of Figures	ix
List of Schemes	xi
List of Tables	xiii
Chapter 1: Introduction	
A. Discovery, basic properties, and uses of phthalocyanines	1
B. Organic photovoltaics using phthalocyanines and other dyes	2
C. Principles of operation of an ultrathin porphyrinic solar cell	7
D. Electrochemistry of phthalocyanines	11
E. Structural aspects of phthalocyanines	12
F. Challenges in the synthesis of phthalocyanines	16
G. Research goals: Synthesis and characterization of novel phthalocyanines	19
H. References	22
Chapter 2: A magnesium phthalocyanine bearing a tripodal linker	28
A. Research objectives	28
B. Synthesis	29

C. Electrochemical studies	33
D. Conclusion	36
E. Experimental Section	37
F. References	41
Chapter 3: Benzimidazoporphyrazines: first synthetic route (failed)	42
A. Published research on benzimidazoporphyrazines	42
B. Synthesis of 2-aryl-5,6-disubstituted-benzimidazoles	44
C. Alkylation of benzimidazoles	48
D. Palladium coupling and Rosenmund-von Braun cyanation reactions	50
E. Synthesis of benzimidazoporphyrazines: model reactions	56
F. Alternative cyanation strategies	58
G. Pursuit of secondary swallowtail alkyl-groups	61
H. Imidazoporphyrazines	63
I. Conclusions	65
J. Experimental Section	67
K. References	81
Chapter 4: Benzimidazoporphyrazines: second synthetic route (successful)	94
A. Synthesis	94
B. Photochemistry	100

C. Conclusion	108
D. Experimental Section	109
E. References	131
Chapter 5: A phthalocyanine and triple decker lanthanide sandwich complex, each	
bearing a tripodal linker	134
A. Background	134
B. Synthesis: strategy and results	140
C. Characterization of surface monolayers	145
D. Outlook	153
E. Experimental Section	155
F. References	163

## LIST OF CHARTS

	Page
Chart 1.1 A family of four tetrapyrrolic macrocycles	1
Chart 5.1 Structure of three known types of heteroleptic triple decker lanthanide sandwich complexes.	135

## **LIST OF EQUATIONS**

	Page
Equation 1.1	9
Equation 1.2	10
Equation 1.3	10
Equation 2.1	35
Equation 2.2	36
Equation 2.3	36

## LIST OF FIGURES

	Page
Figure 1.1. The Schottky diode and the hetero-Schottky diode, two basic examples of organic solar cells.	4
Figure 1.2. A surface-bound molecular wire of pigments.	8
Figure 1.3. Rectification of energy and holes in a molecular wire.	9
Figure 1.4. Two trans-substituted phthalocyanines.	15
Figure 1.5. Regioisomers resulting from the cyclization of a substituted precursor	17
Figure 1.6. A mixed macrocyclization forming lowered-symmetry phthalocyanines.	18
Figure 1.7. Generic Structure of Benzimidazoporphyrazines.	20
Figure 2.1. A Mg-phthalocyanine bearing a tripodal linker.	28
Figure 2.2. Square wave voltammogram of compound <b>10</b> in solution.	33
Figure 2.3. Cyclic voltammogram of compound <b>10</b> bound to a gold electrode.	35
Figure 3.1.	41
Figure 4.1. Absorption and emission spectra for tetrasubstituted benzimidazoporphyrazines.	
	101
Figure 4.2. (A) Absorption spectra for <b>Fb-11</b> . (B) Absorption spectra for <b>Fb-13</b> .	
(C) Emission spectra for <b>Fb-11</b> (excitation at 435, 600, and 630 nm).	
(D) Emission spectra for <b>Fb-13</b> (excitation at 435, 600, and 630 nm).	104
Figure 4.3. Absorption and emission spectra for low symmetry zinc-Benzimidazoporphyrazines.	107
Figure 5.1. A type-c triple decker bearing a tether for surface attachment.	136

Figure 5.2. Camshaft rotation of a type-c triple decker tethered to a surface

(via a surface attachment group, denoted by “S”).

137

Figure 5.3. Architectures containing a type-c triple decker bearing a tripodal thiol

tether.

138

Figure 5.4. A phthalocyanine attached to a tripodal thiol tether. Note the cant angle

of the tripodal axis with respect to the N-N axis of the phthalocyanine.

138

Figure 5.5. Generic structure of A<sub>4</sub> benzimidazoporphyrazines.

139

Figure 5.6. Schematic of Si electrode fabrication.

147

Figure 5.7. IR spectrum of **H**<sub>2</sub>-**7** (KBr pellet).

148

Figure 5.8. IR spectra of compound **9** in KBr (upper) and in a monolayer (lower).

149

Figure 5.9. Apparatus used in electrochemical measurements of electrodes coated

with **H**<sub>2</sub>-**7** or **9**.

150

Figure 5.10. Cyclic voltammogram of compound **9**.

151

Figure 5.11. A longevity study of compound **9** composed of many voltage cycles.

152

Figure 5.12. Representation of the type-a triple decker bearing the compact all-carbon

tether. The tripod is attached to the (central) phthalocyanine ligand and

aligned along one of the N-N axes of the phthalocyanine.

154

## **LIST OF SCHEMES**

	Page
Scheme 2.1.	29
Scheme 2.2.	30
Scheme 2.3.	31
Scheme 2.4.	32
Scheme 3.1.	42
Scheme 3.2.	43
Scheme 3.3.	44
Scheme 3.4.	45
Scheme 3.5.	45
Scheme 3.6.	47
Scheme 3.7.	48
Scheme 3.8.	49
Scheme 3.9	51
Scheme 3.10.	53
Scheme 3.11.	55
Scheme 3.12.	56
Scheme 3.13.	57
Scheme 3.14	58
Scheme 3.15	60
Scheme 3.16	61
Scheme 3.17.	62

Scheme 3.18.	65
Scheme 4.1	85
Scheme 4.2	86
Scheme 4.3	89
Scheme 4.4	91
Scheme 4.5	92
Scheme 4.6	94
Scheme 4.7	96
Scheme 4.8	99
Scheme 5.1	142
Scheme 5.2	143
Scheme 5.3	144

## LIST OF TABLES

	Page
Table 4.1 Photochemical data for benzimidazoporphyrazines	102

# Chapter 1

## A. Discovery, basic properties, and uses of phthalocyanines.

Phthalocyanine dyes were first encountered as byproducts of industrial chemical reactions in the early twentieth century.<sup>1</sup> The first series of academic reports on phthalocyanines were published by Linstead and coworkers in 1934.<sup>2</sup> These dyes, usually blue or green in color, have been widely exploited as colorants.<sup>3</sup> Their electro-optic behavior has led to their use in xerography (photocopying and laser printing).<sup>4</sup> Phthalocyanines have also been investigated for potential use in a variety of other applications, including nonlinear optical generation and limiting,<sup>5,6</sup> photodynamic therapy,<sup>7</sup> photovoltaics,<sup>8,9</sup> sensors,<sup>10</sup> electrochromic displays,<sup>11</sup> and information storage.<sup>12</sup> Phthalocyanines are a member of the class of compounds known as tetrapyrrolic macrocycles. Other members of this class (Chart 1.1) include porphyrins and tetraazaporphyrins (i.e. porphyrazines). A synonym for phthalocyanine is tetrabenzotetraazaporphyrin. Phthalocyanines have a strong optical absorbance in the red and near-IR portions of the electromagnetic spectrum, and are stable under a wide range of thermal and electrochemical conditions.

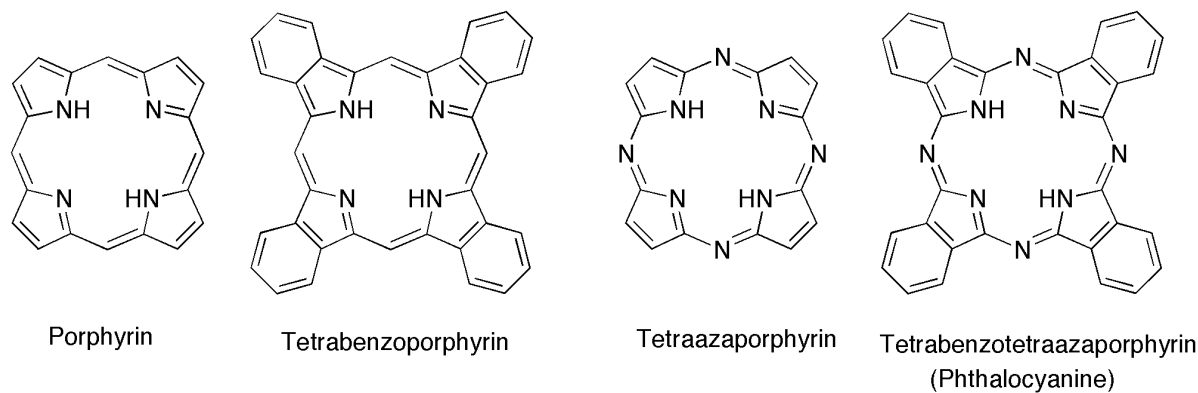


Chart 1.1. A family of four tetrapyrrolic macrocycles.

Besides the optical properties and stability of phthalocyanines, these dyes must be evaluated with regard to their electrochemical suitability and structural suitability for a given application, such as an electronic material. Two electronic applications that are considered in this dissertation are the development of an ultrathin solar cell and the use of tetrapyrroles as charge storage media. In the latter application, the storage of charge is a mechanism for the storage of information, and the information storage application is relevant to the development of new components in computer memory devices.

## **B. Organic photovoltaics using phthalocyanines and other dyes.**

The development of an ultrathin solar cell based on porphyrinic pigments (a classification that includes porphyrins and related pigments, such as phthalocyanines) is an idea that has been patented and published.<sup>13</sup> A brief discussion of the design concept is helpful to understanding the distinguishing features of an ultrathin solar cell and the potential role of phthalocyanines in this proposed electronic device. It is necessary to first consider some more basic organic solar cell designs. An initial distinction must be made between solid-state solar cells and liquid junction solar cells. The solid-state solar cell is a device composed of layers of solid organic material (composed of dye(s), and sometimes hole and/or electron conducting compounds/materials) sandwiched between two electrodes (an anode and a cathode). In the solid-state solar cell, separation of electron/hole pairs must occur at the interface between organic layers, or at the interface of an organic layer and an electrode. The transport of holes and electrons is usually not performed with equivalent efficiency, and recombination between holes and electrons are the major source of power loss in these devices. The liquid junction solar cell has the organic layer(s) deposited at one

electrode (usually the photoanode), with a liquid junction (electrolyte) that contains a redox pair in solution placed between the organic layer and the counterelectrode. The most popular type of liquid junction solar cell in current research is the Grätzel cell, which takes advantage of a colloidal titania photoanode that provides an extremely high surface area for adsorbed dye molecules.<sup>14</sup> The most commonly employed redox pair for the Grätzel cell is iodine/triiodide. Liquid junction solar cells have advantages and disadvantages relevant to solid-state solar cells. Advantages of the liquid junction solar cell include the high surface area of the photoanode, high efficiency of electron injection into the photoanode by excited dyes, and relatively low cost and simplicity of fabrication compared to solid-state solar cells. In particular, the titania photoanode is coated by dip coating, which is far preferable to the chemical vapor deposition and other high vacuum-related techniques used for depositing crystalline layers of organic dyes used in solid-state solar cells. Disadvantages of liquid junctions cells include the corrosive nature of iodine/triiodide (great difficulty has been encountered in trying to replace it with other redox pairs), the photocurrent limitation that is incurred by relying on the diffusion of the redox pair as a transport mechanism, and the risk of leakage of a device containing an electrolyte (usually acetonitrile with dissolved lithium iodide or other salt). Although Grätzel cells are currently outperforming solid-state solar cells in published accounts of academic research (~7-10% efficiency), the potential efficiencies of the solid-state design are greater than those of the liquid junction design, and following this assertion, the remainder of this discussion will be confined to solid-state devices.

The first promising result in the field of solid-state organic photovoltaics came in 1978 from Morel and coworkers at Exxon labs, who reported a 0.7% solar efficiency for

Schottky junction devices (Figure 1.1) using merocyanine dyes as the photoabsorptive material.<sup>15</sup> Previous to their discovery, the best solar efficiency result in this field had been 0.02%.<sup>16</sup> In the case of Morel and coworkers, the merocyanine dyes were vacuum deposited or solution cast onto an aluminium electrode (high work-function photocathode) with a layer of Ag (lower work-function photoanode) vacuum-deposited on top of the prepared organic layer.

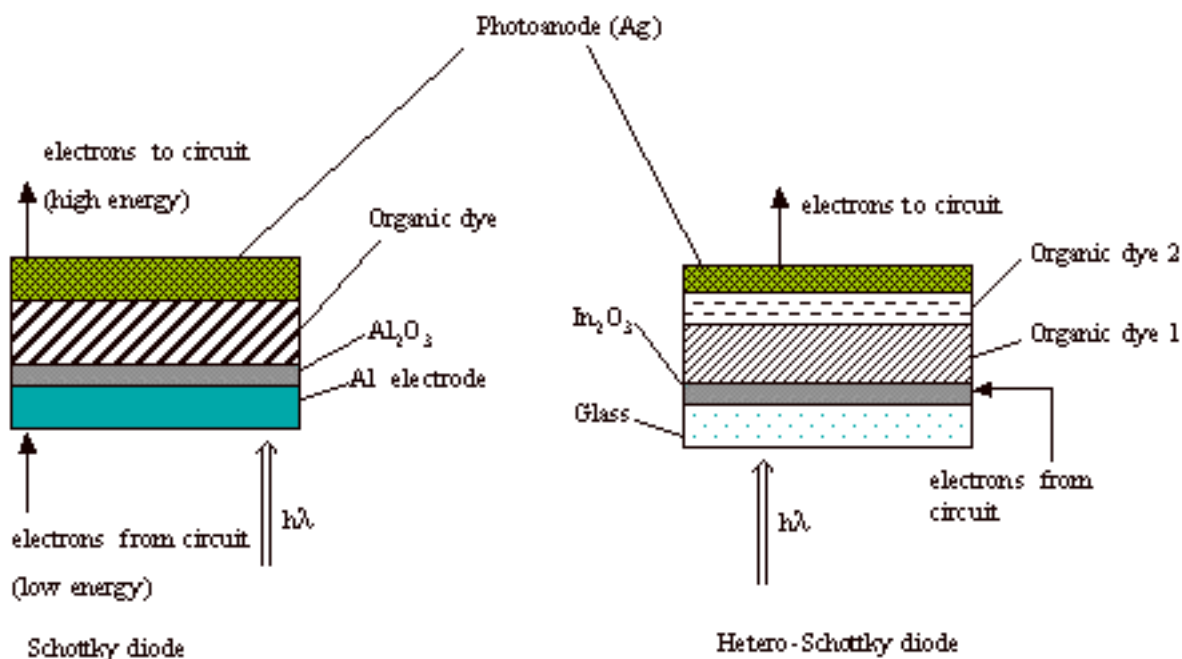


Figure 1.1. The Schottky diode and hetero-Schottky diode, two basic examples of organic solar cells.

In the years since that discovery, there have been many variations of solar cell architecture and fabrication techniques. In addition to high vacuum deposition and spin coating of organic thin films, Schottky junctions have been prepared using electrodeposition of pigment molecules (such as phthalocyanines) onto an electrode,<sup>17</sup> as well as by Langmuir

Blodgett film formation,<sup>18</sup> and in situ self-assembly of liquid-crystalline films.<sup>19</sup> A variety of electrode materials, such as aluminium and indium for the cathode, and silver and gold for the photoanode, have been tested. Polymeric light-absorbing materials have been employed,<sup>20</sup> and pigments have been blended with other substances, such as conducting polymers and buckminsterfullerene, to improve charge transport in the organic layer.<sup>21</sup> Organic Schottky heterojunctions, also called p-n junctions (Figure 1.1), beginning with C. W. Tang's two-layer cell in 1985,<sup>22</sup> have been widely explored in the attempt to broaden spectral coverage and improve charge mobility through organic photovoltaic devices. The Schottky heterojunctions, often employing a phthalocyanine layer and a perylene layer, have been reported with efficiencies of ~2%.<sup>22,23</sup>

The Schottky devices having a single organic layer operate by the generation of excited-states in the individual pigment molecules, followed by migration of the excited-state energy (often referred to as excitons or bound hole/electron pairs) through the material until the excited-state energy reaches the pigments at the interface with the photoanode, whereupon an electron is injected into the photoanode, leaving the hole behind in the organic material. The hole must then be transferred through the organic material by a series of electron transfer events between pairs of pigments, until the hole reaches the cathode where it combines with an electron produced by the cathode, resulting in a neutral pigment molecule (ground-state). The migration of the original excited-state is an undirected process that may result in short or long paths of migration for each excited pigment. Each excited-state has some probability to relax to the ground-state, by fluorescence, by internal conversion, or by intersystem crossing (followed by internal conversion or phosphorescence). The competition between energy transfer and relaxation mechanisms results in a finite number of transfers

that are likely to take place before the energy of a given excited-state is lost. This phenomenon of excited-state energy ( $\Delta E$ , i.e. the difference in energy between ground-state and excited-state) loss is often understood as the diffusion length of an exciton, which is the average distance that an exciton will travel through the organic layer.

The Schottky heterostructure devices, having multiple organic layers, are intended to allow the conversion of the excitons from bound hole/electron pairs to free holes and electrons at the interface of two layers of different pigments. Many of the dissociated hole/electron pairs simply recombine at the interface, but some result in charge migration to the electrodes. Depending on the combination of pigments used, it is also possible that excited-states may migrate from one layer into the other while remaining as bound hole/electron pairs. Due to the different excited-state energies ( $\Delta E$ ) inherent to different pigments, this migration would be expected to occur in a one-way manner from greater  $\Delta E$  to lesser  $\Delta E$ .

Despite the variety of architectures and dye-substances employed in solid-state organic photovoltaic devices, solar efficiencies higher than 1-2% have rarely been reported. The most significant source of inefficiency in existing solid-state photovoltaics, both inorganic and organic, is the combination of light absorption and charge generation within the same zone of a photovoltaic device.<sup>24</sup> The desire to maximize light absorption results in a photoactive layer so thick that charge transport through the material is inefficient due to exciton-pair recombination events (i.e. excited-state relaxation pathways, as discussed above). A few Schottky junction and p-n junction devices with interdigitated layers of dye and electrode have been explored in the hope that by increasing the surface area of ohmic

contact, holes and electrons might be more effectively separated.<sup>25</sup> These attempts did not result in improved solar efficiencies (i.e. >2%).

### C. Principles of operation of an ultrathin porphyrinic solar cell.

The motivation for an ultrathin solar cell is the minimization or elimination of recombination and relaxation events as factors limiting the efficiency of an organic solar cell.<sup>13</sup> By using porphyrinic pigments with very high extinction coefficients, a large portion of the solar flux could be absorbed with a relatively thin organic layer (200-500 nm). In addition to the enhanced electrical performance sought from this design, the thinness of the device is anticipated to allow the use of flexible substrates and/or irregularly-surfaced (i.e. non-flat) solar panels and solar absorptive media. The design for an ultrathin solar cell based on porphyrinic pigments is predicated on the requirement that the light-harvesting and charge generation functions of the organic material must be segregated.<sup>13</sup> This paradigm is an emulation of natural photosynthetic architectures, wherein an absorbed photon may migrate through hundreds of pigment molecules before reaching a reaction center where charge generation occurs. This feature would be achieved in the synthetic solar cell by tailoring the organic material within the device. Principally, the organic material would not consist of monomeric pigments, but rather would be made up of pigment oligomers, that would reach from the photoanode to the cathode (or into an electrolyte having contact with the cathode, as in a liquid junction solar cell). The pigments would be organized into a covalently bonded linear light-harvesting array, also called a “molecular wire”, which would be connected at the terminus to a “charge-separating unit” (CSU) which would itself be bound to the surface of the photoanode (Figure 1.2).

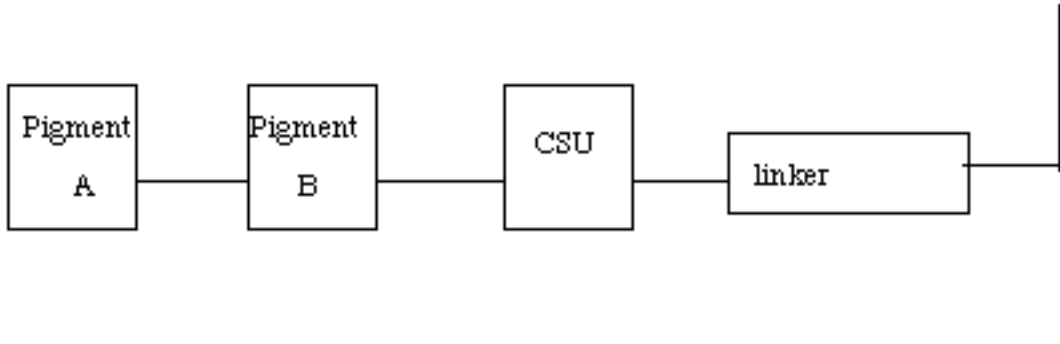


Figure 1.2. A surface-bound molecular wire of pigments.

For simplicity, the example in Figure 1.2 shows two different pigments and the CSU, but the design intends for a large number of pigments in the linear array. The CSU may itself be a porphyrinic pigment. The material is able to direct the flow of photonic energy to the photoanode by virtue of the differences in the excited-state energies ( $\Delta E$ ) (Figure 1.3). Photonic energy would migrate from pigments with greater  $\Delta E$  toward pigments with lesser  $\Delta E$  one-way manner. This design is termed an “energy cascade”. If the oxidation potential of the CSU is more positive than that of its nearest neighbor, then a ground-state electron will be transferred from the neighboring pigment to the CSU. The oxidation potential is an indication of the absolute energy level of a compound’s highest occupied molecular orbital (HOMO). A less positive oxidation potential corresponds to a HOMO at higher absolute energy. Therefore, a molecular wire having pigments in a progressive series of higher HOMO energy levels leading in the direction away from the CSU, will transfer the “hole” away from the photoanode as a series of one-electron movements.

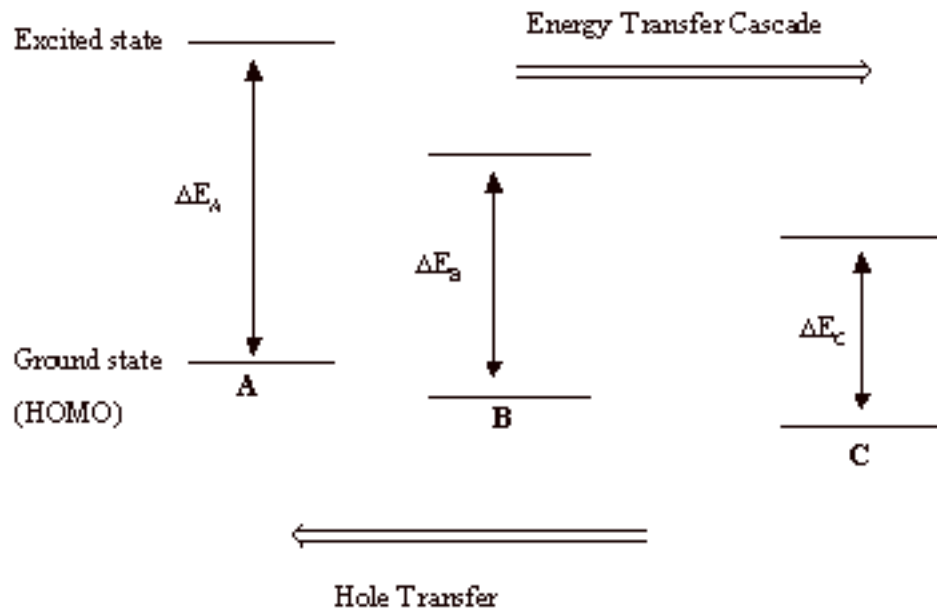


Figure 1.3. Rectification of energy and holes in a molecular wire.

The strength of the design for the ultrathin solar cell is that the properties of the organic material are tailored by the choice and order of pigments in the molecular wires. Phthalocyanines can be incorporated into such molecular wires, provided that they meet certain requirements with regard to their optical and electronic properties, and their structural features. Phthalocyanines have strong light absorption in the longer-wavelength, red to near-IR region of the solar spectrum, whereas porphyrins have strong light absorption in the shorter wavelength, near-UV to blue region of the solar spectrum. This difference in light absorption means that the excited-state energy ( $\Delta E$ ) of phthalocyanines is less than the corresponding  $\Delta E$  of porphyrins. This distinction can be seen via Einstein's relation:

$$\Delta E = h\nu = hc/\lambda \quad (1.1)$$

where  $\Delta E$  is the excited-state energy,  $h$  is Planck's constant,  $\nu$  is the frequency of electromagnetic radiation,  $\lambda$  is the wavelength of electromagnetic radiation, and  $c$  is the speed of light. Therefore, phthalocyanines would likely be near the photoanode end of the molecular wires, and could perhaps serve as the charge-separating unit itself.

If phthalocyanines are used within the light-harvesting section of the molecular wires, then they must have long-lived excited-states to participate efficiently in energy transfer between pigments. The excited-state lifetime ( $\tau$ ) of an uncoupled dye is inversely proportional to the sum of the rates by which that excited-state decays back to the ground-state:

$$1/\tau = k_f + k_{isc} + k_{ic} \quad (1.2)$$

where  $k_f$ ,  $k_{isc}$ , and  $k_{ic}$  are the rates of fluorescence emission, intersystem crossing, and internal conversion, respectively (units =  $s^{-1}$ ). A large value for the excited-state lifetime ( $\tau$ ) indicates slow rates of decay to the ground-state. This is favorable to the scenario where energy transfer from the dye molecule in question is viewed as a competing decay mechanism alongside the abovementioned pathways:

$$1/\tau = k_{trans} + k_f + k_{isc} + k_{ic} \quad (1.3)$$

where  $k_{trans}$  is the rate of energy transfer. A long-lived excited-state for the uncoupled monomer translates to slow competition for the energy transfer mechanism, thus promoting a high value of energy transfer efficiency. The photochemically relevant phthalocyanines that have long excited-state lifetimes (~3-5 ns) include free base phthalocyanines and their zinc and magnesium chelates.<sup>26</sup>

#### **D. Electrochemistry of phthalocyanines.**

Unfortunately, phthalocyanines are often not well behaved in optical and electrochemical measurements due to their tendency to aggregate in solution. This phenomenon and its effect on electrochemistry studies of phthalocyanines has led to disagreement in the literature regarding the oxidation potentials of phthalocyanines. The half-wave reduction-potential of the first oxidation state of an organic compound corresponds to the HOMO energy level of that compound. Methods such as cyclic voltammetry and square wave voltammetry can determine the oxidation/reduction potentials of organic compounds relative to an electrode's potential, which can be corrected to the vacuum scale if necessary. For purposes of designing a molecular wire of pigments, it is sufficient to determine a relative ordering of the oxidation/reduction potentials for pigment compounds within a single electrode potential scale.

There are published reports which describe the first oxidation peak potentials of photochemically relevant phthalocyanines as generally being of less positive than the oxidation peak potential of corresponding porphyrins.<sup>26</sup> This is a counterintuitive result, because the phthalocyanine scaffold is distinguished by the substitution of four carbon atoms of the interior scaffold of a porphyrin with four nitrogen atoms (Chart 1.1). Nitrogen is more electronegative than carbon, and should therefore affect the phthalocyanines by rendering them more difficult to oxidize relative to corresponding porphyrins. An important observation in support of this latter perspective is found in the study of an array of four porphyrins bound to a single phthalocyanine, a compound prepared within the Lindsey research group: When the compound was subjected to one electron oxidation and studied by EPR, it was observed that the “hole” resided only on porphyrins within the array.<sup>28</sup> This

indicated that the phthalocyanine was not capable of transferring a ground-state electron to an oxidized porphyrin, and therefore must have a more positive oxidation potential (and corresponding lower energy of HOMO). Although this observation is encouraging regarding the use of phthalocyanines together with porphyrins in an ultrathin solar cell, it does not allow the assignment of a precise oxidation potential to the phthalocyanine. An ultrathin solar cell may ultimately have a variety of porphyrinic pigments, and it is inconvenient to prepare a model array and conduct EPR studies for every possible pigment that might be placed adjacent to a phthalocyanine in the molecular wire. A study that could more precisely characterize the oxidation potentials of phthalocyanines, without suffering from perturbation caused by aggregation of the macrocycles, is needed.

#### **E. Structural aspects of phthalocyanines.**

Another category of consideration for the use of phthalocyanines in molecular wires is their structural suitability. There is a need for phthalocyanines bearing useful substituents in precise alignments for incorporation of the pigments into macromolecules and materials. For a rod-like molecular wire of phthalocyanines, new methods must be developed towards the backbone polymerization of phthalocyanines. Backbone polymerization of phthalocyanines is distinguished from the axially connected or “shish-kebab” phthalocyanines, wherein each monomer is connected via its central atom.<sup>29</sup> Backbone polymerization of phthalocyanines is difficult, owing partly to the limited solubility of most phthalocyanines and partly to limitations of the geometry of phthalocyanines. The advantages of backbone polymers of phthalocyanines relative to non-covalently assembled phthalocyanines are (1) improved thermal and chemical stability of the short and long range

structure, (2) reproducible preparation of materials without the use of expensive or delicate instrumentation, and sometimes (3) the addition of through-bond mechanisms of electronic communication between the component monomers as a complement to through-space mechanisms of energy transfer and/or conductivity.

Most efforts at preparing phthalocyanine polymers have utilized the phthalocyanine macrocyclization reaction as the material-forming step, with bridged or bilateral building blocks such as 1,2,4,5-tetracyanobenzene or dicyanobenzenes linked by alkyl chains or other intermediary groups.<sup>30,31</sup> This strategy typically results in two-dimensional sheets of fused or linked pigments. Another approach is to prepare square oligomers of fused phthalocyanines with polymerizable end groups,<sup>32,33</sup> which also gives two-dimensional products. The ladder oligomers prepared by Hanack and coworkers are the best example of a linear one-dimensional phthalocyanine material.<sup>34</sup> However, the stepwise synthesis used for such oligomers is not well suited to the preparation of polymers bearing many phthalocyanine macrocycles. Kingsborough and Swager prepared a thiophene-linked metallophthalocyanine polymer via electropolymerization of thiophene end groups.<sup>35</sup> The resulting material is described as “nearly linear”, but this polymer allows for rotation of the phthalocyanines and is not likely to be shape-persistent. The electroactive linking groups play a large role in the character of the resulting polymer. The fused linkages in the ladder oligomers and the phthalocyanine sheets also have a significant effect on the photochemical and electrochemical properties of the individual chromophores of the resulting material. In many cases this perturbation may be beneficial and intentional. However, these perturbation effects are not easily predicted and therefore complicate the design of electronic materials.

Lindsey and coworkers have prepared backbone polymers of diethynylporphyrins via chemical as well as thermal polymerization of ethyne end groups.<sup>36,37</sup> Chemically polymerized porphyrins are of interest as “light-harvesting rods” in the capture of solar energy,<sup>36</sup> whereas the thermally polymerized porphyrins have been examined as electroactive films for information storage.<sup>37</sup> The linkages between porphyrins in the light-harvesting rods are made by Glaser coupling and are phenyl-butadiynyl-phenyl groups, which allow for through-bond communication (excited-state energy, ground-state hole/electron transfer) without perturbing the native properties of the porphyrin monomers.<sup>36,38</sup> A one-dimensional all-phthalocyanine polymer derived from monomers that similarly retain their native properties while engaging in such through-bond communication would be a useful counterpart to the porphyrin-based rods.

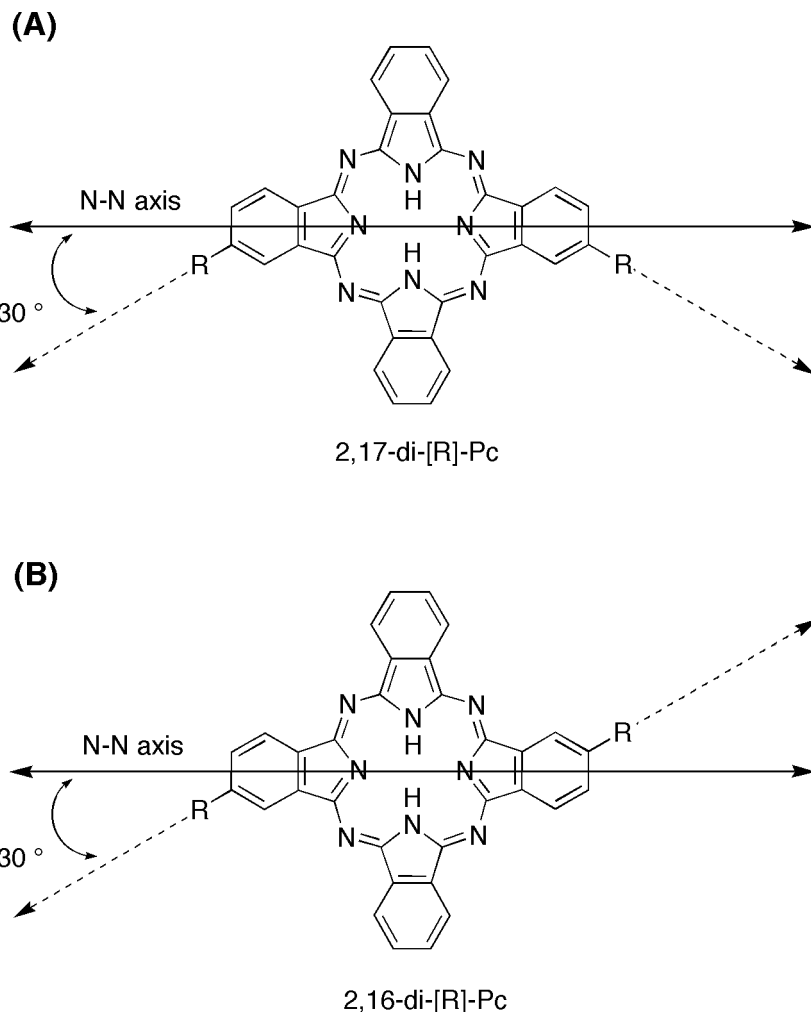


Figure 1.4. Two *trans*-substituted phthalocyanines.

The inherent geometry of phthalocyanines is an important consideration in approaches to a linear phthalocyanine polymer. In Figure 1.4, two possible ABAB phthalocyanines are shown, having 2,16- and 2,17-substitution patterns. The substituents of the 2,17 isomer are at a  $120^\circ$  angle with respect to each other, whereas those of the 2,16-isomer are parallel but not collinear. This is the result of the fact that each of the peripheral substituents shown in these structures is offset with respect to one of the central N-N axes by a  $30^\circ$  angle (see Figure 1 for definition of the N-N axis). A polymer prepared from a mixture

of these isomers could not be expected to afford a linear alignment. Even a polymer produced solely from the 2,17-isomer would be unlikely to hold a 180° alignment over long range due to rotation about the bonds between the phthalocyanines and their linkages.

#### F. Challenges in the synthesis of phthalocyanines.

Even if either or both of the two types of *trans*-phthalocyanines shown in Figure 1.4 were suitable, the preparation of such lowered-symmetry phthalocyanines is a difficult task. Typical phthalocyanine-forming conditions involve the refluxing of a suitable building block (such as a phthalonitrile) in a high boiling alcohol solvent (such as pentanol) in the presence of a strong base (such as DBU or an alkoxide). The reaction is oxidative, requiring the input of an equivalent of molecular hydrogen (two protons, two electrons) to transform the starting material(s) to product. As a result of these harsh and oxidative conditions, the reaction intermediates are highly unstable, and not readily isolable for the pursuit of stepwise syntheses. Moreover, the number and geometry of the substituent positions allows for the formation of regioisomers (such as the two *trans*-phthalocyanines in Figure 1.4). Figure 1.5 shows the macrocyclization of a monosubstituted phthalonitrile. This reaction provides four distinct regioisomers, which can be tedious to separate (if separable at all), depending on the nature of the substituent.

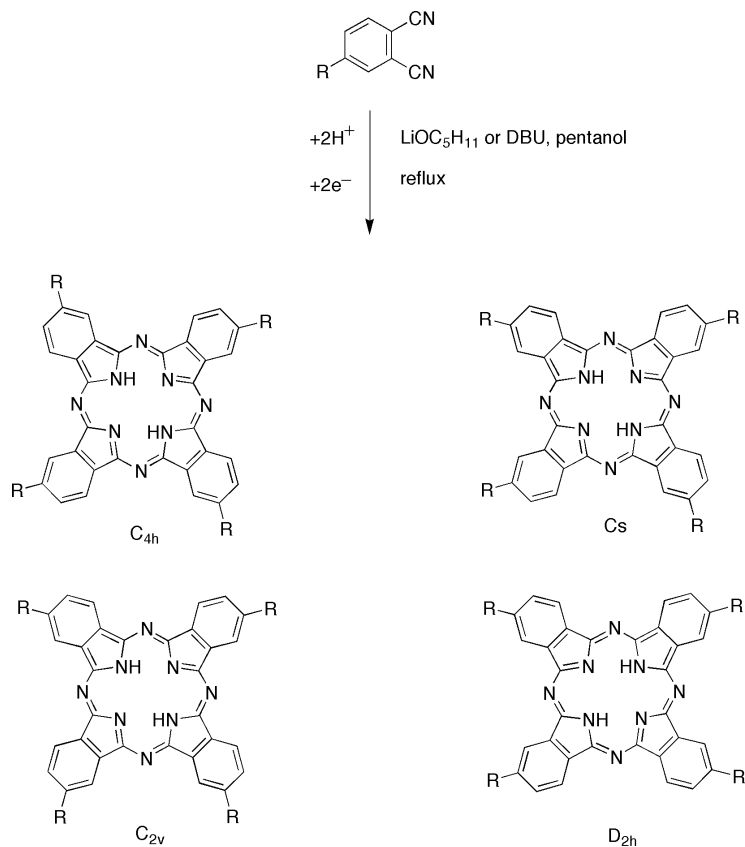


Figure 1.5. Regioisomers resulting from the cyclization of a substituted precursor.

Attempts to prepare lowered-symmetry phthalocyanines from mixtures of precursors result more complex product mixtures. Figure 1.6 shows the mixed macrocyclization of a monosubstituted phthalonitrile with dicyanobenzene, resulting in 15 distinct phthalocyanines due to compositional and regiosomeric differences. The same tetrasubstituted products that are shown in Figure 1.4 are present, together with four trisubstituted products, five disubstituted products, one monosubstituted product, and the unsubstituted phthalocyanine. Either of the two *trans*-substituted products (left end of center row) would likely be extremely difficult to isolate from this mixture, and available only in very low yield.

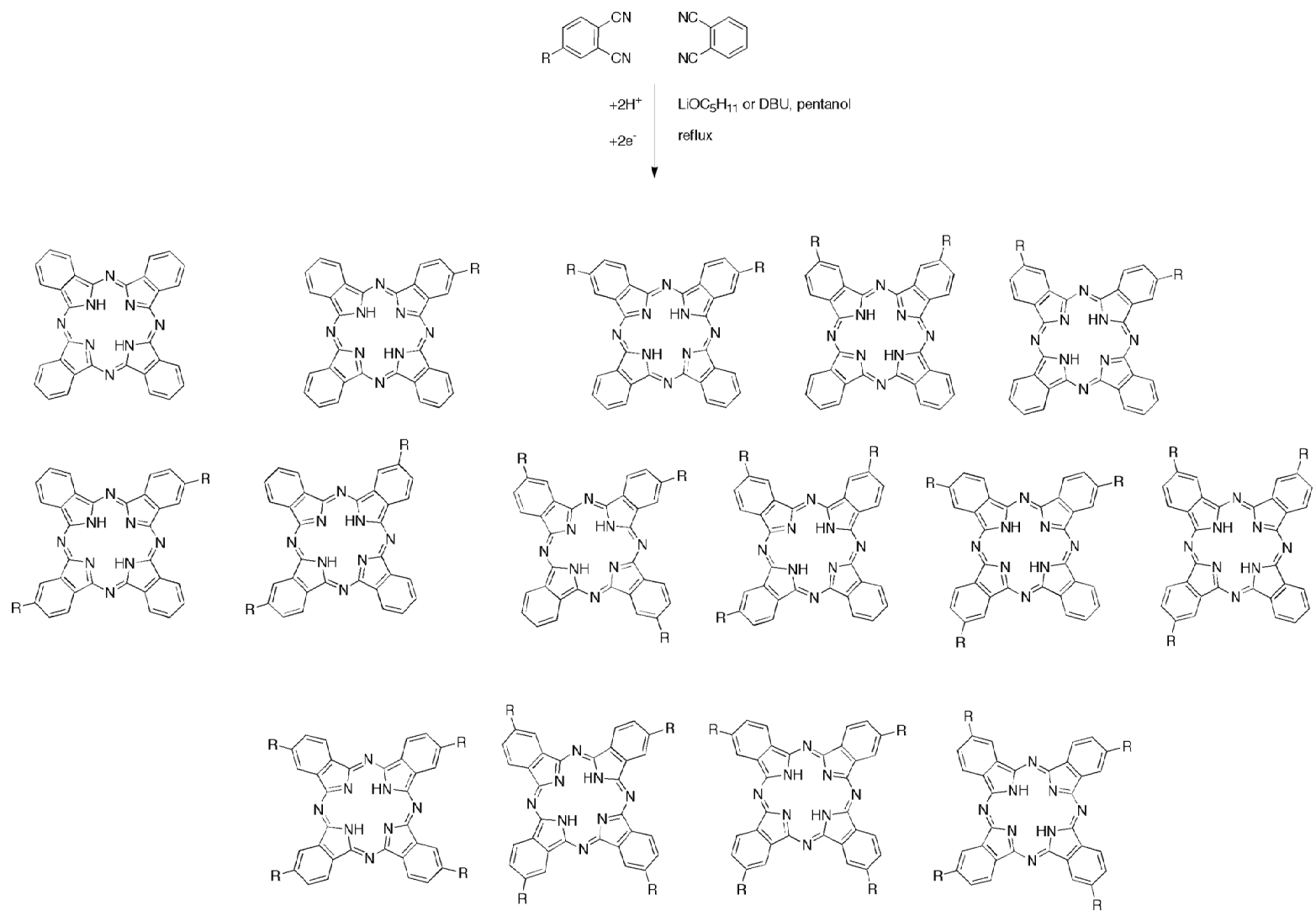


Figure 1.6. A mixed macrocyclization forming lowered-symmetry phthalocyanines.

A few synthetic methodologies have been developed for the directed synthesis of low symmetry phthalocyanines. Phthalocyanines having an AAAB (also termed A<sub>3</sub>B) substitution pattern have been prepared by the ring expansion of subphthalocyanines.<sup>39</sup> Phthalocyanines with an AABB substitution pattern (also termed *cis*-A<sub>2</sub>B<sub>2</sub>) have been prepared via reactive intermediates called “half-phthalocyanines”.<sup>40</sup> Some examples of *cis*-A<sub>2</sub>B<sub>2</sub> phthalocyanines have also been prepared by the macrocyclization of linked phthalonitriles.<sup>41</sup> Lastly, a direct approach to ABAB phthalocyanines (also termed *trans*-A<sub>2</sub>B<sub>2</sub>) is available via the “crossed-condensation” method.<sup>42</sup> One example of an in-plane linear polymerization strategy has come from this technique via a fused ladder-type oligomerization by Hanack and coworkers (Scheme 7).<sup>34</sup> These challenging procedures require the preparation of very reactive precursors, and typically give low yields. Nevertheless, they are the best routes available for the preparation of lowered-symmetry phthalocyanines.

#### **G. Research goals: Synthesis and characterization of novel phthalocyanines.**

A modification of the core pigment scaffold such that substituents are collinear with the N-N axes of the macrocycles should result in a monomer suitable for rod-like polymers. Such an architecture can be achieved with phthalocyanines bearing five-membered outer rings, either in place of the standard benzo rings, or by extra-annulation. Since a five-membered all-carbon ring would break the aromaticity of the macrocycle, the outermost ring must be heterocyclic. There are reported syntheses for phthalocyanines bearing diverse five-membered heterocyclic outer rings.<sup>43</sup> Some are obtained by the use of heterocyclic building blocks, whereas others are achieved by peripheral modification of substituted

phthalocyanines. Those that permit substitution at the outermost position include pyrrole, indole, imidazole, and thiophene. From this shortened list, the extra-annulated imidazole appeared the most accessible in terms of numbers and types of synthetic steps. Phthalocyanines bearing this motif (Figure 1.7) have been previously termed imidazophthalocyanines,<sup>44</sup> as well as benzimidazoloporphyrnazines.<sup>45</sup> (Note that a tetrabenzoporphyrnazine is synonymous with a phthalocyanine.) This report uses the term benzimidazoporphyrnazines, a slight abbreviation of the previous moniker, and still unambiguous with respect to the motif.

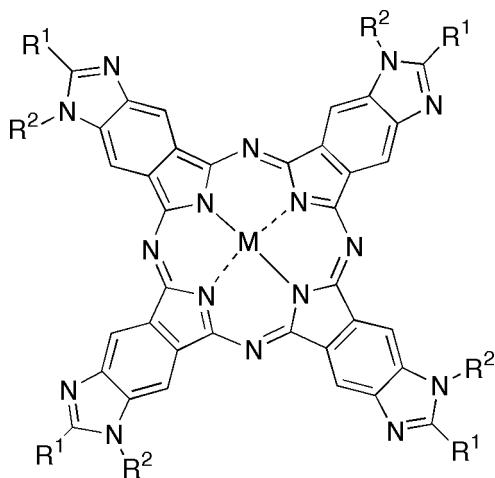


Figure 1.7. Generic Structure of Benzimidazoporphyrnazines (A<sub>4</sub>-type, C<sub>4h</sub> geometry).

This dissertation describes the development of new synthetic methodology for benzimidazoporphyrnazines (BzImPAs). BzImPAs having four benzimidazole moieties (A<sub>4</sub>-type) have been prepared, bearing a variety of substituents at the outermost positions. These new pigments have been studied with regard to structural confirmation and photochemical behavior. A *trans*-ABAB benzimidazoporphyrnazine has been prepared for application to polymerization into a molecular wire for an ultrathin solar cell. Two kinds of AB<sub>3</sub>

benzimidazoporphyrazines have been prepared, and one has been used to prepare a lanthanide sandwich complex that is of interest in the application of information storage.

Additionally, two different phthalocyanines have been prepared that bear tripodal linkers for attachment to electrode surfaces. One of the phthalocyanines is a benzimidazoporphyrazine and the other is not. One of the phthalocyanines is intended for attachment to a silican electrode, whereas the other is intended for a gold electrode. These phthalocyanines bearing tripodal linkers were prepared for the purpose of determining the oxidation potentials of surface-bound phthalocyanines, with the expectation that the artifactual electrochemical responses normally attributed to phthalocyanine aggregates would be absent from the resulting studies. One of the phthalocyanines has also been used to prepare the abovementioned type-a triple decker lanthanide sandwich. A separate short introduction has been included in the chapter describing the triple decker. As a final note, this dissertation is not intended as a catalog of all work performed in my graduate experience. This report is confined to projects ongoing from the time of my preliminary defense, concerning the synthesis of phthalocyanines. Projects completed before the defense and later projects that were unrelated to the synthesis of phthalocyanines have been omitted for the purpose of brevity. Much of this omitted work can be found in published articles.<sup>12f,36,38,46</sup>

## G. References:

- (1) McKeown, N. B. *Phthalocyanine Materials* 1998, Cambridge University Press, pp 1–3.
- (2) (a) Linstead, R. P. *J. Chem. Soc.* **1934**, 1016–1017; (b) Byrne, G. T.; Linstead, R. P.; Lowe, A. R. *J. Chem. Soc.* **1934**, 1017–1022; (c) Linstead, R. P.; Lowe, A. R. *J. Chem. Soc.* **1934**, 1022–1027; (d) Dent, C. E.; Linstead, R. P. *J. Chem. Soc.* **1934**, 1027–1031; (e) Linstead, R. P.; Lowe, A. R. *J. Chem. Soc.* **1934**, 1031–1033; (f) Dent, C. E.; Linstead, R. P.; Lowe, A. R. *J. Chem. Soc.* **1934**, 1033–1039.
- (3) Christie, R. M. *Colour Chemistry*, Royal Society of Chemistry: Cambridge, UK, 2001.
- (4) Law, K.-Y. *Chem. Rev.* **1993**, *93*, 449–486.
- (5) de la Torre, G.; Vazquez, P.; Agullo-Lopez, F.; Torres, T. *J. Mater. Chem.* **1998**, *8*, 1671–1683.
- (6) Calvete, M.; Yang, G. Y.; Hanack, M. *Synth. Met.* **2004**, *141*, 231–243.
- (7) Allen, C. M.; Sharman, W. M.; Van Lier, J. E. *J. Porphyrins Phthalocyanines* **2001**, *5*, 161–169.
- (8) Nazeeruddin, M. K.; Humphry-Baker, R.; Grätzel, M.; Wörhle, D.; Schnurpeil, G.; Hirth, A.; Trombach, N. *J. Porphyrins Phthalocyanines* **1999**, *3*, 230–237.
- (9) Petritsch, K.; Friend, R. H.; Lux, A.; Rozenberg, G.; Moratti, S. C.; Holmes, A. B. *Synth. Met.* **1999**, *102*, 1776–1777.
- (10) Zhou, R.; Josse, F.; Gopel, W.; Ozturk, Z. Z.; Bekaroglu, O. *Appl. Organomet. Chem.* **1996**, *10*, 557–577.

- (11) Jiang, J.; Kasuga, K.; Arnold, D. P. In *Supramolecular Photosensitive and Electroactive Materials*, Nalwa, H. S. Ed., Academic Press: San Diego, CA, 2001, 188–189 and references cited therein.
- (12) (a) Li, J.; Gryko, D.; Dabke, R. B.; Diers, J. R.; Bocian, D. F.; Kuhr, W. G.; Lindsey, J. S. *J. Org. Chem.* **2000**, *65*, 7379–7390; (b) Gryko, D.; Li, J.; Diers, J. R.; Roth, K. M.; Bocian, D. F.; Kuhr, W. G.; Lindsey, J. S. *J. Mater. Chem.* **2001**, *11*, 1162–1180; (c) Gross, T.; Chevalier, F.; Lindsey, J. S. *Inorg. Chem.* **2001**, *40*, 4762–4774; (d) Schweikart, K.-H.; Malinovskii, V. L.; Diers, J. R.; Yasseri, A. A.; Bocian, D. F.; Kuhr, W. G.; Lindsey, J. S. *J. Mater. Chem.* **2002**, *12*, 808–828; (e) Schweikart, K.-H.; Malinovskii, V. L.; Yasseri, A. A.; Li, J.; Lysenko, A. B.; Bocian, D. F.; Lindsey, J. S. *Inorg. Chem.* **2003**, *42*, 7431–7446; (f) Wei, L.; Padmaja, K.; Youngblood, W. J.; Lysenko, A. B.; Lindsey, J. S.; Bocian, D. F. *J. Org. Chem.* **2004**, *69*, 1461–1469.
- (13) (a) Lindsey, J. S.; Meyer, G. J. U.S. Patent 6,407,330, June 18, 2002; (b) Loewe, R.S.; Lammi, R. K.; Diers, J. R.; Kirmaier, C.; Bocian, D. F.; Holten, D.; Lindsey, J. S. *J. Mater. Chem.*, **2002**, *12*, 1530–1552.
- (14) O'Regan, B.; Grätzel, M. *Nature* **1991**, *353*, 737–740.
- (15) Morel, D. L.; Ghosh, A. K.; Feng, T.; Stogryn, E. L.; Purwin, P. E.; Shaw, R. F.; Fishman, C. *Appl. Phys. Lett.* **1978**, *32*, 495–497.
- (16) Merritt, V. Y.; Hovel, H. J. *Appl. Phys. Lett.* **1976**, *29*, 953.
- (17) (a) Harima, Y.; Yamashita, K.; Saji, T. *Appl. Phys. Lett.* **1988**, *52*, 1542–1543. (b) Durstock, M. F.; Taylor, B.; Spry, R. J.; Chiang, L.; Reulback, S.; Heitfeld, K.; Baur, J. W. *Synth. Met.* **2001**, *116*, 373–377.

- (18) Hua, Y. L.; Petty, M. C.; Roberts, G. G.; Ahmad, M. M.; Hanack, M.; Rein, M. *Thin Solid Films* **1987**, *149*, 163–170.
- (19) Schmidt-Mende, L.; Fechtenkötter, A.; Müllen, K.; Moons, E.; Friend, R. H.; Mackenzie, J. D. *Science* **2001**, *293*, 1119–1122.
- (20) van Duren, J. K. J.; Dhanabalan, A.; van Hal, P. A.; Janssen, R. A. J. *Synth. Met.* **2001**, *121*, 1587–1588.
- (21) (a) Dittmer, J. J.; Marseglia, E. A.; Friend, R. H. *Adv. Mater.* **2000**, *12*, 1270–1274; (b) Panneman, C.; Dyakonov, V.; Parisi, J.; Hild, O.; Wörhle, D. *Synth. Met.* **2001**, *121*, 1585–1586.
- (22) Tang, C. W. *Appl. Phys. Lett.* **1985**, *48*, 183–185.
- (23) Hiramoto, M.; Fujiwara, H.; Yokoyama, M. *Appl. Phys. Lett.* **1991**, *58*, 1062–1064.
- (24) Nelson, J. *Current Opinion in Solid State and Materials Science* **2002**, *6*, 87–95.
- (25) (a) Takada, J.; Awaji, H.; Nakajima, A.; Nevin, W. A. *Appl. Phys. Lett.* **1992**, *61*, 2184–2186; (b) Murgia, M.; Biscarini, M.; Taliani, C.; Ruani, G. *Synth. Met.* **2001**, *121*, 1533–1534; (c) Ahn, Y. J.; Kang, G. W.; Lee, C. H. *Mol. Cryst. Liq. Cryst.* **2002**, *301*–304.
- (26) (a) data for (*t*-Bu)<sub>4</sub>H<sub>2</sub>Pc and (*t*-Bu)<sub>4</sub>MgPc: Teuchner, K.; Pfarrherr, A.; Stiel, H.; freyer, W.; Leupold, D. *Photochem. Photobiol.* **1993**, *57*, 465–471; (b) additional data for (*t*-Bu)<sub>4</sub>MgPc: Freyer, W.; Dähne, S.; Minh, L. Q.; Teuchner, K. Z. *Chem.* **1986**, *26*, 334–336; (c) data for (*t*-Bu)<sub>4</sub>ZnPc: Tran-Thi, T.-H.; Desforge, C.; Thiec, C.; Gaspard, S. *J. Phys. Chem.* **1989**, *93*, 1226–1233; (d) data for (n-heptyl)<sub>8</sub>MPc, where M = H<sub>2</sub>, Mg, or Zn: Yang, S. I.; Li, J.; Cho, H. S.; Kim, D.; Bocian, D. F.; Holten, D.; Lindsey, J. S. *J. Mater. Chem.* **2000**, *10*, 283–296.

- (27) L'Her, M.; Pondaven, A. In *The Porphyrin Handbook*; Kadish, K. M., Smith, K. M., Guilard, R., Eds.; Academic Press: San Diego, CA, 2003; Vol. 16, pp 117-169.
- (28) Li, J.; Diers, J. R.; Seth, J.; Yang, S. I.; Bocian, D. F.; Holten, D.; Lindsey, J. S. *J. Org. Chem.* **1999**, *64*, 9090–9100.
- (29) Hanack, M.; Hees, M.; Stihler, P.; Winter, G.; Subramanian, L. R. In *Handbook of Conducting Polymers*, Skotheim, T. A., Elsenbaumer, R. L., and Reynolds, J. R., Eds., Marcel Dekker, New York, 1998, 381.
- (30) (a) Gürek, A. G.; Bekaroglu, O. *J. Porphyrins Phthalocyanines* **1997**, *1*, 67–76. (b) Gürek, A. G.; Bekaroglu, O. *J. Porphyrins Phthalocyanines* **1997**, *1*, 227–237.
- (31) Wörhle, D.; Benters, R.; Suvorova, O.; Schurpfeil, G.; Trombach, N.; Bogdahn-Rai, T. *J. Porphyrins Phthalocyanines* **2000**, *4*, 491–497.
- (32) Achar, B. N.; Fohlen, F. M.; Parker, J. A. *J. Polym. Sci. Polym. Chem. Ed.* **1982**, *20*, 1785–1790.
- (33) Venkatachalam, S.; Rao, K. V. C.; Manoharan, P. T. *J. Polym. Sci. Part B* **1994**, *32*, 37-52.
- (34) (a) Hauschel, B.; Ruff, D.; Hanack, M. *J. Chem. Soc., Chem. Commun.* **1995**, 2449–2451. (b) Hanack, M.; Stihler, P. *Eur. J. Org. Chem.* **2000**, *39*, 303–311.
- (35) Kingsborough, R. P.; Swager, T. M. *Angew. Chem. Int. Ed.* **2000**, *39*, 2897–2900.
- (36) Loewe, R. S.; Tomizaki, K.; Youngblood, W. J.; Bo, Z.; Lindsey, J. S. *J. Mater. Chem.* **2002**, *12*, 3438–3451.
- (37) Liu, Z.; Schmidt, I.; Thamyongkit, P.; Loewe, R. S.; Syomin, D.; Diers, J. R.; Zhao, Q.; Misra, V.; Lindsey, J. S., Bocian, D. F. *Chem. Mater.* **2005**, in press.

- (38) Youngblood, W. J.; Gryko, D. T.; Lammi, R. K.; Bocian, D. F.; Holten, D.; Lindsey, J. S. *J. Org. Chem.* **2002**, *67*, 2111–2117.
- (39) (a) Kobayashi, N.; Kondo, R.; Nakajima, S.; Osa, T. *J. Am. Chem. Soc.* **1990**, *112*, 9640–9641; (b) Musluoglu, E.; Gürek, A.; Ahsen, V.; Bekaroglu, Ö. *Chem. Ber.* **1992**, *125*, 2337–2339; (c) Sastre, A.; Torres, T.; Hanack, M. *Tetrahedron Lett.* **1995**, *36*, 8501–8504; (d) Weitemeyer, A.; Kliesch, H.; Wörhrle, D. *J. Org. Chem.* **1995**, *60*, 4900–4904; (e) Kudrevich, S. V.; Gilbert, S.; van Lier, J. E. *J. Org. Chem.* **1996**, *61*, 5706–5707.
- (40) Nolan, K. J. M.; Hu, M.; Leznoff, C. C. *Synlett* **1997**, 593–594.
- (41) (a) Kobayashi, N.; Kobayashi, Y.; Osa, T. *J. Am. Soc. Chem.* **1993**, *115*, 10994–10995; (b) Drew, D. M.; Leznoff, C. C. *Synlett* **1994**, 623–624.
- (42) (a) Idelson, Elbert (Polaroid Corp.), U. S. Patent 4,061,654; Dec. 6, 1977. (b) Young, J. G.; Onyebuagu, W. *J. Org. Chem.* **1990**, *55*, 2155–2159; (c) Stihler, P.; Hauschel, B.; Hanack, M. *Chem. Ber.* **1997**, *130*, 801–806; (d) Dabak, S.; Bekâroglu, Ö. *J. Chem. Res. (S)* **1997**, 8–9.
- (43) Stuzhin, P. A.; Ercolani, C. In *The Porphyrin Handbook*; Kadish, K. M., Smith, K. M., Guillard, R., Eds.; Academic Press: San Diego, 2003; Vol. 15, pp 263–364.
- (44) Pardo, C.; Yuste, M.; Elguero, J. *J. Porphyrins Phthalocyanines* **2000**, *4*, 505–509.
- (45) (a) Kudrik, E. V.; Shaposhnikov, G. P. *Mendeleev Commun.* **1999**, 85–86. (b) Kudrik, E. V.; Shaposhnikov, G. P.; Balakirev, A. E. *Russ. J. Gen. Chem.* **1999**, *69*, 1321–1324. (c) Balakirev, A. E.; Kudrik, E. V.; Shaposhnikov, G. P. *Russ. J. Gen. Chem.* **2002**, *72*, 1616–1619.

- (46) Tamaru, S.-I.; Yu, L.; Youngblood, W. J.; Muthukumaran, K.; Taniguchi, M.; Lindsey, J. S. *J. Org. Chem.* **2004**, *69*, 765–777.

## Chapter 2

### A. Research objectives.

This chapter describes the synthesis and characterization of a phthalocyanine bearing a tripodal linker for attachment to a gold electrode (Figure 2.1). The motivation for this work is twofold: Electrochemical studies on a monolayer of phthalocyanines bound to an electrode surface might be a viable alternative to solution phase voltammetry; and if phthalocyanines can be electrochemically addressed in this manner, then they might be useful as a charge storage material for information storage in the same manner that porphyrins have recently been studied.<sup>1</sup> We felt that surface-bound monomeric phthalocyanines would be unable to aggregate, thereby ensuring that any electrochemical measurements of the phthalocyanines would be free of artifactual response caused by phthalocyanine aggregates. The tripodal linker was intended to promote a vertical orientation of the phthalocyanines relative to the electrode surface.

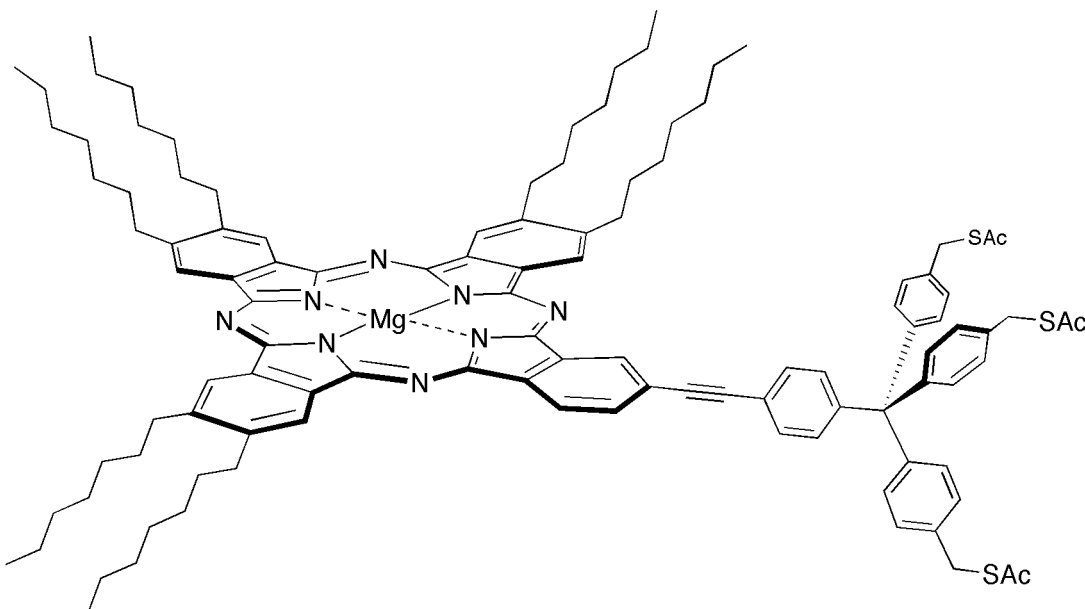
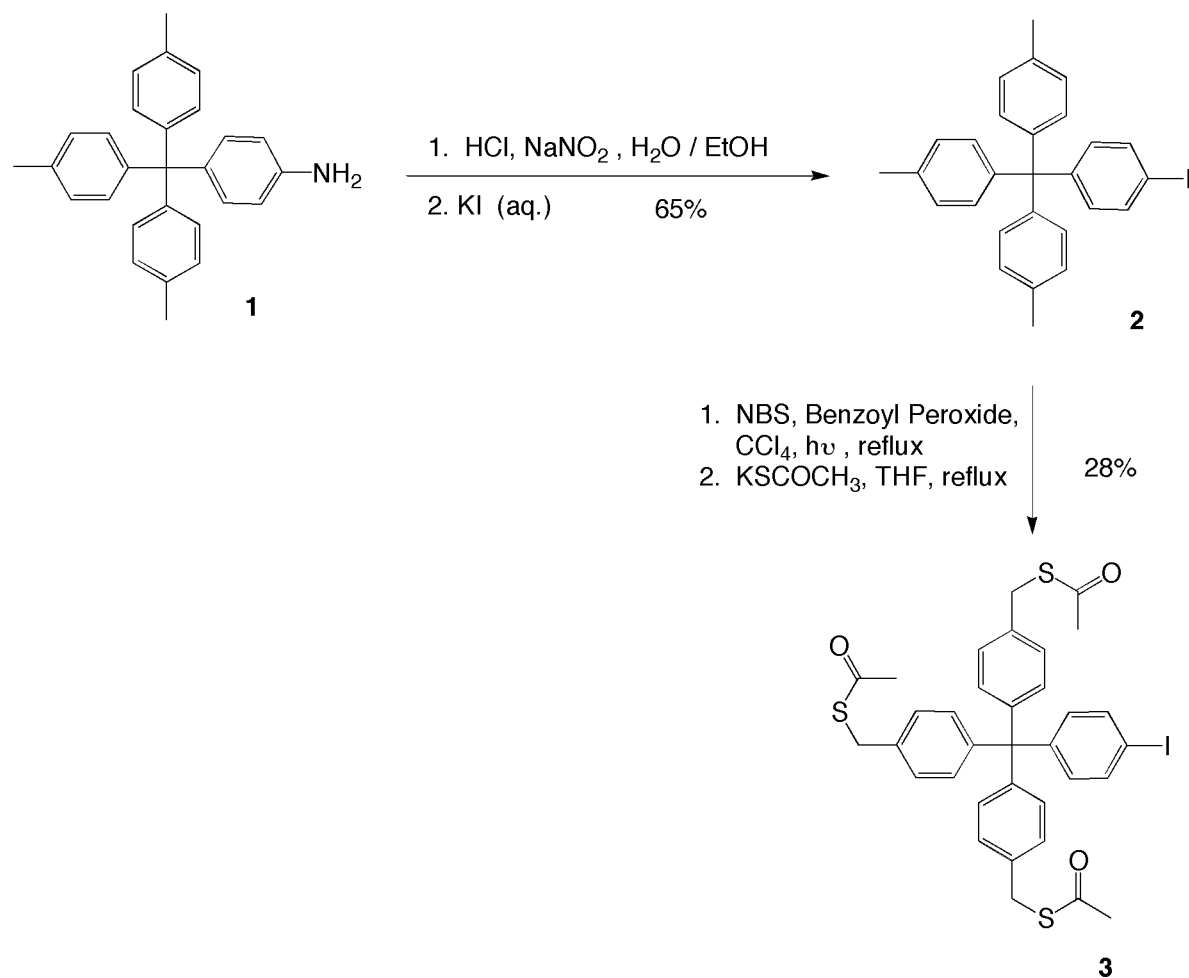


Figure 2.1. A Mg-phthalocyanine bearing a tripodal linker for attachment to a gold surface.

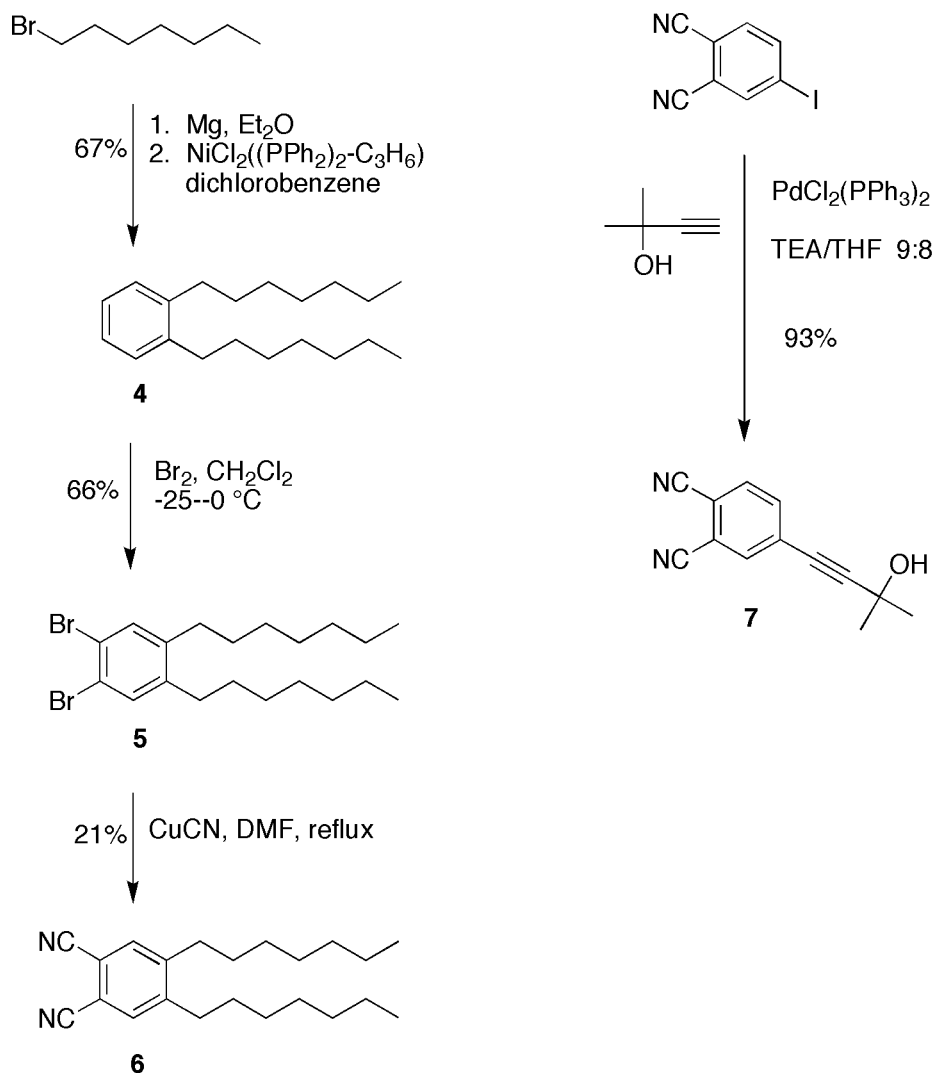
## B. Synthesis.

The synthesis of this phthalocyanine was achieved by the union of a monoethynyl phthalocyanine with the *S*-acetylthio-capped tripodal linker **3** (Scheme 1), which is a new compound, albeit similar to a previously-prepared tripodal linker in the literature.<sup>2</sup> Compound **3** was desired so that the palladium-coupling between the tripodal linker and any ethyne-terminated electroactive species could employ the most gentle conditions. The use of the corresponding linker compound with an aryl bromide requires elevated temperature, whereas the aryl iodide reacts at room temperature.



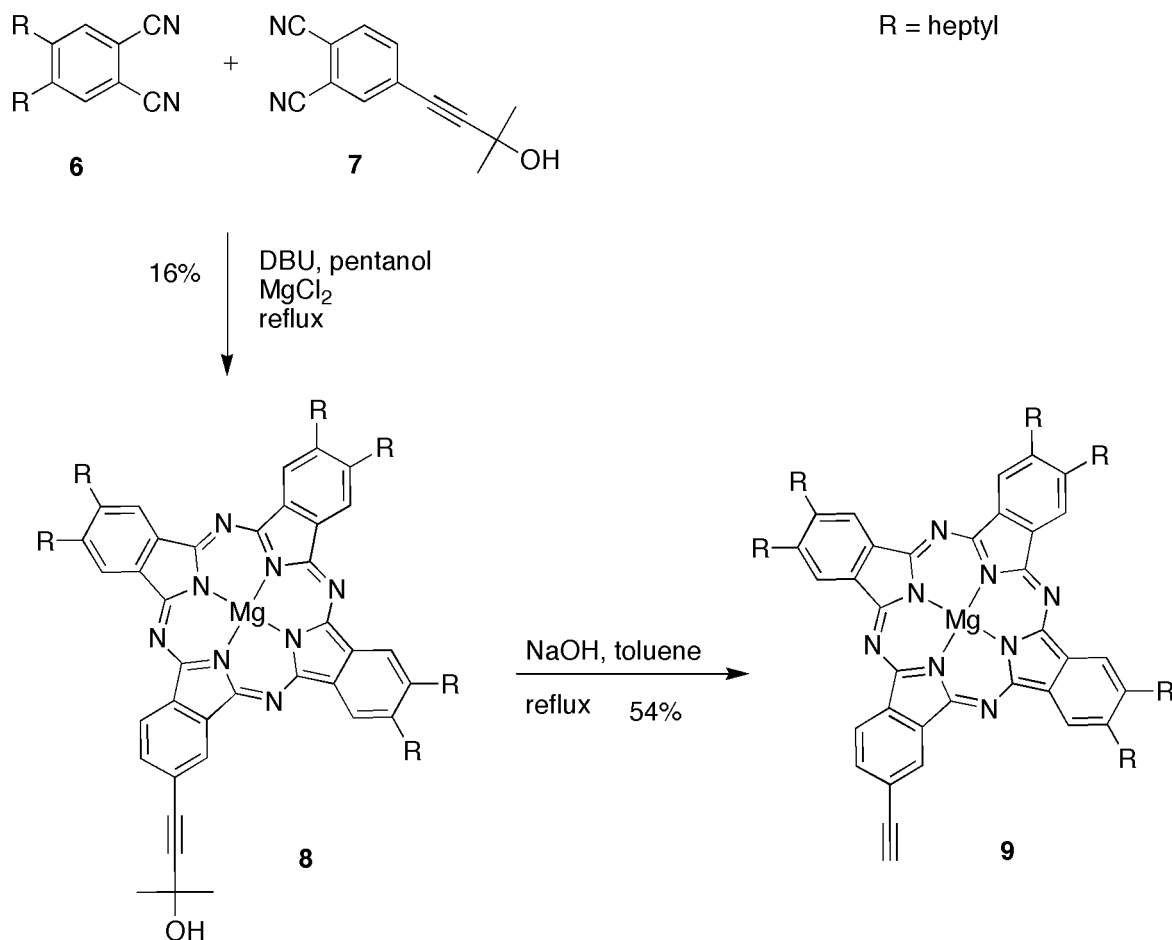
Scheme 2.1. Synthesis of a tripodal linker.

Starting from the known compound **1**,<sup>3</sup> it is possible to arrive at the desired aryl iodide **2** via an arene-diazonium intermediate. Treatment of the resulting arene-diazonium compound with aq. KI provided a good yield of **2** with minimal workup and simple recrystallization. The radical bromination of **2** gave a mixture of mono-, di-, and tri-brominated products. The products could not be separated due to their poor solubility. The mixture was carried on, and upon nucleophilic substitution of the benzyl bromides with potassium thioacetate, chromatographic separation of the desired product **3** was achieved.

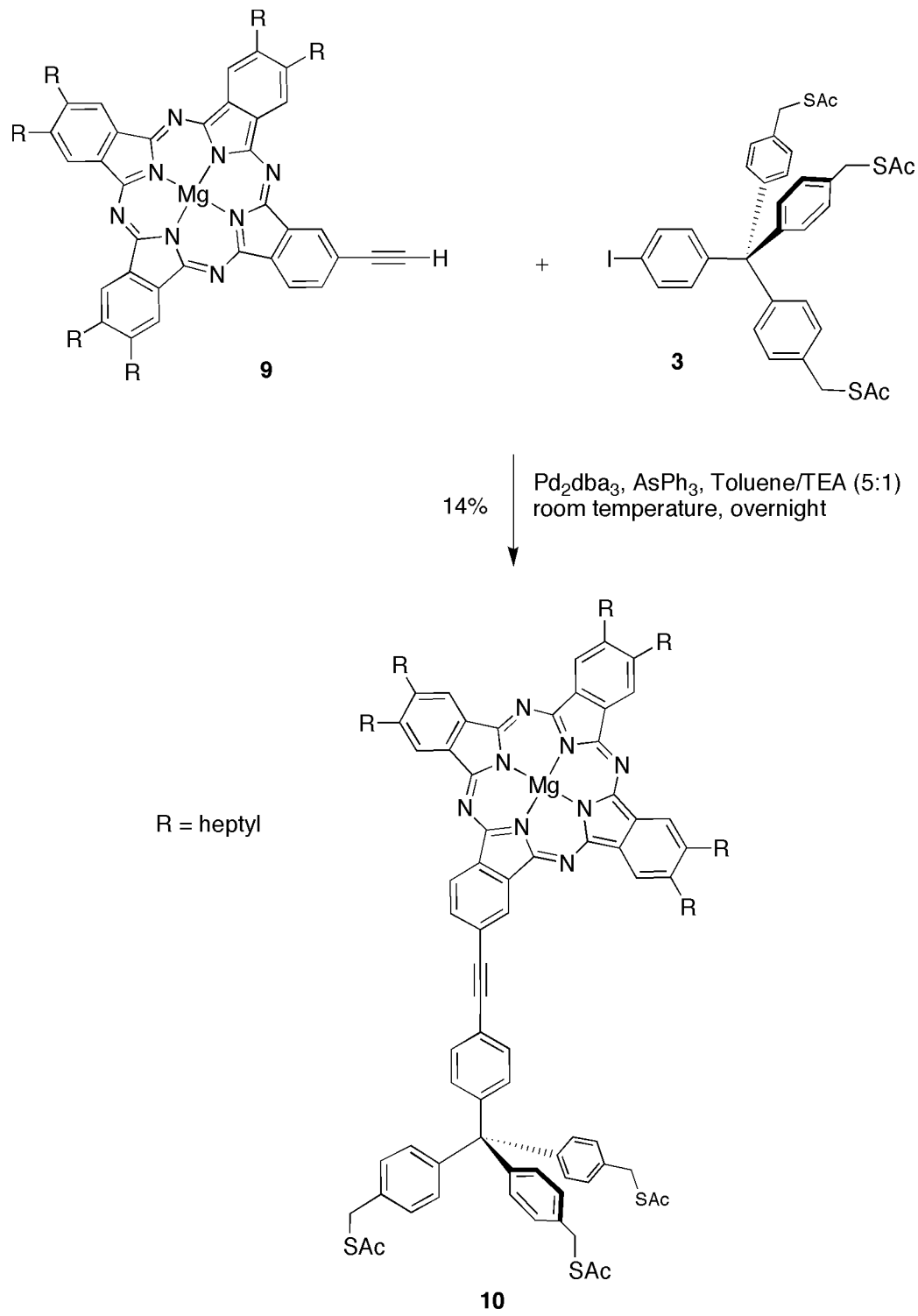


Scheme 2.2. Synthesis of substituted phthalonitriles.

Compound **9** has been previously synthesized in our group for the preparation of porphyrin-phthalocyanine dyads, and was prepared using the published procedures (Schemes 2,3).<sup>4</sup> Pd-mediated coupling of **9** and **3** (Scheme 4) was done in the absence of copper to avoid any deleterious transmetallation of copper for magnesium. Analytical SEC of the reaction mixture suggested a high yield of coupling for the reaction (>70%). However, the recovered yield of the desired product was low (14%), possibly due to instability of the acetylthio groups.



Scheme 2.3. Synthesis of a monoethynyl phthalocyanine.



Scheme 2.4. Synthesis of the Mg-phthalocyanine bearing a tripodal linker.

### C. Electrochemical Studies.

Electrochemical studies on compound **10** were conducted at the University of California at Riverside, in the laboratory of Prof. David Bocian. The measurements were conducted by Dr. James Diers (Research Scientist) and Lingyun Wei (graduate student). Figure 2.1 shows the square-wave voltammogram of compound **10**. This experiment is conducted by preparing a sample of compound **10** as a dilute solution in purified CH<sub>2</sub>Cl<sub>2</sub> and addressing the sample with three electrodes: a working electrode, a counter electrode, and a reference electrode, which contains a silver wire bathed in an aqueous solution of silver hexafluorophosphate.

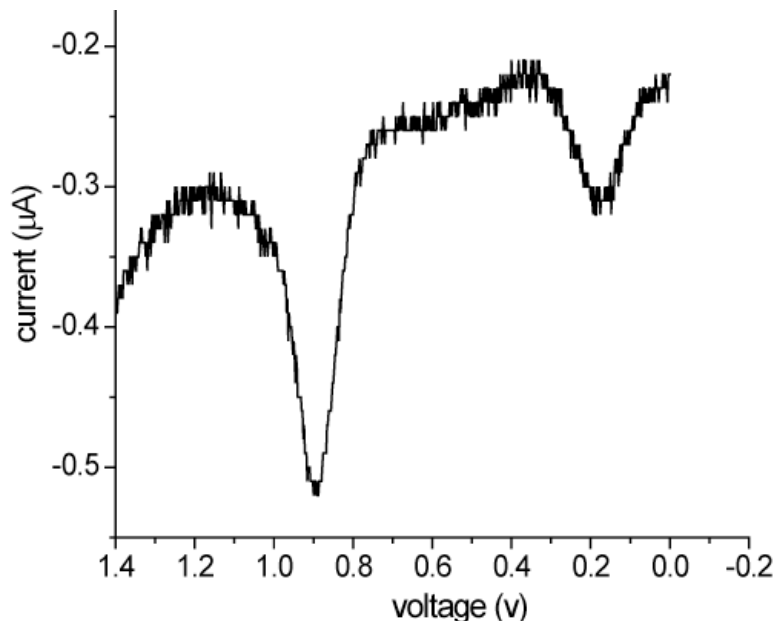


Figure 2.2 Square wave voltammogram of compound **10** in solution (Courtesy of Dr. James Diers).

The voltammogram in Figure 2.2 shows two oxidation peaks for compound **10**, at 0.15 V and 0.9 V (vs. Ag/Ag<sup>+</sup>). Although the area of the peaks has not been mathematically

integrated, it is evident from the amplitude of the two peaks that they are significantly unequal. Upon dilution of the sample the peaks were attenuated, but the first peak was attenuated more strongly than the second peak. The different amplitude of the first peak, and its greater attenuation at lower concentrations, suggests that it may represent an oxidation state corresponding to an aggregate of phthalocyanines, whereas the second peak is likely due to the monomeric pigments. The similar square wave voltammetry measurement for a zinc porphyrin with the same tripodal linker gave oxidation peaks at 0.6 V and 0.9 V (vs. Ag/Ag<sup>+</sup>). If the first peak of the voltammogram of compound **10**, at 0.15 V, is due to an aggregate species, then the peak at 0.9 V must be the first oxidation peak potential of the monomeric species, which would qualify the magnesium phthalocyanine as a suitable component in a light-harvesting array containing porphyrins. If the peak at 0.15 V is not due to an aggregate species, then the magnesium phthalocyanine must have a higher energy ground-state than the zinc porphyrin. This result would be unfavorable for the use of magnesium phthalocyanines with porphyrins in a light-harvesting array.

For the cyclic voltammogram shown in Figure 2.3, the adsorption was accomplished by dip coating of the gold electrode into a solution of compound **10** in organic solvent, followed by rinsing of the electrode to remove unbound pigment molecules. The integrals for the first and second oxidation peaks do not match, although the difference is only ~10%. These data do not suggest as compellingly as the square wave voltammogram that the first oxidation peak is due to an aggregate. For an aggregate to be responsible for the first peak, either some of the anchored molecules must lean over toward each other, or additional unanchored molecules are closely associated with the bound molecules.

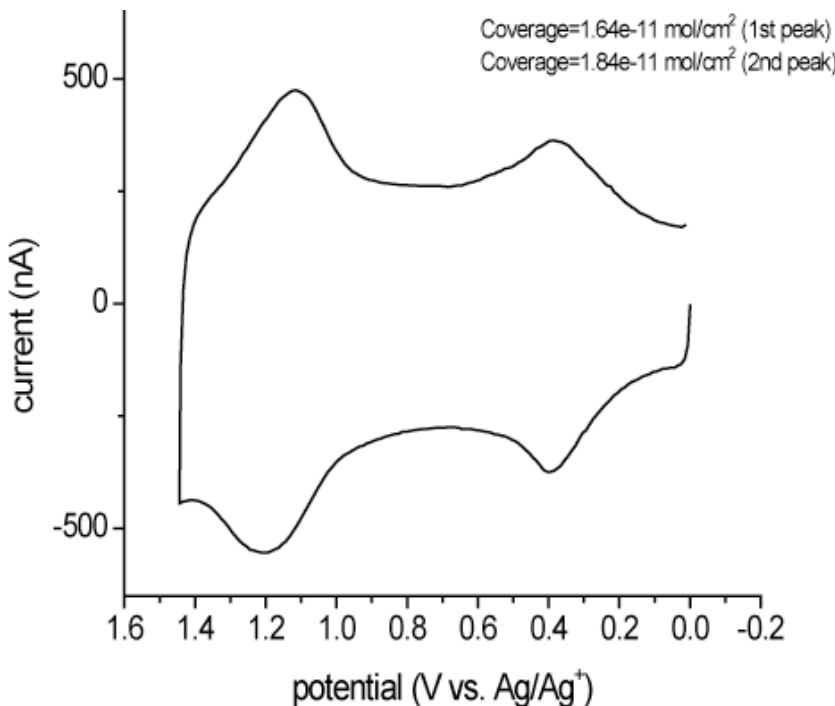


Figure 2.3. Cyclic voltammogram of compound **10** bound to a gold electrode (Courtesy of Lingyun Wei).

The cyclic voltammogram does allow for an estimation of the density of molecules in the self-assembled monolayer. The area within each oxidation peak has been integrated. These data are initially expressed as pico-Coulombs (pC), and are translated to moles of compound **10** by means of the Faraday constant:

$$[X] \text{ pC} \div 9.65e^9 \text{ C/mol} = [Y] \text{ mol} \quad (2.1)$$

The molar quantity is then divided by the electrode area, giving the expression shown in Figure 2.3 as moles per square centimeter. This quantity can then be adjusted to square nanometers, and multiplied by Avogadro's number to give an expression of molecules per square nanometer. For the second oxidation peak shown in Figure 2, this treatment gives:

$$\begin{aligned}
 [8.14e^{-11} \text{ mol/cm}^2] \times [1e^{-14} \text{ cm}^2/\text{nm}^2] \times [6.023e^{23} \text{ molecules/mol}] \\
 = 0.49 \text{ molecules / nm}^2.
 \end{aligned} \tag{2.2}$$

By inverting the result of the calculation, the average “footprint” of each molecule in the monolayer is deduced:

$$1 \div 0.49 \text{ molecules / nm}^2 = 2.0 \text{ nm}^2 / \text{molecule} \tag{2.3}$$

Given that the phthalocyanine macrocycle is roughly 2 nm wide (not considering the alkyl chains), this result indicates that the phthalocyanines are closely packed. Unfortunately, the monolayer of phthalocyanines proved to be unstable to the cyclic voltammetry experiment, because the first measurement could never be repeated for any electrode coated with compound **10**. Multiple electrodes were fairly consistent with respect to the first cyclic measurement of each.

#### D. Conclusion.

The apparent aggregation behavior of the phthalocyanine prepared for this study, and the instability of the monolayer prepared from this compound, indicate that phthalocyanines would not serve well as candidates for information storage media. Porphyrins, by contrast, have been shown to survive through many thousands of cycles of oxidation/reduction.<sup>4</sup> This study also failed to provide a definitive result as to the potential for the first oxidation state of the phthalocyanine. Another phthalocyanine-linker candidate would be needed to provide better data. A better candidate for this study would need some substituents that could provide steric hindrance against coplanar stacking of the macrocycles. The preparation of **10** provided an opportunity to hone many important techniques in the synthesis and purification of organic compounds. This work was included in a published article.<sup>5</sup>

## E. Experimental Section.

**General.**  $^1\text{H}$  (400 MHz) and  $^{13}\text{C}$  (100 MHz) NMR spectra were obtained in  $\text{CDCl}_3$  unless noted otherwise. Melting points are uncorrected. Silica gel (Scientific Adsorbents, 40  $\mu\text{m}$  average particle size) was used for column chromatography. THF was distilled from sodium chips under argon with benzophenone/ketyl as indicator. Dry toluene and dry TEA were prepared by distillation over  $\text{CaH}_2$ . The  $\text{CHCl}_3$  was reagent grade and contained 0.75% ethanol. All other chemicals were reagent grade and were used as received. Preparative SEC was conducted using Bio-Rad Bio-Beads SX-1<sup>®</sup> as the stationary phase, in THF.

**Non-commercial Compounds:** Compounds **1**<sup>3</sup> and **9**<sup>4</sup> were prepared as previously described.

**1-(4-Iodophenyl)-1,1,1-tris(*p*-tolyl)methane (**2**).** A three-necked 1 L round bottom flask was charged with **1** (15.6 g, 41.3 mmol), aqueous HCl (36 mL of a 6.1 M solution), and a magnetic stirring bar. EtOH was added slowly until all of the solid material was dissolved (total ~400 mL). The reaction flask was placed in an ice bath. An ice-cold solution of  $\text{NaNO}_2$  (5.33 g, 76.7 mmol) in water (25 mL) was slowly added to the reaction vessel, followed by slow addition (via syringe) of an aqueous KI solution (12 g, 72 mmol, 13 mL), at all times keeping the temperature of the mixture <5 °C. Gas evolution was observed, and an orange-brown precipitate appeared. The reaction mixture was allowed to reach room temperature and stirred overnight. The mixture was neutralized with solid  $\text{K}_2\text{CO}_3$  (16 g) and extracted with toluene. The toluene layer was separated, dried ( $\text{Na}_2\text{SO}_4$ ), filtered, and evaporated. The residue was dissolved in  $\text{CH}_2\text{Cl}_2$ , poured over a pad of silica (prepared in hexanes), and eluted with hexanes/ $\text{CH}_2\text{Cl}_2$  (2.5:1). The first fraction was rose-colored and this was set aside. Later fractions containing product were brown-colored and were

reconcentrated and put to a second silica pad so that the eluent came through with only the rose color. All the rose-colored fractions were combined and dissolved in warm toluene and concentrated to saturation on a rotary evaporator. The rose-color evaporated away with the solvent and was thereby identified as iodine. This coloration continued to form in the solution until cooling to room temperature, indicating a mild instability of the compound. Upon sitting overnight, large colorless crystals (4.6 g) were obtained. The mother liquor was evaporated and the residue was recrystallized from hexanes/CH<sub>2</sub>Cl<sub>2</sub> (2.5:1), yielding another 8.4 g of colorless crystals. The total recovered product was 13.0 g (65%): mp >270 °C; <sup>1</sup>H NMR (CDCl<sub>3</sub>) δ 2.34 (s, 9H), 7.01 (d, 2H, *J* = 8.8 Hz), 7.07 (d, 6H, *J* = 8.4 Hz), 7.10 (d, 6H, *J* = 8.8 Hz), 7.57 (d, 2H, *J* = 8.8 Hz); <sup>13</sup>C NMR (CDCl<sub>3</sub>) δ 21.18, 63.97, 91.80, 128.54, 131.06, 133.39, 135.72, 136.72, 143.90, 147.55; Anal. Calcd for C<sub>28</sub>H<sub>25</sub>I: C, 68.86; H, 5.16; Found: C, 69.03; H, 5.18.

**1-(4-Iodophenyl)-1,1,1-tris[4-(S-acetylthiomethyl)phenyl]methane (3).** A solution of **2** (7.67 g, 15.7 mmol) in CCl<sub>4</sub> (30 mL) under argon was treated with NBS (8.66 g, 48.6 mmol) and a solution of benzoyl peroxide (38 mg, 0.16 mmol) in CCl<sub>4</sub> (200 μL). The flask was exposed to a 300 MW lamp (held next to the flask) for 30 s. Some bubbling began in the mixture. Then the flask was placed in an oil bath and refluxed for 5 h, upon which bubbling was no longer observed in the mixture. The mixture was filtered and the filter cake was washed with hot toluene. The toluene washing and the filtrate were combined and evaporated. The residue was dissolved in warm CH<sub>2</sub>Cl<sub>2</sub>, eluted through a pad of silica, and the filtrate was concentrated to dryness. <sup>1</sup>H NMR of the residue confirmed the elimination of succinimide from the mixture, but the tribrominated product could not be separated from the side products due to the poor solubility of the residue. The residue was dried under high

vacuum for 5 h, then dissolved in 200 mL of dry THF. A slurry of KSCOCH<sub>3</sub> (5.38 g, 47.1 mmol) in dry THF (30 mL) was added and the mixture was refluxed under argon for 7 h. The solution was cooled to room temperature, poured into toluene, and washed with water. The organic layer was washed with aq. NaHCO<sub>3</sub>, and brine. The organic layer was separated, dried (Na<sub>2</sub>SO<sub>4</sub>) and concentrated to dryness. The residue was redissolved and chromatographed twice (SiO<sub>2</sub>, CH<sub>2</sub>Cl<sub>2</sub>; SiO<sub>2</sub>, CHCl<sub>3</sub>). Fractions containing the pure product were evaporated, yielding a tan powder (3.11 g, 28%): mp = 54–5 °C ; <sup>1</sup>H NMR (CDCl<sub>3</sub>) δ 2.35 (s, 9H), 4.08 (s, 6H), 6.91 (d, 2H, *J* = 8.8 Hz), 7.06 (d, 6H, *J* = 8.4 Hz), 7.14 (d, 6H, *J* = 8.8 Hz), 7.54 (d, 2H, *J* = 8.8 Hz); <sup>13</sup>C NMR (CDCl<sub>3</sub>) δ 30.60, 33.12, 92.08, 128.16, 128.31, 131.29, 133.21, 135.57, 136.88, 145.29, 195.38; FAB-MS obsd 710.0480, calcd 710.0496 (C<sub>34</sub>H<sub>31</sub>IO<sub>3</sub>S<sub>3</sub>).

**2-[2-{4-(1,1,1-Tris[4-(S-acetylthiomethyl)phenyl]methyl)phenyl}ethynyl]-9,10,16,17,23,24-hexaheptylphthalocyanatomagnesium (II) (5).** A flask containing **3** (74 mg, 100 μmol), **4** (119 mg, 100 μmol), Pd<sub>2</sub>dba<sub>3</sub> (14 mg, 15 μmol), AsPh<sub>3</sub> (37 mg, 120 μmol) and a magnetic stirring bar was alternately evacuated and purged with Ar three times successively. A mixture of dry toluene (10 mL) and dry TEA (2 mL) was added and the reaction mixture was stirred overnight at room temperature. The reaction mixture was chromatographed (silica, CHCl<sub>3</sub>/diethyl ether, 9:1). One blue band was collected and concentrated to dryness. The residue was then dissolved in CHCl<sub>3</sub> and chromatographed (SiO<sub>2</sub>, CHCl<sub>3</sub>/acetone, 50:1). From this second column, the second blue band was collected, concentrated, and purified by SEC (5 cm diameter by 100 cm height, THF, 1 drop/6 s) over 12 h. The second blue band was collected and concentrated to dryness. The residue was dissolved in CHCl<sub>3</sub> and chromatographed over a short silica column (CHCl<sub>3</sub>/acetone, 50:1).

The first blue band was collected and filtered through a 0.25  $\mu\text{m}$  teflon membrane, and concentrated to dryness, yielding a blue solid (25 mg, 14%):  $^1\text{H}$  NMR (THF-d<sub>8</sub>)  $\delta$  0.99 (t, 18H,  $J$  = 13.2 Hz), 1.47 (br s, 24H), 1.60 (br s, 12 H), 1.73 (br s, 12 H), 2.06 (br s, 12 H), 2.34 (s, 9H), 3.26 (br s, 12H), 4.15 (s, 6H), 7.23 (d, 6H,  $J$  = 8.8 Hz), 7.25 (d, 6H,  $J$  = 8.43 Hz), 7.36 (d, 2H,  $J$  = 8.07 Hz), 7.80 (d, 2H,  $J$  = 8.07 Hz), 8.25 (d, 1H,  $J$  = 7.7 Hz), 9.23 (m, 6H), 9.42 (d, 1H,  $J$  = 7.7 Hz), 9.59 (s, 1H);  $^{13}\text{C}$  NMR (THF-d<sub>8</sub>)  $\delta$  13.79, 22.94, 29.30, 29.65, 30.40, 32.24, 32.43, 32.67, 34.17, 64.59, 90.54, 90.87, 121.52, 122.69, 123.28, 123.46, 125.95, 128.19, 131.02, 131.22, 131.28, 136.28, 137.84, 138.12, 139.08, 142.45, 142.73, 145.55, 147.49, 151.25, 153.16, 153.36, 154.50, 154.77, 193.55; LD-MS obsd 1730.62, calcd 1730.93 ( $\text{C}_{110}\text{H}_{130}\text{MgN}_8\text{O}_3\text{S}_3$ );  $\lambda_{\text{abs}}$  358, 684, 702 nm.

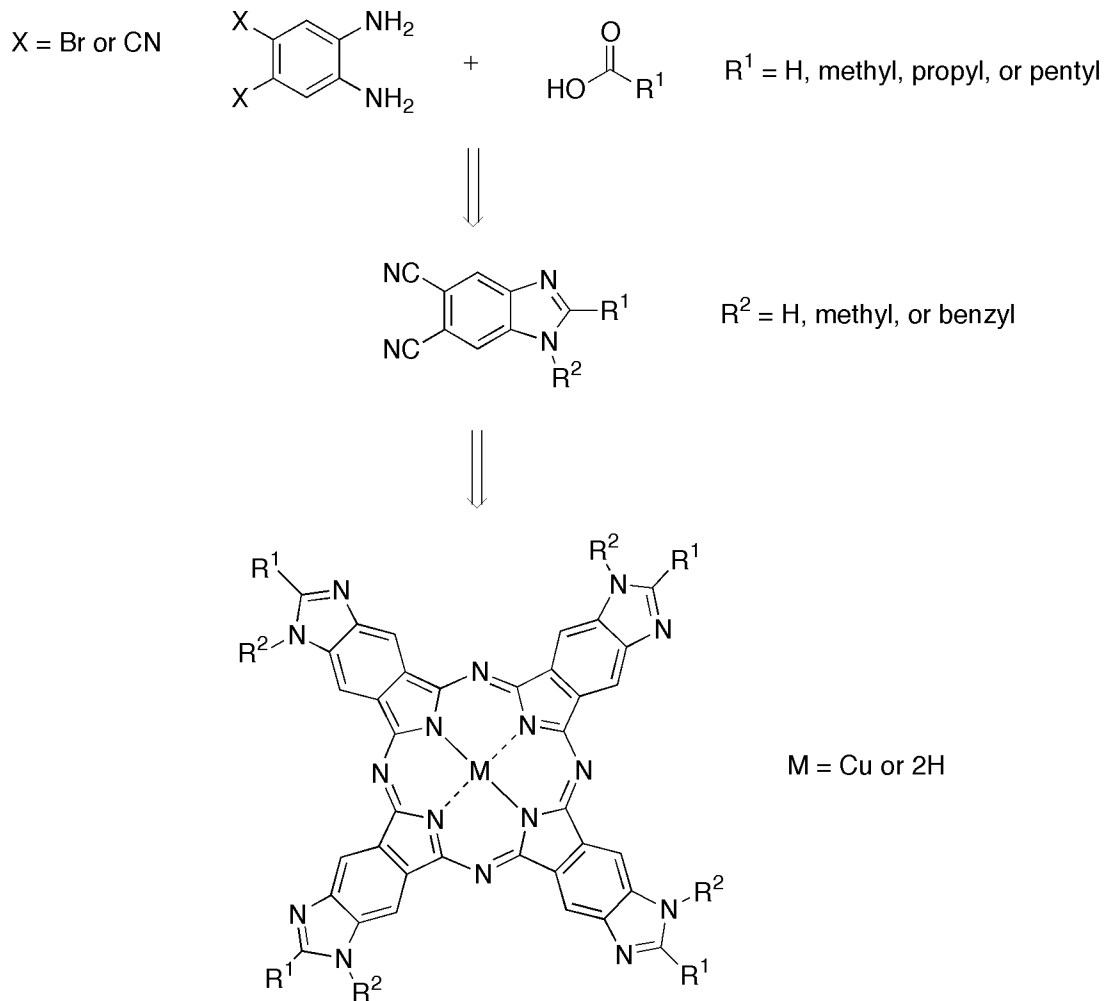
## References:

- (1) (a) Li, J.; Gryko, D.; Dabke, R. B.; Diers, J. R.; Bocian, D. F.; Kuhr, W. G.; Lindsey, J. S. *J. Org. Chem.* **2000**, *65*, 7379–7390; (b) Gryko, D.; Li, J.; Diers, J. R.; Roth, K. M.; Bocian, D. F.; Kuhr, W. G.; Lindsey, J. S. *J. Mater. Chem.* **2001**, *11*, 1162–1180; (c) Gross, T.; Chevalier, F.; Lindsey, J. S. *Inorg. Chem.* **2001**, *40*, 4762–4774; (d) Schweikart, K.-H.; Malinovskii, V. L.; Diers, J. R.; Yasseri, A. A.; Bocian, D. F.; Kuhr, W. G.; Lindsey, J. S. *J. Mater. Chem.* **2002**, *12*, 808–828; (e) Schweikart, K.-H.; Malinovskii, V. L.; Yasseri, A. A.; Li, J.; Lysenko, A. B.; Bocian, D. F.; Lindsey, J. S. *Inorg. Chem.* **2003**, *42*, 7431–7446.
- (2) Hirayama, D.; Takimiya, K.; Aso, Y.; Otsubo, T.; Hasobe, Yamada, H.; Imahori, H.; Fukuzumi, S.; Sakata, Y. *J. Am. Chem. Soc.* **2002**, *124*, 532-533.
- (3) Heim, C.; Affeld, A.; Neiger, M.; Vögtle, F. *Helv. Chim. Acta* **1999**, *82*, 746-759.
- (4) Yang, S. I.; Li, J.; Cho, H. S.; Kim, D.; Bocian, D. F.; Holten, D.; Lindsey, J. S. *J. Mater. Chem.* **2000**, *10*, 283-296.
- (5) Wei, L.; Padmaja, K.; Youngblood, W. J.; Lysenko, A. B.; Lindsey, J. S.; Bocian, D. F. *J. Org. Chem.* **2004**, *69*, 1461–1469.

## Chapter 3

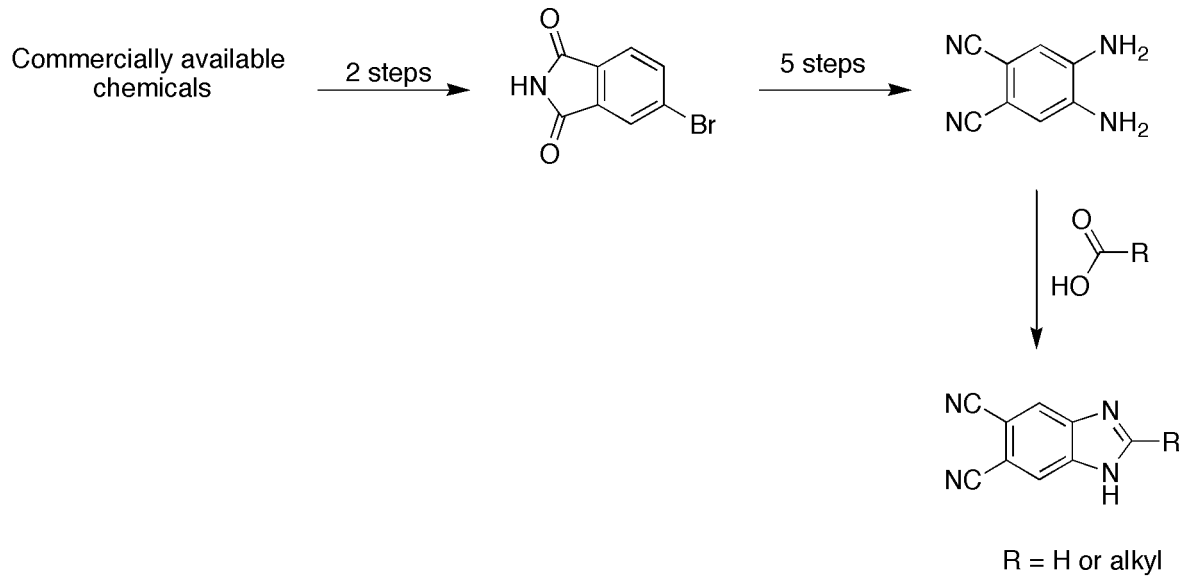
### A. Published research on benzimidazoporphyrazines.

This chapter describes some exploratory work towards the synthesis of benzimidazoporphyrazines (BzImPAs). This work was begun as an emulation of the existing syntheses of BzImPAs. There are two known routes to benzimidazoporphyrazines, and the key building blocks for both are dicyanobenzimidazoles (Scheme 3.1).<sup>1-3</sup>



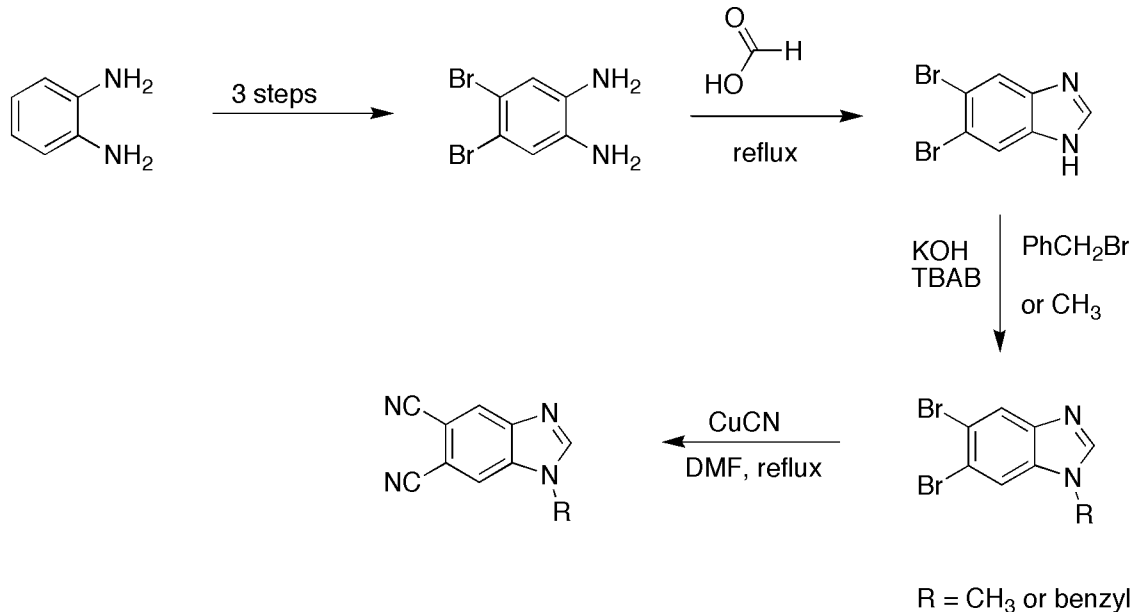
Scheme 3.1 Generalization of published synthetic routes to BzImPAs.

Each route forms a benzimidazole from a reaction between a carboxylic acid of low molecular weight (1 to 6 carbon atoms) and a disubstituted phenylenediamine. The first synthesis of benzimidazoporphyrazines, by Kudrik and coworkers,<sup>1</sup> arrived at dicyanobenzimidazoles from dicyanophenylenediamine (Scheme 3.2). The synthesis of this precursor requires a large number of steps and results in a low overall yield (~7%).<sup>2</sup> The advantage of this route is that there are no additional steps between the benzimidazole cyclization and the macrocyclization of the resulting benzimidazoporphyrazines, or “benzimidazoloporphyrazines”, as they were called in these reports.<sup>1</sup> It is surprising that the protic benzimidazoles were reported to react in the macrocyclization process, as the benzimidazole proton should be acidic enough to quench the lithium pentoxide base used in the macrocyclization. Alkylation of the protic nitrogen is necessary to render the pigments less polar. Combining this additional step with the existing steps adds to an eight-step synthesis.



Scheme 3.2. Synthesis of dicyanobenzimidazoles from references 1-2.

The second route for benzimidazoporphyrazines was reported by Pardo and coworkers.<sup>3</sup> This route used dibromophenylenediamine, which is reportedly available in good overall yield (55-81%) in only three steps from phenylenediamine (Scheme 3.3).<sup>3,4</sup> This route is only six steps including the alkylation of the secondary nitrogen.



Scheme 3.3. Synthesis of dicyanobenzimidazoles from reference 3.

### B. Synthesis of 2-aryl-5,6-disubstituted-benzimidazoles.

The target compound for synthesis of new BzImPAs was a dicyanobenzimidazole bearing a protected phenylethyne group at the 2-position (Figure 3.1).

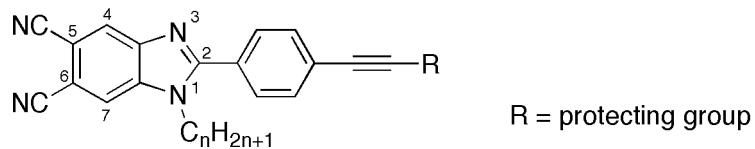
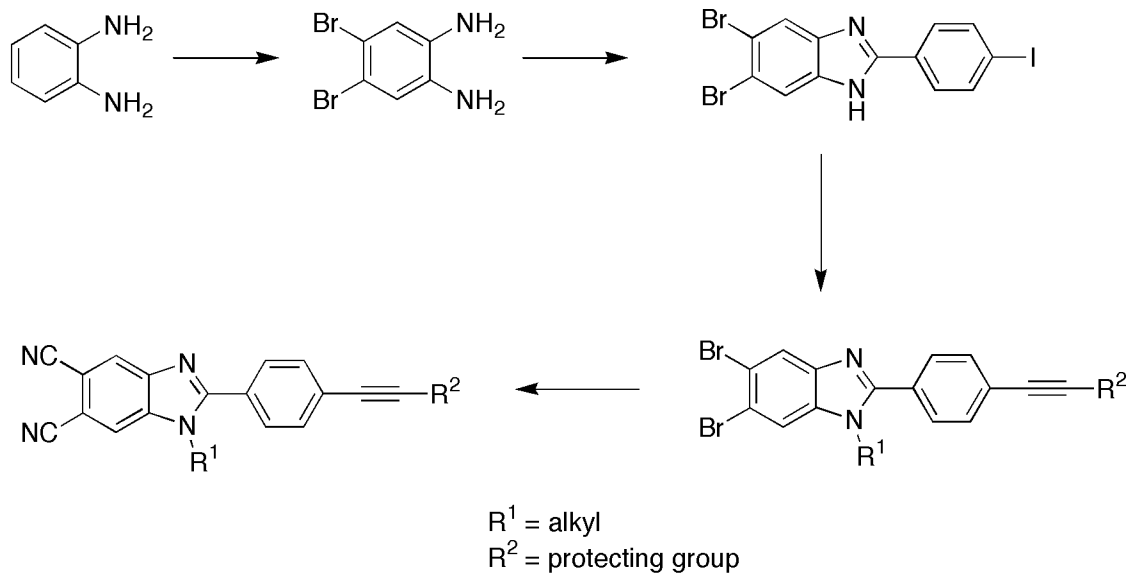


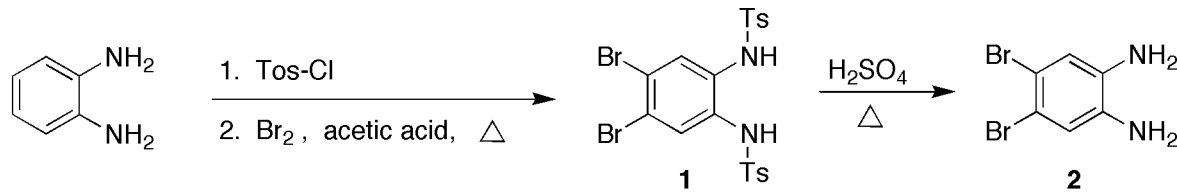
Figure 3.1.

The synthetic route chosen for this building block was adapted from the report of Pardo and coworkers, because their route was the shorter of the two published routes (Scheme 3.4).



Scheme 3.4. Proposed sequence of transformations for synthesis of an ethynylphenyl-dicyanobenzimidazole.

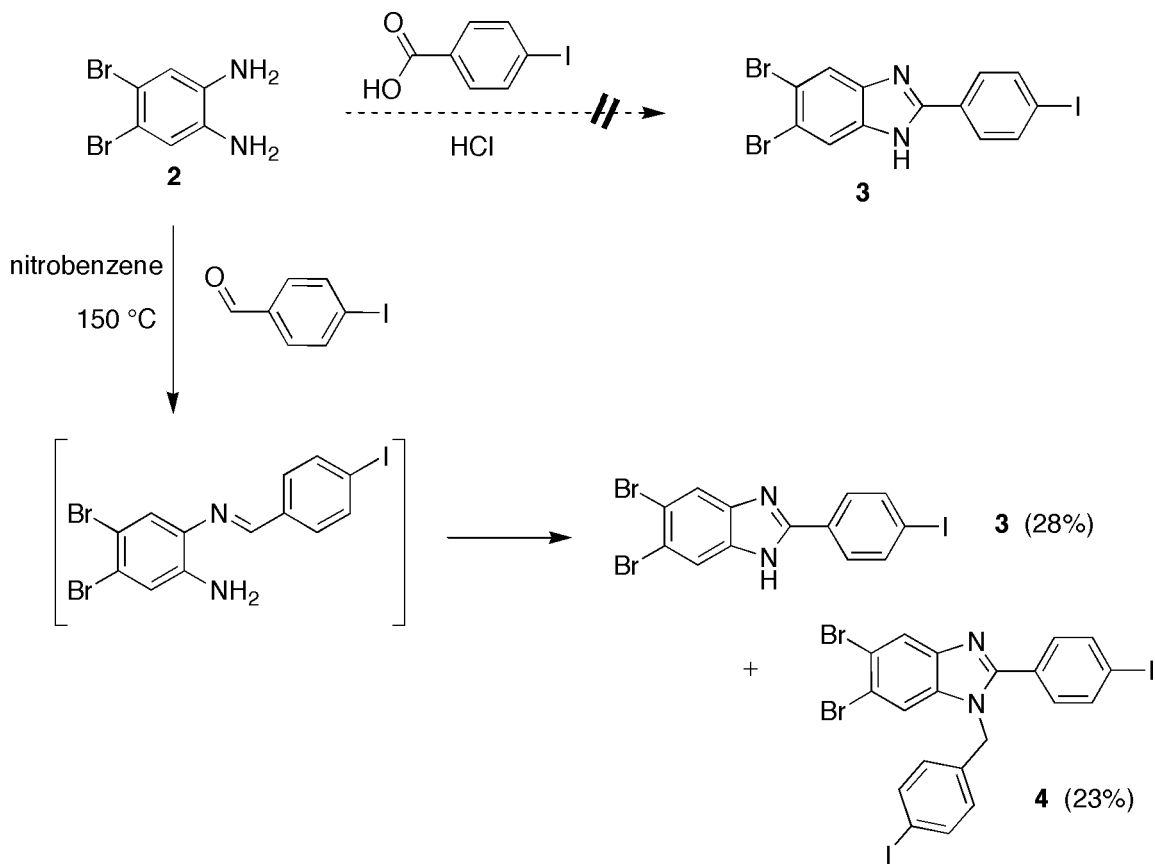
This route began with the preparation of 4,5-dibromophenylenediamine **2** from *o*-phenylenediamine. This three-step preparation proceeded smoothly according to literature conditions, and gave yields consistent with previous reports (Scheme 3.5).<sup>4</sup>



Scheme 3.5.

The cyclization of compound **2** with a substituted benzoic acid, to form a 2-aryl-5,6-dibromobenzimidazole (Scheme 3.6), could not easily be adapted from the previous reports of dicyanobenzimidazole syntheses. The previous syntheses had each employed an aliphatic carboxylic acid of low molecular weight, which served as the reagent, solvent, and acid catalyst for the cyclization reaction. When crystals of compound **2** were mixed with crystals of *p*-iodobenzoic acid and the mixture was ground together and heated in the absence of any added solvent or acid, the mixture appeared to be inert at first, but then suddenly decomposed, and the evolution of a purple vapor (possibly Br<sub>2</sub>) was observed. No soluble species could be extracted from the resulting black residue. A similar trial employing a small amount of concentrated HCl as an intended catalyst resulted in the same purple vapor and black residue.

There are precedents for benzimidazole cyclization from *o*-phenylenediamine and benzoic acids, using hygroscopic acids at high temperatures as catalytic solvent media.<sup>5</sup> Examples of such acids include concentrated HCl, polyphosphoric acid, HBO<sub>3</sub>, and Ti(OBu)<sub>4</sub>. Because these conditions are rather severe, and compound **2** had already demonstrated some instability in the initial cyclization attempts, a milder procedure was sought via an oxidative cyclization using *p*-iodobenzaldehyde (Scheme 3.6).



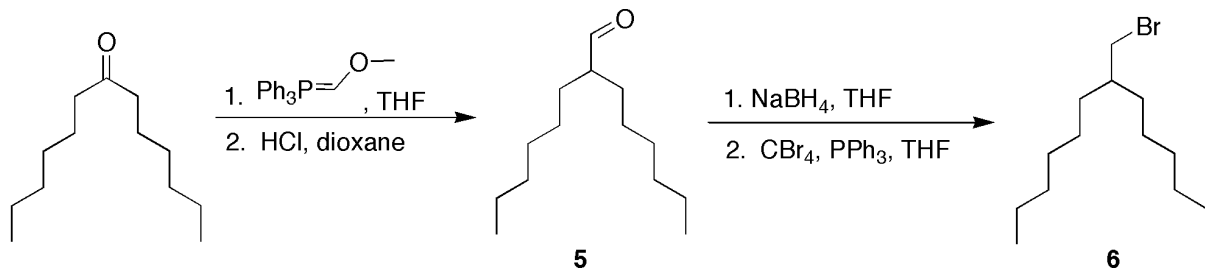
Scheme 3.6.

The first reports of the oxidative cyclization of benzimidazoles from aldehydes and phenylenediamine were published in the 1930's by Weidenhagen and coworkers.<sup>6</sup> These conditions used copper acetate and other Cu(II) salts as oxidants. Since that time, other metal salts have been used,<sup>7</sup> and some recent reports cite the use of hot nitrobenzene as a suitable oxidant for this reaction.<sup>8</sup> The reaction of compound **2** with *p*-iodobenzaldehyde was performed using hot nitrobenzene as the solvent/oxidant (Scheme 3.6), producing the desired 2-aryl-5,6-dibromobenzimidazole **3**, along with the 1,2-disubstituted benzimidazole byproduct **4**. The poor solubility of both products made their separation difficult. Although the byproduct could be isolated in pure form, the desired product **3** could only be purified to

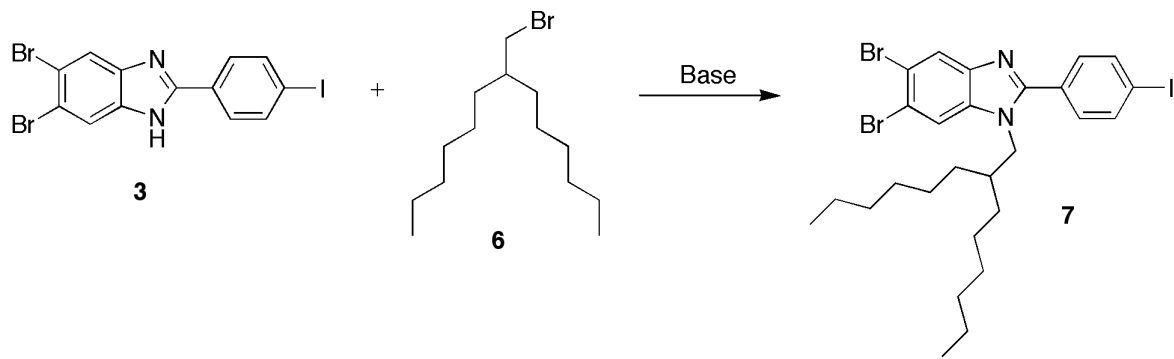
~90% purity, with the 10% impurity comprised of the byproduct and the diamine starting material. Byproducts of the type observed in this reaction were not reported for those reactions using metal salts as oxidants, but were reported for some reactions using hot nitrobenzene, and also for the heating of phenylenediamine with benzaldehyde in the absence of an added oxidant.<sup>9</sup> This reaction was not further optimized.

### C. Alkylation of benzimidazoles.

To improve the solubility of compound **3**, as well as the ultimate target phthalocyanines, we chose to install a 2-hexyloctyl chain at the benzimidazole 1-position, because such “swallowtail” alkyl groups have been shown to improve solubility for perylene dyes.<sup>10</sup> The alkyl bromide **6** is known in the literature and was prepared in four steps in good yield according to the previous report (Scheme 3.7).<sup>11</sup>



Scheme 3.7.



Entry	3 (eq)	6 (eq) <sup>a</sup>	Base (eq) <sup>a</sup>	Solvent	Temp. (°C)	Time (h)	Yield (%)
1	1	1	KOH (2)	-- <sup>b</sup>	25 <sup>d</sup>	2 h	0
2	1	1	KOH (2)	pyridine <sup>b</sup>	25 <sup>d</sup>	14	29
3	1	2 <sup>e</sup>	KOH (4)	pyridine	80	4	40
4	1	1.1	KOtBu (1)	pyridine	115	24	14
5	1	1	DBU (1)	acetone	56	4	0
6	1	2	KOH (10)	acetone <sup>b</sup>	56	12	14
7	1	0 <sup>c</sup>	NaH	DMF	25	0 <sup>b</sup>	0 <sup>c</sup>
8	1	1	--	DMF	100	2.5	0
9	1	1	DBU (1)	DMF	100	19	32
10	1	3 <sup>e</sup>	DBU (3) <sup>e</sup>	DMF	155	36	38
11	1	2 <sup>e,g</sup>	DBU (2) <sup>e,f</sup>	DMF	155	2	66

- a) Reagent quantities are expressed in molar equivalents, relative to the benzimidazole 3;
- b) TBAI (0.02 equiv.) was added to the reaction;
- c) The reaction mixture decomposed rapidly prior to addition of 6;
- d) Prolonged sonication was used, making the temperature an uncertain parameter;
- e) Quantity was added in portions during the reaction;
- f) Base was added 2-5 min before alkyl halide.

Scheme 3.8.

Various reaction conditions were explored to alkylate the benzimidazole in reasonable yield (Scheme 3.8). Pardo and coworkers followed an alkylation protocol using sonication of the ground mixture of their benzimidazole, alkyl halide, KOH, and a phase

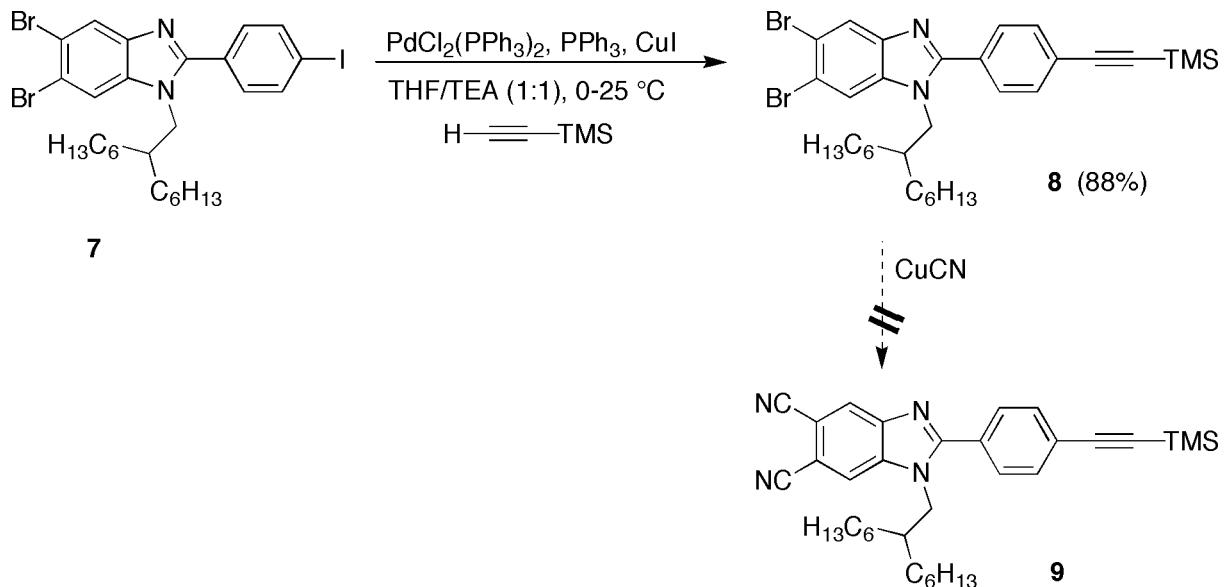
transfer catalyst.<sup>12</sup> For the reaction with compound **3** (entry 1), tetrabutylammonium iodide was chosen as the phase transfer catalyst, in the hope that the iodide ions might catalyze the substitution via the Finkelstein reaction. This procedure was ineffective until a small quantity of pyridine was added to the mixture, resulting in some product formation (entry 2, 29%). A second trial used enough pyridine to dissolve the benzimidazole (~1 M) and gave an increased yield (40%, entry 3). The reaction was still heterogeneous due to the choice of the inorganic base. Further experiments were predicated on the assumption that a completely homogeneous reaction would give the best result.

The homogeneity of the reaction was improved by changing the base to potassium *t*-butoxide, but this resulted in a lower yield. Heating was substituted for sonication, without improvement. The reaction using DBU in acetone was homogeneous, but gave no product. The alkylation reaction in DMF was homogeneous, and the access to higher temperature gave improved yields compared to the use of acetone. The use of successive rounds of addition of DBU and alkyl bromide during the reaction was effective, and the best yield (66%) was obtained when DBU was added a few minutes before the alkyl bromide in each round of reagent addition (entry 11). The use of excess DBU at the beginning of the reaction was ineffective at raising the yield (no entry).

#### **D. Palladium coupling and Rosenmund-von Braun cyanation reactions.**

The iodophenylbenzimidazole **7** could now be transformed to a protected ethynylphenylbenzimidazole (Scheme 3.9). This coupling step had to precede the final cyanation reaction at the 5 and 6 positions, because the iodoaryl group was also susceptible to cyanation. In coupling reactions mediated by palladium (0) reagents, iodoaryl compounds

have been shown to be more reactive than corresponding bromoaryl compounds.<sup>13</sup> To achieve selectivity in compounds bearing both types of functionality, the temperature of the reaction must be kept low (0-25 °C), whereas a reaction without regard to such selectivity would typically run at elevated temperature, sometimes even with refluxing of the solvent.

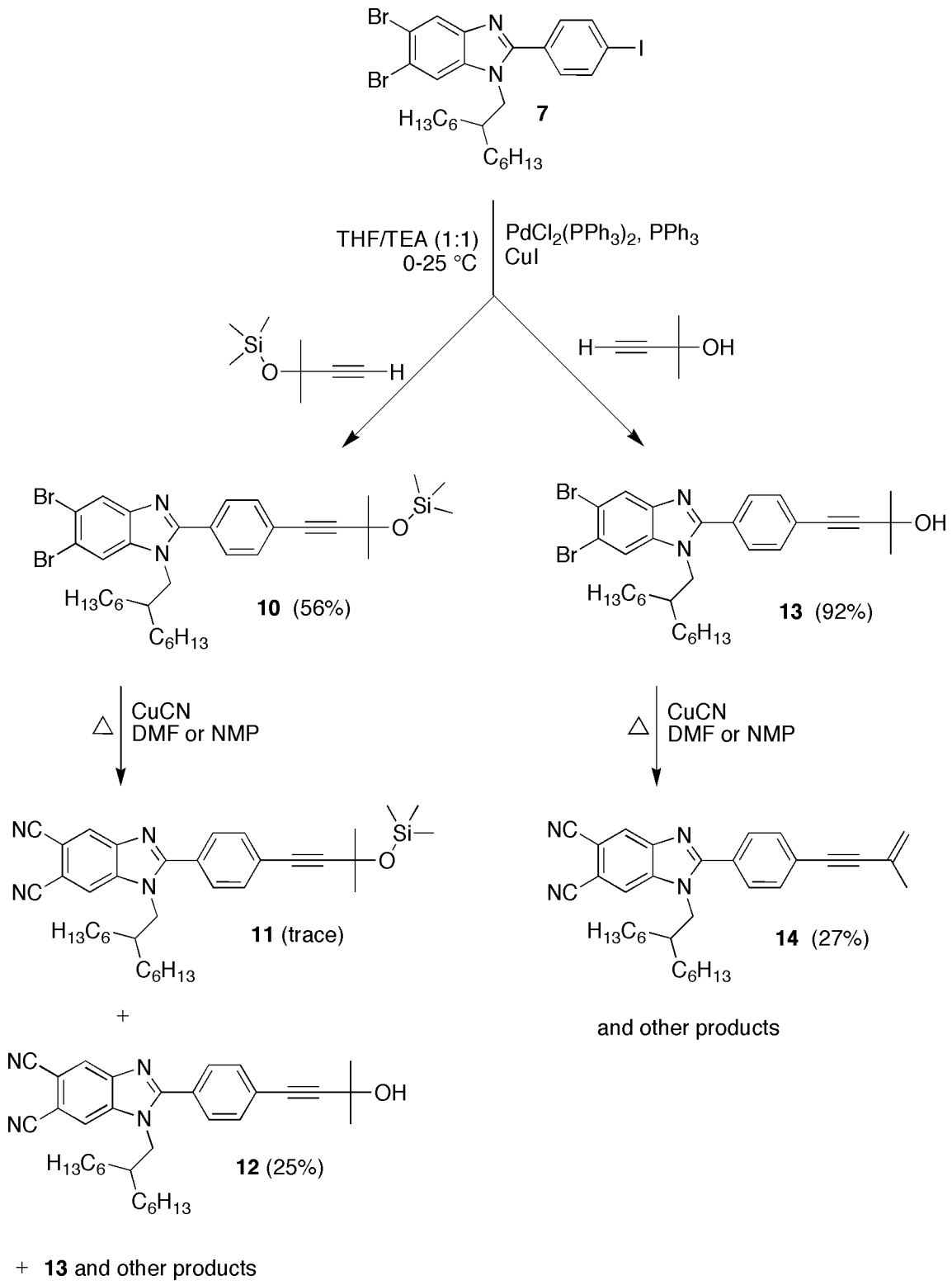


Scheme 3.9.

The cross-coupling reaction was adopted from a previous report of selective palladium coupling,<sup>13c</sup> and used trimethylsilylacetylene to replace the iodoaryl group. The product **8** was identified by <sup>1</sup>H NMR spectroscopy and carried forward to the cyanation step (Scheme 3.8) to complete the synthesis of this key building block. Unfortunately, the cyanation (Rosenmund-Von Braun reaction) produced a mixture of several (>10) products. The expected behavior of the reaction would result in only four species: starting material, product **9**, and two monocyanated intermediates. One interpretation of the complex product mixture is that the trimethylsilyl (TMS) group may have been displaced by nucleophilic

attack of the cyanide anion, and the resulting deprotected ethynyl byproduct could prove susceptible to Glaser coupling: given that the reaction is conducted under air with excess Cu(I), there is a potential for the presence of Cu(II) in the reaction, which, together with Cu(I), can mediate a coupling reaction between two deprotected ethyne groups.

A particular distinction was observed in TLC analyses of the products of this first cyanation reaction, in comparison to the benzimidazoles **3** and **7**. The products of the cyanation reaction gave a blue fluorescence (at varying intensities) when illuminated with short-wave or long-wave UV light, whereas the ethynylbenzimidazole **8** exhibited visible blue fluorescence only under long-wave UV light, and the iodoaryl precursor **7** did not present visible fluorescence under any illumination. The blue fluorescence was likely due to the electronic transitions of the substituted benzimidazole's  $\pi$ -orbital system. The synthesis progression from **7** to **8** and then to the cyanation reaction served to remove the halogens, which can have a quenching effect (via spin-orbit coupling) on molecular fluorescence. This quenching behavior is called the "heavy atom effect". The correlation between substitution at the halogen positions with the intensity of the blue fluorescence would become a useful tool in identifying the dicyanated compounds from complex reaction mixtures in the ensuing attempts at completing this synthetic route.



Scheme 3.10.

The next approach was the use of [(1,1-dimethylprop-2-ynyl)oxy]trimethylsilane in place of the trimethylsilylacetylene (Scheme 3.10). Whereas the TMS group is easily deprotected by mildly basic conditions, the silyloxy bond of the [(trimethylsilyl)oxy]isopropyl group is reputed to impart greater stability, making it removable only by treatment with fluoride. The palladium coupling of compound **7** with the protected acetylene proceeded in moderate yield after overnight reaction (56%), and a substantial quantity of **7** was recovered from the purification (42%).

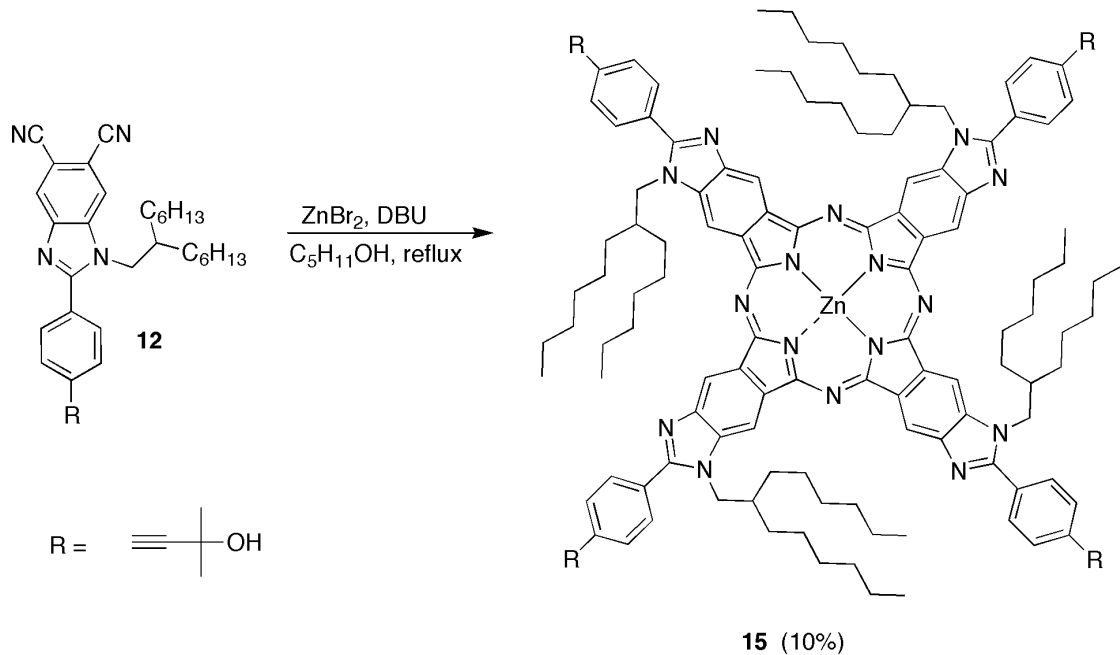
The cyanation of the protected ethynylbenzimidazole **10** (Scheme 3.10) gave a complex mixture of products. In addition to the expected cyanation products, the reaction had given byproducts that had lost the TMS group, and now bore either the remaining hydroxyisopropyl protecting group at the ethyne, or its dehydrated isopropene derivative. This assessment was supported by synthesizing the benzimidazole **13** and comparing it with the cyanation reaction mixture by TLC analysis: the reaction mixture had a species that matched precisely to **13**. From this complex mixture, the two species that exhibited the strongest blue fluorescence were isolated and identified as the expected product **11** and the partially deprotected product **12**. This reaction was repeated in both DMF and NMP at varying temperatures. The reaction always produced a mixture of deprotected/decomposed cyanated byproducts. No acceptable conditions were found.

Since the hydroxyisopropyl group had survived the cyanation reaction, the benzimidazole **13** was considered a reasonable candidate for a cyanation reaction that might give a less complex product mixture. Unfortunately, the cyanation of **13** (Scheme 3.10) also gave a complex product mixture. The major product of the reaction was isolated and identified as dicyanobenzimidazole **14** wherein the hydroxyisopropyl group was dehydrated,

resulting in an irremovable isopropylene cap at the ethyne group. The harsh conditions of the Rosenmund-Von Braun reaction appeared to be a roadblock in the overall route toward dicyanobenzimidazoles bearing any useful ethynylphenyl group.

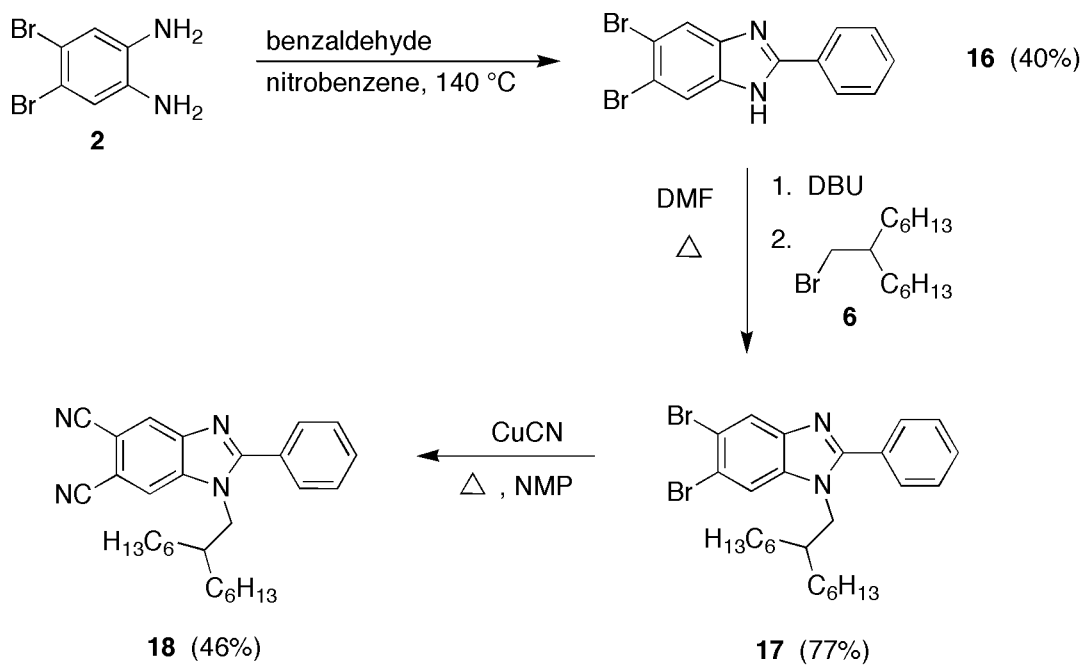
### E. Synthesis of Benzimidazoporphyrazines: model reactions.

Before the synthesis methodology would be pursued further, the utility of dicyanobenzimidazoles as precursors to benzimidazoporphyrazines had to be established. A sample of the benzimidazole **12** was converted to the corresponding zinc benzimidazoporphyrazine by heating in pentanol, using DBU as a base and ZnBr<sub>2</sub> as a templating agent (Scheme 3.11). The desired pigment was obtained in a 10% yield, which is low compared to typical yields for synthesis of zinc phthalocyanines.<sup>14</sup> The quantity (3.2 mg) was quite small, and not helpful in carrying out a thorough characterization of the product.



Scheme 3.11.

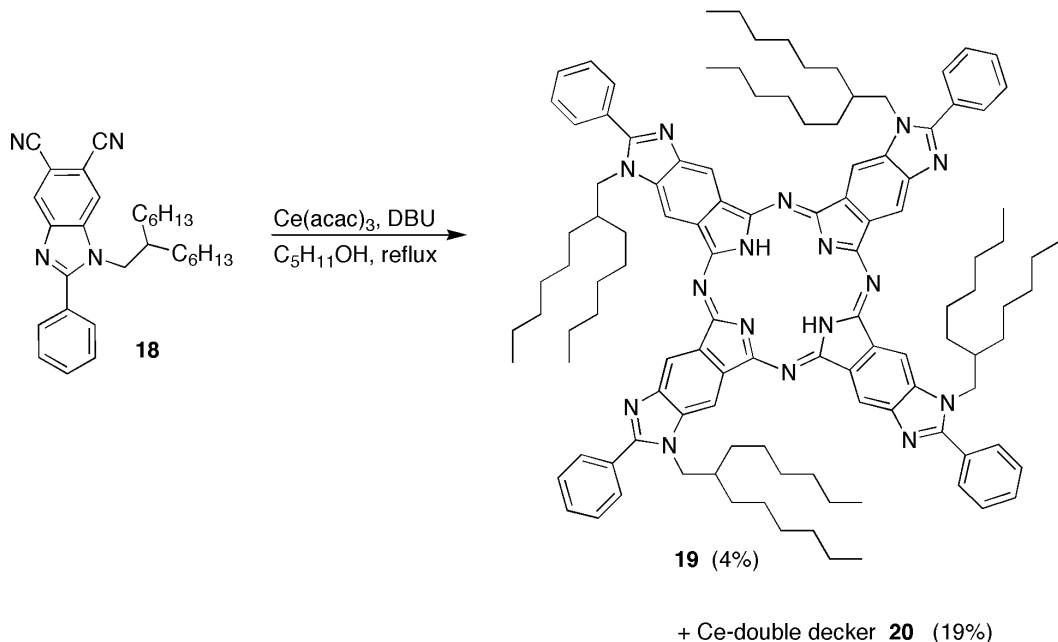
More dicyanobenzimidazole material was needed to prepare a larger sample of benzimidazoporphyrazine. Since the ethynyl group was not needed, a 2-phenyldicyanobenzimidazole **18** was pursued instead. This compound was prepared using the same methodology that had been used for the earlier benzimidazole syntheses (Scheme 3.12) in a 14% overall yield from dibromophenylenediamine **2**. The cyanation reaction gave no surprises, showing only 4 spots upon TLC analysis (starting material, two intermediates, and product).



Scheme 3.12.

The dicyanobenzimidazole **18** was used to prepare a free base benzimidazoporphyrazine. Macrocyclization reactions often give better yields when templates are employed, and the use of cerium(III) acetylacetone has been reported to improve the yield of free base phthalocyanines by a templating effect.<sup>15</sup> Unfortunately, the

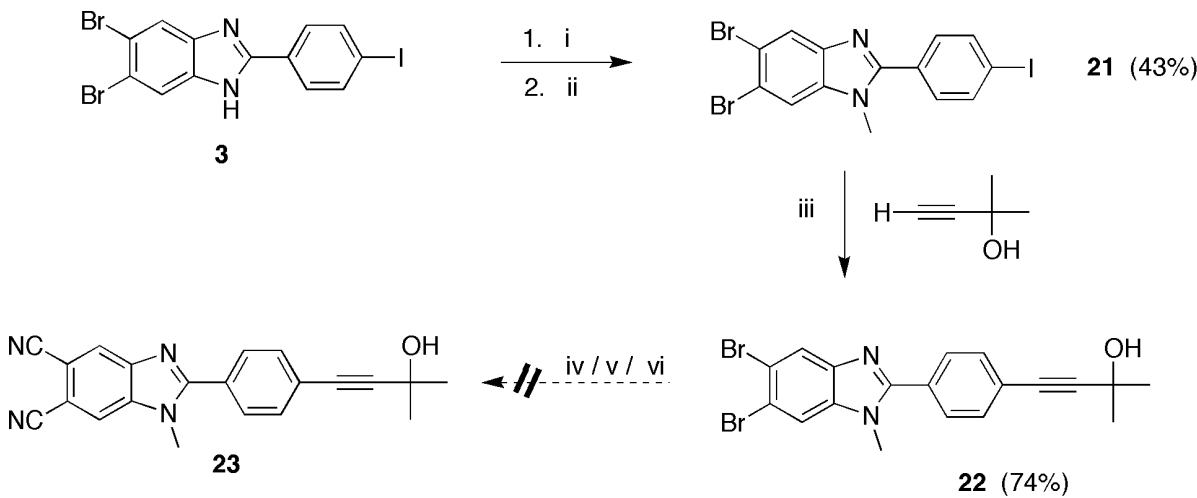
macrocyclization using cerium(III) acetylacetone with **18** resulted in the formation of only a small quantity of free base benzimidazoporphyrazine, and a greater quantity of a sandwich compound that held two molecules of the target benzimidazoporphyrazine complexed to a cerium atom (Scheme 3.13). It may be argued that the overall macrocyclization yield was improved by using the cerium template, but the recovered yield of the desired free base macrocycle was still quite low (7 mg, 4%). Some analyses were performed for the free base and zinc benzimidazoporphyrazines: UV-Vis absorbance and fluorescence spectra, and fluorescence quantum yields (relative to known phthalocyanine standards). The data supported the identification of benzimidazoporphyrazines as a class of phthalocyanines, and thus provided the impetus for continued efforts toward the efficient synthesis of this new class of pigments (see Chapter 4 for a detailed study of photochemical behavior of BzImPAs).



Scheme 3.13.

## F. Alternative cyanation strategies.

The aforementioned macrocyclization experiments demonstrated that 2-aryl-dicyanobenzimidazoles are viable precursors to phthalocyanines. But a reliable conversion of the dibromobenzimidazoles to dicyanobenzimidazoles was still needed. Additionally, around this time, the wisdom of putting the 2-hexyloctyl chains on the benzimidazoles was reconsidered. Because the benzimidazoporphyrazines are intended for incorporation into materials, the side chains should be considered with respect to their influence on the closest packing of molecules in a polymeric phthalocyanine material. The proper alkyl groups should be able to either lie in the plane of the macrocycle, or project above and below the plane of the macrocycle in a symmetrical manner. Efforts toward the latter strategy were put off until the cyanation strategy could be resolved. Therefore, a methyl group was chosen for continued studies of cyanation procedures (Scheme 3.14).



- i. DBU, NMP, 25 °C;
- ii. CH<sub>3</sub>I;
- iii. PdCl<sub>2</sub>(PPh<sub>3</sub>)<sub>2</sub>, PPh<sub>3</sub>, CuI, TEA/THF, 25 °C;
- iv. CuCN, NMP, 115-170 °C;
- v. CuI (10 mol%), NaCN (4 equiv.), NMP, 190 °C;
- vi. CuI (20 mol%), N,N'-dimethylethylenediamine (2 equiv.), KI (40 mol%), NaCN (2.2 equiv.), toluene, reflux.

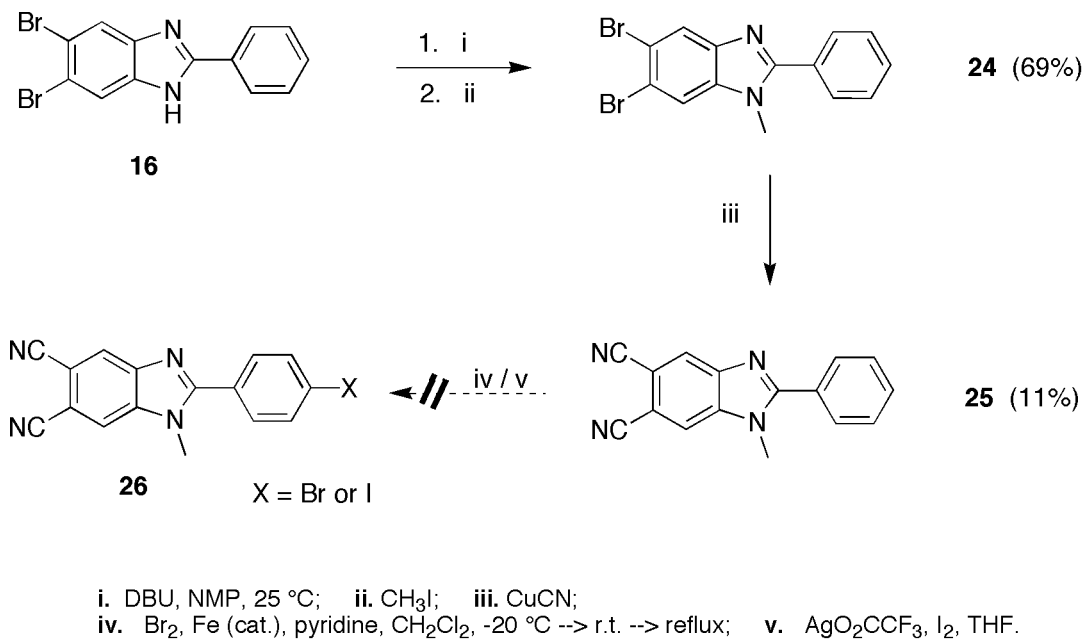
Scheme 3.14.

The Rosenmund Von-Braun reaction was reattempted with dibromobenzimidazole **22** (Schemes 3.14), in the hope that the minimum temperature necessary for cyanation would be lower than the temperature at which dehydration of the protecting group would occur. No significant reaction progress was observed below 170 °C. After 3 h at 170 °C, much of the starting material had been converted to a new compound, which was isolated and identified as the dehydrated derivative of the desired benzimidazole **23**.

To find out whether the copper catalyst was at all responsible for the dehydration of the hydroxyisopropyl group, a reaction was attempted using sodium cyanocuprate ion as the cyanating agent (Scheme 3.14). Although the sodium cyanocuprate ion is described in the literature as less reactive than copper cyanide,<sup>16</sup> it was hoped that the sacrifice for a slower rate or lower yield might be rewarded with an intact protecting group on the product. No significant reaction progress was observed below 190 °C. After 3 h at 190 °C, the organic material of the reaction appeared to have decomposed entirely.

The final attempt at cyanation of an ethynylphenyl-dibromobenzimidazole was taken from a report by Buchwald and coworkers.<sup>17</sup> This two-step, one-pot procedure combines a Finkelstein reaction (at an sp<sup>2</sup> hybridized carbon atom) with the desired cyanation. This method is extremely oxygen-sensitive. All of the reactions in the published report were conducted in Schlenkware, using substrate quantities in the range of 2-30 mmol, whereas the benzimidazole cyanation experiments used substrate typically in the range of 0.1-0.2 mmol. The attempt at cyanating **22** with these conditions failed due to exposure of the reaction to oxygen, as evidenced by the blue Cu(II) residue found in the vessel. Although this procedure could possibly be developed for the cyanation of dibromobenzimidazoles, it did not seem sufficiently robust for routine use at the microscale.

Since no successful cyanation procedure had been found, a new strategy was needed. The halogenation of a phenyl-substituted dicyanobenzimidazole was attempted twice (Scheme 3.15), first with bromine, and later with a hypoiodite reagent generated *in situ*. This strategy was based on an assumption that the imidazole ring would operate as an electron-releasing substituent on the phenyl ring. This strategy is precedented in the literature, in the successful para-directed nitration of 2-phenyl-4,5-dibromoimidazole, and 2-phenyl-4-carboxyimidazole.<sup>18</sup> Even 2-phenyl-4,5-dicarboxyimidazole was reported to nitrate, albeit at the meta-position. Unfortunately, the halogenation conditions attempted for the 2-phenyl-4,5-dicyanobenzimidazole **25** were not aggressive enough, as no reaction was observed for either of the halogenation attempts.



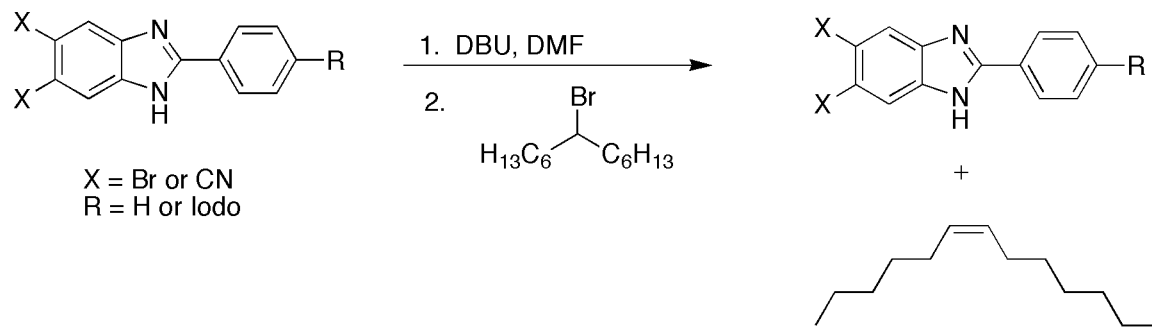
Scheme 3.15.

At this point of the research, the pursuit of benzimidazoporphyrazines through the dibromobenzimidazole intermediates was concluded. The work had provided access to a

variety of dibromobenzimidazoles, but the desired ethynyl-substituted dicyanobenzimidazole could not be prepared in reasonable yield or adequate quantity.

#### G. Pursuit of secondary swallowtail alkyl-groups.

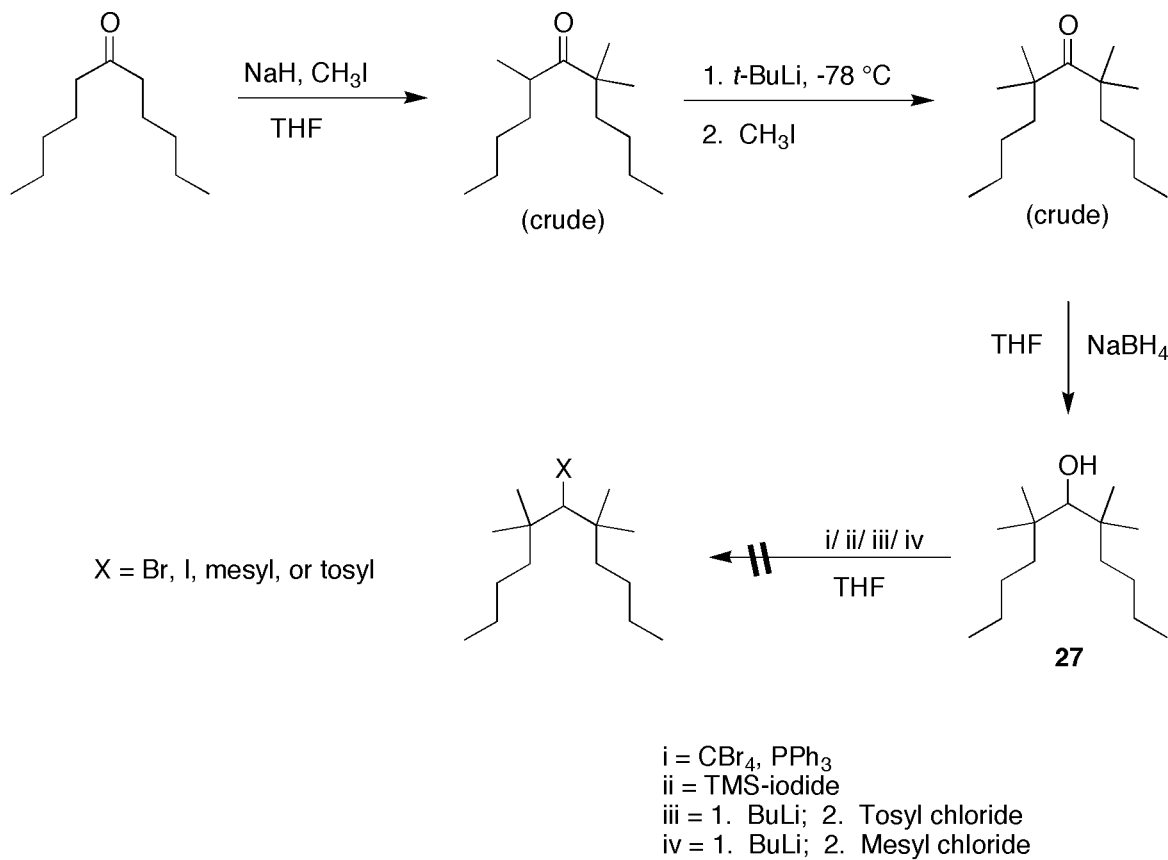
The alkylated benzimidazoles bearing methyl groups (**21**, **22**, **24**, **25**) were generally less soluble and more polar (with respect to adsorption media) than the corresponding benzimidazoles bearing the swallowtail groups (**7**, **8**, **10-14**). The swallowtail groups so far employed were attached by a primary carbon and were anticipated to hinder to close packing of molecules in any polymeric material composed of benzimidazoporphyrazines. Swallowtail groups that could be attached via a secondary carbon might provide steric bulk against aggregation by projecting above and below the plane of the resulting benzimidazoporphyrazine macrocycles. Such an arrangement might also allow for more orderly close packing of the pigment molecules.



Scheme 3.16.

Unfortunately, the attempt to alkylate various benzimidazoles with 7-bromotridecane was unsuccessful (Scheme 3.16). A phase separation was observed in each reaction, resulting in the appearance of a colorless oil that was immiscible with the solvent (whereas 7-

bromotridecane was fully miscible). Analysis of one of the reaction mixtures by GC-MS indicated that the reaction was producing a tridecene product (presumably 6-tridecene). No alkylated benzimidazole was evident by TLC analysis of the reaction mixture. It seemed that the benzimidazole anion was of too strong basicity, and was therefore directing the reaction toward elimination reaction rather than nucleophilic substitution. Even the use of dicyanobenzimidazoles (available via chemistry discussed in Chapter 4 that was ongoing at the time of this alkylation study) resulted in the formation of the tridecene product, without any detectable alkylation. In hindsight, it is possible that the Mitsunobu reaction could have effected this desired alkylation.



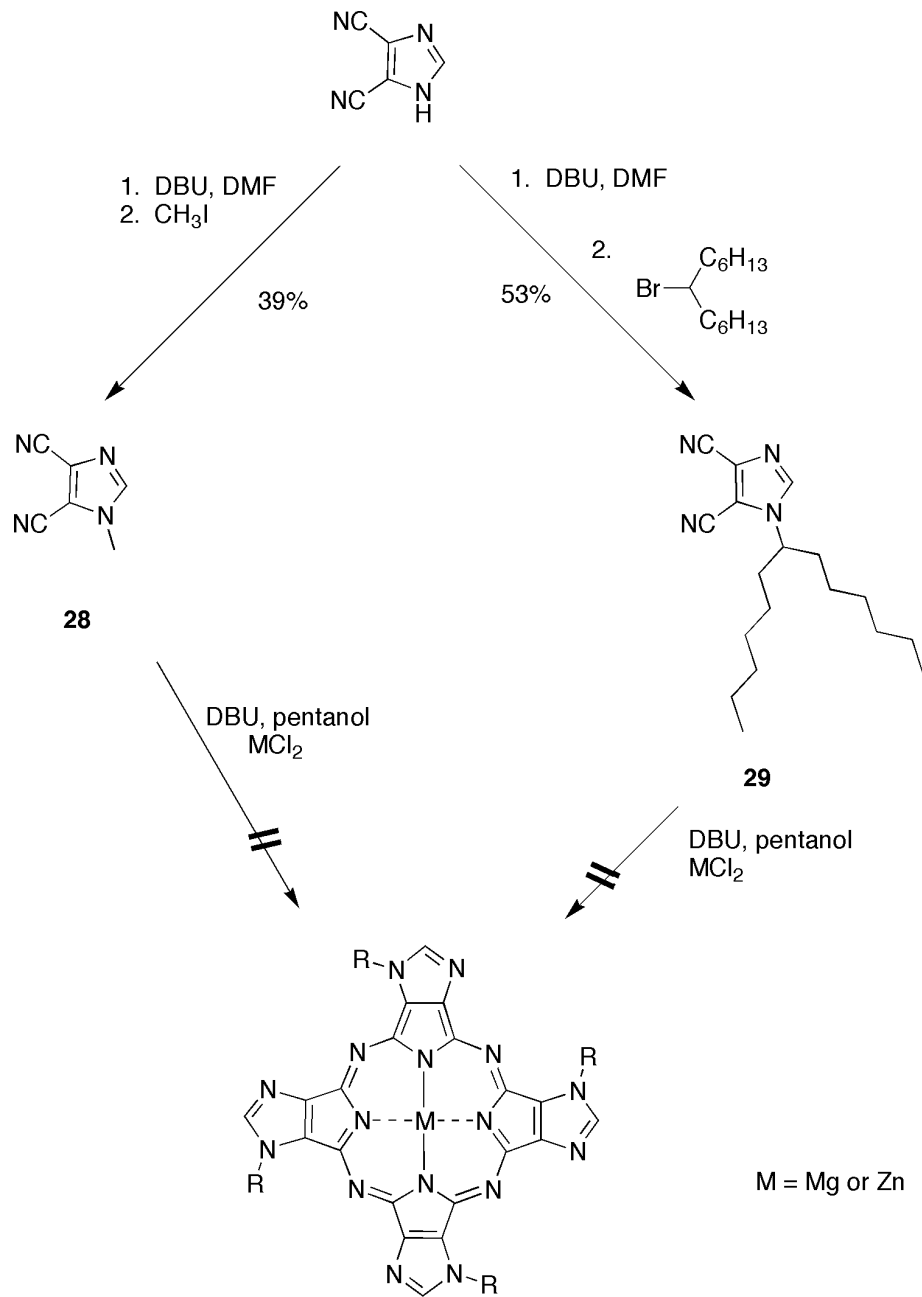
Scheme 3.17.

To prepare an alkylating group that could not undergo elimination, dihexyl ketone was transformed to its tetramethylated alcohol derivative **27**. There are a few reports in the literature that describe tetramethylated ketones, usually as compounds of interest to NMR-related phenomena.<sup>19</sup> The product mixture of the initial methylation reaction was resubmitted to stronger methylation conditions to drive the intermediates toward the tetramethylketone, but the intermediates were not fully consumed by the reaction and could not be separated, so the residue was reduced to alcohol **27**, which was purified by chromatography ( $\text{SiO}_2$ , hexanes with 1% ethyl acetate). The tetramethylketone intermediate was distinguished by its singlet resonance in the  $^1\text{H}$  NMR spectrum, for its equivalent methyl groups, whereas the spectrum of alcohol **27** exhibited two singlets for the methyl groups, as a result of the prochirality induced by the reduction of the carbonyl position. Unfortunately, **27** could not be transformed into a stable alkylating agent. The alcohol was inactive to  $\text{CBr}_4/\text{PPh}_3$ , and decomposed during the attempts to iodinate or sulfonate the compound. If any successful transformation of the alcohol to a good leaving group (such as a halide or sulfonyl group) had occurred, it may be that the product was unstable. The secondary carbocation left behind by loss of the leaving group would be readily transformed by methyl shift from one of the  $\alpha$ -methyl groups.

## H. Imidazoporphyrazines.

Dicyanoimidazole is commercially available. The alkylation conditions developed for the benzimidazoles described above were useful in alkylating dicyanoimidazole. Dicyanoimidazole was susceptible to alkylation with 7-bromotridecane (Scheme 3.18), which was a surprising result, given that imidazoles are typically more basic than

benzimidazoles.<sup>20</sup> The effectiveness of the cyano groups in dicyanoimidazole for withdrawing the electron density of the imidazole anion is sufficient to weaken the basicity of the compound and render it an effective nucleophile. A dicyanobenzimidazole was tried in this reaction (Scheme 3.16), but the cyano groups must be too far removed from the imidazole ring to have a sufficient electron-withdrawing effect. Unfortunately, alkylated dicyanoimidazoles were unreactive in macrocyclization reactions (Scheme 3.18). Sometime after these attempts, I learned of unsuccessful attempts at this reaction that were carried out by another research group but were never published.<sup>21</sup>



Scheme 3.18.

### I. Conclusions.

The general synthetic route to dicyano-ethynylbenzimidazoles through dibromobenzimidazole intermediates (Scheme 3.4) was unsuccessful. The harsh conditions

of the cyanation reaction were prohibitive to the use of protected ethynyl groups. The lesson to be learned from these efforts is that the aspects of the synthesis that require severe reaction conditions must be carried out as early in the synthetic route as possible. A new route for 2-substituted dicyanobenzimidazoles would follow the example of Kudrik and coworkers,<sup>1</sup> but a new preparation of dicyanophenylenediamine would be needed to minimize the labor of the synthetic route. Also, swallowtail alkyl groups would have to be abandoned. The benzimidazoporphyrazines prepared with small alkyl groups could be expected to have limited solubility and to be quite polar, but improvements in this regard would be the task of a later generation in this research area (if ever). The second route to benzimidazoporphyrazines is detailed in the following chapter.

## J. Experimental Section.

**General.**  $^1\text{H}$  (400 MHz) and  $^{13}\text{C}$  (100 MHz) NMR spectra were obtained in  $\text{CDCl}_3$  unless noted otherwise. Silica gel (Scientific Adsorbents, 40  $\mu\text{m}$  average particle size) was used for column chromatography. THF was dried over sodium/benzophenone. Reagents were purchased from Aldrich or Acros and used as received.

**4,5-Dibromo-N,N'-di-p-toluenesulfonyl-o-phenylenediamine (1).** This compound was prepared according to a previous report.<sup>4a</sup> Analytical data were consistent with the published results.

**4,5-Dibromo-o-phenylenediamine (2).** This compound was prepared according to a previous report.<sup>4a</sup> Analytical data were consistent with the published results.

**5,6-Dibromo-2-p-iodophenylbenzimidazole (3).** A 250 mL round bottom flask was charged with a magnetic stirring bar, nitrobenzene (150 mL) and **2** (3.68 g, 13.8 mmol). When all of **2** had dissolved, p-iodobenzaldehyde (3.21 g, 13.8 mmol) was added. When the mixture was homogeneous, the flask was placed in an oil bath and heated to 150 °C overnight. The mixture was allowed to cool to room temperature, and upon cooling, tan crystals of the pure product were formed (227 mg.). The liquid portion was poured onto a large column of silica gel (packed in  $\text{CHCl}_3$ , 6 cm diameter x 20 cm height), and eluted with  $\text{CHCl}_3$ . As the components of the mixture were separated, the band that contained product appeared to precipitate and redissolve continually as it progressed through the column. Column fractions that contained the product were checked by TLC for purity, and appeared to contain ~10% of the starting diamine **2**. The samples were pooled and concentrated to dryness, giving the product as a tan powder (2.70 g, 41%). Data for crystals (227 mg, 3%): mp 292-294 °C ;  $^1\text{H}$  NMR ( $d_4$ -MeOH)  $\delta$  7.82 (d,  $J$  = 8.7 Hz, 2H), 8.01–8.06 (m, 3H).

Preparation without chromatography: A 500 mL round bottom flask was charged with a magnetic stirring bar, nitrobenzene (264 mL) and **2** (7.03 g, 26.4 mmol). When all of **2** had dissolved, p-iodobenzaldehyde (6.13 g, 26.4 mmol) was added slowly, in portions. When the mixture was homogeneous, the flask was placed in an oil bath heated to 150 °C for 20 h. The mixture was then cooled to room temperature and concentrated in vacuo. The residue was treated with hot acetone and filtered. The filter cake was set aside. The filtrate was heated to boiling and water was added until the solution was turbid. The mixture was allowed to stand overnight, and the resulting precipitate was filtered, reheated in a water/acetone mixture, and the mixture was hot filtered and allowed to stand overnight, producing tan crystals of **3** (1.75 g). The mother liquor was diluted with water, producing a tan precipitate of **3** (1.80 g). The crystals and the tan precipitate were each ≈90% pure by <sup>1</sup>H NMR, and were therefore combined (3.55 g, 28%). Spectral data, although impure, were consistent with the pure sample described above.

The initial filter cake was treated with additional portions of hot acetone to obtain:

**5,6-Dibromo-1-(4-iodobenzyl)-2-p-iodophenylbenzimidazole (4)** (3.29 g, 23%):  
mp 240-242 °C; <sup>1</sup>H NMR δ 5.31 (s, 2H), 6.79 (d, *J* = 8.4 Hz, 2H), 7.35 (d, *J* = 8.4 Hz, 2H), 7.47 (s, 1H), 7.70 (d, *J* = 8.4 Hz, 2H), 7.82 (d, *J* = 8.4 Hz, 2H), 8.12 (s, 1H).

**2-Hexyloctanal (5).** This compound was prepared according to a previous report.<sup>12</sup> Analytical data were consistent with the published results.

**7-Bromomethyltridecane (6).** This compound was prepared according to a previous report.<sup>12</sup> Analytical data were consistent with the published results.

**5,6-Dibromo-1-(2-hexyloctyl)-2-p-iodophenylbenzimidazole (7).** A 20 mL reaction vial was charged with a magnetic stirring bar, **3** (717 mg, 1.50 mmol), and DMF (1.0 mL).

The vial was placed in an oil bath heated to 155 °C. When the mixture was homogeneous, DBU (224  $\mu$ L, 1.5 mmol) was added. After 2-3 min, **6** (416 mg, 1.50 mmol) was added. After 15 min, TLC indicated that the reaction had progressed to  $\approx$ 30-40% yield. After an additional 15 min, no further change was observed by TLC, so another 1.50 mmol of DBU was added. After 2-3 min, another 1.50 mmol of **6** was added. The reaction was allowed to stir at 155 °C for another 1 h, after which it was cooled to room temperature, and the mixture was chromatographed without workup ( $\text{SiO}_2$ ,  $\text{CHCl}_3$ ). The product was obtained as a light tan solid that formed soft crystals upon storage ( $\approx$ 2 weeks) at room temperature (667 mg, 66%):  $^1\text{H}$  NMR  $\delta$  0.84 (t,  $J$  = 7.2 Hz, 6H), 0.89–1.38 (m, 20H), 1.65–1.80 (m, 1H), 4.06 (d,  $J$  = 7.2 Hz, 2H), 7.38 (d,  $J$  = 7.2 Hz, 2H), 7.62 (s, 1H), 7.84 (d,  $J$  = 7.2 Hz, 2H), 8.03 (s, 1H).

**5,6-Dibromo-1-(2-hexyloctyl)-2-[4-(2-trimethylsilylethynyl)phenyl]-benzimidazole (8).** A 20 mL reaction vial was charged with a magnetic stirring bar, **7** (195 mg, 0.29 mmol), bis(triphenylphosphino)palladium dichloride (4.1 mg, 5.8  $\mu$ mol), triphenylphosphine (3.0 mg, 12  $\mu$ mol) and copper iodide (1.1 mg, 5.8  $\mu$ mol). The vial was sealed with a septum and flushed with argon for 30 min. The vial was placed in an ice bath. After 15 min, freshly dried TEA (2 mL) was added. The organic material did not dissolve, so the reaction vessel was allowed to warm to room temperature. The organic material still had not dissolved after 30 min, so freshly dried THF (2 mL) was added, upon which the mixture became homogeneous. Then trimethylsilylacetylene (41  $\mu$ L, 0.29 mmol) was added, and the mixture was stirred at room temperature for 24 h, and during this time, a precipitate formed in the mixture. The precipitate was filtered from the liquid using a pasteur pipette that had been plugged with cotton. The filtrate was concentrated in vacuo and the residue was chromatographed ( $\text{SiO}_2$ ,  $\text{CHCl}_3$ ). Fractions containing the desired compound were

concentrated to a white solid (164 mg, 88%):  $^1\text{H}$  NMR  $\delta$  0.23 (s, 9H), 0.84 (t,  $J$  = 7.2 Hz, 6H), 0.91–1.15 (m, 16H), 1.17–1.28 (m, 4H), 1.70–1.80 (m, 1H), 4.41 (d,  $J$  = 7.2 Hz, 2H), 7.56 (d,  $J$  = 8.4 Hz, 2H), 7.60 (d,  $J$  = 8.4 Hz, 2H), 7.76 (s, 1H), 8.17 (s, 1H).

**5,6-Dibromo-1-(2-hexyloctyl)-2-(4-[2-(2-trimethylsilyloxyprop-2-**

**yl)ethynyl]phenyl)-benzimidazole (10).** A 20 mL reaction vial was charged with a magnetic stirring bar, **7** (219 mg, 0.325 mmol), bis(triphenylphosphino)palladium dichloride (5.3 mg, 7.5  $\mu\text{mol}$ ), triphenylphosphine (3.4 mg, 13  $\mu\text{mol}$ ) and copper iodide (1.4 mg, 7.5  $\mu\text{mol}$ ). The vial was sealed with a septum. The vial was connected to a Schlenk line via a needle and then evacuated and purged with argon three times successively. The vial was placed in an ice bath with continuous flushing of argon. Freshly dried TEA (2 mL) and freshly dried THF (2 mL) were added. When the mixture became homogeneous, trimethylsilyloxyisopropylacetylene (63  $\mu\text{L}$ , 0.33 mmol) was added, and the mixture was stirred at 0–5 °C for 1 h and then allowed to warm to room temperature overnight. The reaction mixture was then diluted into diethyl ether and washed with water, aq NH<sub>4</sub>Cl, and brine. The organic layer was then separated and dried over Na<sub>2</sub>SO<sub>4</sub>, and concentrated to dryness. The residue was chromatographed (SiO<sub>2</sub>, hexanes/ether, 9:1‡ 5:1). Fractions containing the desired compound were concentrated to a light tan solid (147 mg, 64%):  $^1\text{H}$  NMR  $\delta$  0.24 (s, 9H), 0.84 (t,  $J$  = 7.2 Hz, 6H), 0.90–1.15 (m, 16H), 1.15–1.25 (m, 4H), 1.59 (s, 6H), 1.70–1.80 (m, 1H), 4.09 (d,  $J$  = 7.2 Hz, 2H), 7.54 (d,  $J$  = 8.2 Hz, 2H), 7.62 (d,  $J$  = 8.2 Hz, 2H), 7.64 (s, 1H), 8.05 (s, 1H);  $^{13}\text{C}$  NMR  $\delta$  2.15, 14.31, 22.81, 26.09, 29.58, 31.26, 31.86, 33.18, 37.83, 49.13, 67.14, 82.35, 96.94, 115.21, 117.84, 118.21, 124.63, 125.28, 129.44, 129.89, 131.99, 136.35, 143.60, 155.36.

**5,6-Dicyano-1-(2-hexyloctyl)-2-(4-[2-(2-trimethylsilyloxyprop-2-yl)ethynyl]phenyl)-benzimidazole (11).**

A 5 mL round bottom flask was charged with CuCN (89 mg, 0.99 mmol), NMP (0.5 mL), and a magnetic stirring bar. The vessel was heated in an oil bath to 170 °C, and a solution of **10** (174 mg, 0.248 mmol) in NMP (0.5 mL) was added. The temperature of the oil bath was raised to 200 °C and the reaction was stirred for 45 min. TLC of the reaction mixture (hexanes/EtOAc, 2:1) showed several (>10) species present, and very little starting material. Judging by the intensity of the blue fluorescence of the spots upon illumination of the plate with a short-wave UV lamp, the sixth and eleventh spots were identified as dicyanobenzimidazoles. The reaction was cooled to ≈50 °C, and diluted with EtOAc. Then aq NH<sub>4</sub>OH was added and the mixture was stirred for 1 h. The organic layer was then separated, dried over Na<sub>2</sub>SO<sub>4</sub>, filtered, and concentrated to dryness. The residue was chromatographed (hexanes/EtOAc 3:1, then 2:1). Fractions containing the sixth band were collected and concentrated. <sup>1</sup>H NMR indicated that the sample was impure, hindering the confirmation of the product's identity. Mass spectrometry was performed to confirm the presence of the product: FABMS obsd 595.3842, calcd 595.3754 [(M + H)<sup>+</sup>; M = C<sub>37</sub>H<sub>50</sub>N<sub>4</sub>OSi].

The eleventh band of the column was collected and concentrated to give the deprotected dicyanobenzimidazole (**12**, 32 mg, 25%): **5,6-Dicyano-1-(2-hexyloctyl)-2-(4-[2-(2-hydroxyprop-2-yl)ethynyl]phenyl)-benzimidazole (12):** <sup>1</sup>H NMR δ 0.84 (t, *J* = 7.2 Hz, 6H), 0.92–1.25 (m, 20H), 1.64 (s, 6H), 1.68–1.78 (m, 1H), 2.49 (brs, 1H), 4.24 (d, *J* = 7.6 Hz, 2H), 7.58 (d, *J* = 8.4 Hz, 2H), 7.60 (d, *J* = 8.4 Hz, 2H), 7.82 (s, 1H), 8.21 (s, 1H).

**5,6-Dibromo-1-(2-hexyloctyl)-2-(4-[2-(2-hydroxyprop-2-yl)ethynyl]phenyl)-benzimidazole (13).** A 20 mL reaction vial was charged with a magnetic stirring bar, **7** (470

mg, 0.68 mmol), bis(triphenylphosphino)palladium dichloride (20 mg, 30  $\mu$ mol), triphenylphosphine (15 mg, 56  $\mu$ mol) and copper iodide (5.3 mg, 28  $\mu$ mol). The vial was sealed with a septum and flushed with argon for 30 min. Freshly dried TEA (2.5 mL) and freshly dried THF (2.5) were mixed together and added to the reaction vessel. When the mixture became homogeneous, hydroxyisopropylacetylene (70 mg, 0.84 mmol) was added, and the mixture was stirred at room temperature for 36 h. The reaction mixture was then diluted into ethyl acetate, washed with aq NH<sub>4</sub>Cl, dried over Na<sub>2</sub>SO<sub>4</sub>, and concentrated to dryness. The residue was chromatographed (SiO<sub>2</sub>, hexanes/ethyl acetate, 3:1). Fractions containing the desired compound were concentrated to a light tan solid (403 mg, 92%): <sup>1</sup>H NMR  $\delta$  0.81 (t, *J* = 7.6 Hz, 6H), 0.90–1.10 (m, 16H), 1.10–1.22 (m, 4H), 1.60 (s, 6H), 1.64–1.76 (m, 1H), 4.06 (d, *J* = 7.2 Hz, 2H), 4.31 (br s, 1H), 7.41 (d, *J* = 8.2 Hz, 2H), 7.58 (d, *J* = 8.2 Hz, 2H), 7.61 (s, 1H), 8.08 (s, 1H); <sup>13</sup>C NMR  $\delta$  14.33, 22.81, 26.05, 29.58, 31.22, 31.69, 31.86, 37.74, 49.13, 65.32, 81.05, 96.99, 115.24, 117.97, 118.32, 124.47, 125.28, 129.38, 132.23, 136.19, 143.22, 155.29.

**5,6-Dicyano-1-(2-hexyloctyl)-2-(4-[2-(propen-2-yl)ethynyl]phenyl)-benzimidazole (14).** A 10 mL 2-necked round bottom flask was charged with CuCN (143 mg, 1.60 mmol) and magnetic stir bar. The flask was fitted with a condenser and the condenser and the second neck of the flask were capped with septa. The vessel was flushed with argon for 20 min. A solution of **13** (403 mg, 0.64 mmol) in NMP (1.5 mL) was added to the vessel and the flask was heated to 140 °C in an oil bath. After 25 min, the temperature of the bath was increased to 150 °C. TLC of the reaction mixture indicated that very little starting material had been consumed. After a total of 45 min, the temperature of the bath was raised to 190 °C. After a total of 2 h, TLC indicated that most of the starting material **13** had been

consumed, and five new species had formed. The fourth spot on the TLC exhibited strong blue fluorescence under illumination of a short-wave UV lamp. The reaction was cooled to ~50 °C, and diluted with EtOAc. Then aq NH<sub>4</sub>OH was added and the mixture was stirred for 1 h. The organic layer was then separated and washed with brine. The organic layer was then dried over Na<sub>2</sub>SO<sub>4</sub>, filtered, and concentrated to dryness. The residue was chromatographed (SiO<sub>2</sub>, hexanes/EtOAc, 5:1), and the fractions containing the fourth band were collected and concentrated to give the product as a colorless solid (86 mg, 27%): <sup>1</sup>H NMR δ 0.84 (t, *J* = 6.8 Hz, 6H), 0.92–1.30 (m, 20H), 1.65–1.80 (m, 1H), 2.01 (s, 3H), 4.25 (d, *J* = 7.6 Hz, 2H), 5.38 (s, 1H), 5.46 (s, 1H), 7.63 (d, *J* = 8.0 Hz, 2H), 7.67 (d, *J* = 8.0 Hz, 2H), 7.82 (s, 1H), 8.21 (s, 1H); <sup>13</sup>C NMR δ 14.27, 22.79, 23.52, 26.13, 29.58, 31.30, 31.84, 38.33, 49.76, 87.34, 93.71, 108.80, 116.59, 116.71, 117.15, 123.46, 126.63, 126.69, 128.47, 129.42, 132.43, 138.09, 145.25, 159.10; LDMS obsd 504.0, calcd 504.3 (C<sub>34</sub>H<sub>40</sub>N<sub>4</sub>).

**Tetrakis[1-(2-hexyloctyl)-2-(4-[2-(2-hydroxyprop-2-yl)ethynyl]phenyl)-5,6-benzimidazo]porphyrazinatozinc (15).** A 0.5 mL reacti-vial was charged with **14** (32 mg, 61 μmol), ZnBr<sub>2</sub> (4.0 mg, 15 μmol), pentanol (244 μL), DBU (9.2 mg, 61 μmol), and a magnetic stirring bar. The vial was capped and heated overnight at 140 °C with an oil bath. The reaction mixture was then cooled to room temperature, diluted with EtOAc, and washed with water. The organic layer was separated, dried over Na<sub>2</sub>SO<sub>4</sub>, filtered, and concentrated to dryness. The residue was chromatographed (SiO<sub>2</sub>, hexanes/EtOAc 2:1). Fractions containing the desired product were collected and concentrated, giving the compound as a green solid (3.2 mg, 10%): LDMS obsd 2152.2, calcd 2153.3; λ<sub>abs</sub> (nm) 319, 645, 688, 720; λ<sub>em</sub> 728 nm; Φ<sub>f</sub> = 0.63.

**5,6-Dibromo-2-phenylbenzimidazole (16).** A 250 mL round bottom flask was charged with a magnetic stirring bar, nitrobenzene (87 mL), and **2** (2.31 g, 8.70 mmol). When the mixture was homogeneous, benzaldehyde (879  $\mu$ L, 8.70 mmol) was slowly added. The reaction vessel was placed in an oil bath heated to 140 °C and the mixture was heated overnight (14 h). The mixture was then allowed to cool to room temperature and stand for 2 h, during which time a precipitate appeared. The mixture was filtered. The precipitate was washed with hexanes, and dried under vacuum, giving the product as a tan powder (675 mg). The hexanes filtrate and the nitrobenzene filtrate were combined and the mixture was then poured onto a silica gel column (packed in CHCl<sub>3</sub>, 6 cm diameter x 20 cm height), and eluted with CHCl<sub>3</sub>. Column fractions that contained the product were checked by TLC for purity, and appeared to contain  $\approx$ 10% of the starting diamine **2**. The samples were pooled and concentrated to dryness, giving the product as a tan powder (538 mg, 18%). Data for pure product from reaction precipitate (675 mg, 22%): <sup>1</sup>H NMR (d<sub>6</sub>-acetone)  $\delta$  7.50–7.59 (m, 3H), 7.98 (s, br, 2H), 8.22–8.70 (m, 2H).

**5,6-Dibromo-1-(2-hexyloctyl)-2-phenylbenzimidazole (17).** A 5 mL conical reaction vial was charged with a stirring bar, **16** (400 mg, 1.14 mmol), and DMF (0.75 mL). The vial was sealed with a perforated screwcap that held a silicon wafer. The vial was placed in an oil bath that was heated to 155 °C. When the mixture was homogeneous, DBU (173 mg, 1.14 mmol) was added. After 2 min, **6** (316 mg, 1.14 mmol) was added. After 15 min, DBU (173 mg, 1.14 mmol) was added again, and after 2 min, **6** (316 mg, 1.14 mmol) was also added. After 15 min, the mixture was allowed to cool to room temperature, and directly chromatographed (SiO<sub>2</sub>, hexanes/EtOAc, 9:1). Fractions containing the product were concentrated to a tan solid (484 mg, 77%): <sup>1</sup>H NMR  $\delta$  0.84 (t, *J* = 7.2 Hz, 6H), 0.98–1.15 (m,

16H), 1.15–1.25 (m, 4 H), 1.72–1.81 (m, 1H), 4.11 (d,  $J$  = 7.2 Hz, 2H), 7.50–7.54 (m, 3H), 7.63–7.68 (m, 3H), 8.07 (s, 1H).

**5,6-Dicyano-1-(2-hexyloctyl)-2-phenylbenzimidazole (18).** A 5 mL reaction vial was charged with a stirring bar, **17** (455 mg, 0.83 mmol), and CuCN (186 mg, 2.08 mmol). The vial was sealed with a septum and flushed with argon. NMP (1 mL) was added and the vessel was placed in an oil bath that was heated to 170 °C. After 1.5 h, TLC analysis (SiO<sub>2</sub>, hexanes/EtOAc, 5:1) showed that only a trace of starting material remained, and that three new species were present. The temperature of the oil bath was raised to 190 °C and the reaction was allowed to continue for 2 h, but no significant progress was evident by TLC analysis. The mixture was allowed to cool, and diluted into EtOAc. The mixture was then washed with aq NH<sub>4</sub>OH, followed by brine, dried over Na<sub>2</sub>SO<sub>4</sub>, and concentrated to dryness. The residue was chromatographed (SiO<sub>2</sub>, hexanes/EtOAc, 5:1), and fractions of the most polar species ( $R_f$  = 0.27) were concentrated, giving the product as a white solid (170 mg, 46%): <sup>1</sup>H NMR δ 0.83 (t,  $J$  = 7.6 Hz, 6H), 0.92–1.23 (m, 20H), 1.67–1.80 (m, 1H), 4.25 (d,  $J$  = 7.2 Hz, 2H), 7.54–7.63 (m, 3H), 7.66–7.73 (m, 2H), 7.83 (s, 1H), 8.22 (s, 1H).

**Tetrakis[1-(2-hexyloctyl)-2-phenyl-5,6-benzimidazo]porphyrzinatozinc (19).** A two-necked 5 mL round bottom flask was charged with Cerium (III) acetylacetone (10.0 mg, 23 µmol) and a magnetic stirring bar. The flask was fitted with a condenser and septa were used to cap the condenser and the second neck of the flask. The vessel was flushed with argon for 20 min. A solution of **18** (170 mg, 0.39 mmol) in pentanol (1.0 mL) was added. Then DBU (234 mg, 1.54 mmol) was added and the mixture was refluxed for 8 h. The reaction mixture was then allowed to cool, diluted with CH<sub>2</sub>Cl<sub>2</sub>, and washed with water. The organic layer was separated, dried over Na<sub>2</sub>SO<sub>4</sub>, and concentrated to dryness. The

residue was chromatographed ( $\text{SiO}_2$ , hexanes/EtOAc 3:1). Two green bands were observed on the column. The title compound eluted as the first green band. Fractions containing the product were concentrated to give a green solid (7.2 mg, 4%): LDMS obsd, 1762.0, calcd 1763.2;  $\lambda_{\text{abs}}$  (nm) 315, 381, 646, 683, 719, 740;  $\lambda_{\text{em}}$  745 nm;  $\Phi_f = 0.61$ .

**(20).** The second green band eluted from the column after the eluent was changed (hexanes/EtOAc, 1:1). LDMS of this sample indicated that it is a sandwich complex containing one cerium atom and two molecules of compound **19**. Fractions containing this compound were concentrated to give a green solid (33 mg, 19%): LDMS obsd, 3666.1, calcd 3662.2.

**5,6-Dibromo-1-methyl 2-p-iodophenylbenzimidazole (21).** A 20 mL reaction vial was charged with a magnetic stirring bar, **3** (1.23 g, 2.58 mmol), and NMP (10 mL). The vial was capped with a septum. The mixture was sonicated until it was homogeneous, and then DBU (302 mg, 2.58 mmol) was added. Then  $\text{CH}_3\text{I}$  (161  $\mu\text{L}$ , 2.58 mmol) was added, and the mixture was stirred at room temperature for 2 h. The reaction mixture was then poured into water and the resulting precipitate was recovered by filtration. The solid material was subjected to recrystallization (acetone/ $\text{H}_2\text{O}$ , 10:1) without success. The mixture was concentrated and dried in vacuo, and chromatographed ( $\text{SiO}_2$ ,  $\text{CHCl}_3$ , 1% EtOAc). Fractions containing the product were concentrated, giving the product as a tan solid (550 mg, 43%): mp 212-213 °C;  $^1\text{H}$  NMR  $\delta$  3.80 (s, 3H), 7.47 (d,  $J = 8.4$  Hz, 2H), 7.66 (s, 1H), 7.88 (d,  $J = 8.4$  Hz, 2H), 8.04 (s, 1H).

**5,6-Dibromo-1-methyl-2-(4-[2-(2-hydroxyprop-2-yl)ethynyl]phenyl)-benzimidazole (22).** A 20 mL reaction vial was charged with a magnetic stirring bar, **21** (550 mg, 1.12 mmol), bis(triphenylphosphino)palladium dichloride (31 mg, 45  $\mu\text{mol}$ ),

triphenylphosphine (23 mg, 89  $\mu$ moL) and copper iodide (8.5 mg, 45  $\mu$ moL). The vial was sealed with a septum and flushed with argon for 2 h. Freshly dried TEA (5 mL) and freshly dried THF (5) were mixed together, and sparged with argon for 15 min. Hydroxyisopropylacetylene (113 mg, 1.34 mmol) was added to the solvent mixture, and then the resulting mixture was added to the reaction vessel. The benzimidazole **21** did not dissolve, so NMP (2 mL) was added, and the mixture became homogeneous. The reaction was stirred at room temperature for 40 h. The reaction mixture was then diluted with aq NH<sub>4</sub>Cl (7 mL) and water (20 mL), and the resulting mixture was filtered. The filter cake was washed with CH<sub>2</sub>Cl<sub>2</sub> and then dissolved in a hot mixture of toluene/THF (4:1). Hexanes was added to the mixture until it was turbid, and the mixture was allowed to stand overnight. Upon standing, the mixture had produced the product as tan crystals (316 mg). The mother liquor was combined with the CH<sub>2</sub>Cl<sub>2</sub> filtrate and the mixture was concentrated chromatographed (SiO<sub>2</sub>, CH<sub>2</sub>Cl<sub>2</sub>, 3% MeOH). Fractions containing the desired compound were concentrated to a light tan solid (55 mg), which was combined with the tan crystals (total yield = 371 mg, 74%): <sup>1</sup>H NMR  $\delta$  1.65 (s, 6H), 2.28 (s, OH), 3.83 (s, 3H), 7.66 (d, *J* = 8.4 Hz, 2H), 7.68–7.73 (m, 3H), 8.07 (s, 1H).

**5,6-Dibromo-1-methyl-2-phenylbenzimidazole (24).** A 20 mL reaction vial was charged with a magnetic stirring bar, **16** (205 mg, 0.58 mmol), NMP (1.25 mL) and DBU (88 mg, 58 mmol). Once the mixture was homogeneous, it was stirred for 5 min at room temperature, and then CH<sub>3</sub>I (82 mg, 0.58 mmol) was added. After stirring for 2 h, the mixture was chromatographed without workup (alumina, CH<sub>2</sub>Cl<sub>2</sub>, column: 5 cm diameter x 20 cm height). The fractions containing product were concentrated and the residue was recrystallized (EtOH:H<sub>2</sub>O, 1.5:1) to give the product as a light tan solid (147 mg, 69%): mp

83–84 °C;  $^1\text{H}$  NMR  $\delta$  3.83 (s, 3H), 7.50–7.58 (m, 3H), 7.69 (s, 1H), 7.70–78 (m, 2H), 8.06 (s, 1H).

**5,6-Dicyano-1-methyl-2-phenylbenzimidazole (25).** A 20 mL vial was charged with **24** (132 mg, 0.36 mmol), CuCN (129 mg, 1.44 mmol), and a magnetic stirring bar. The vial was capped with a septum and flushed with argon for 30 min. Then NMP (1.0 mL) was added and the vial was placed in an oil bath heated to 170 °C for 2 h. TLC ( $\text{SiO}_2$ , hexanes/EtOAc 2:1) indicated that the starting material was consumed, so the reaction was cooled to  $\approx$ 60 °C and diluted with EtOAc. The mixture was treated with aq  $\text{NH}_4\text{OH}$  and heating was continued for 20 min. The mixture was diluted with satd aq  $\text{NH}_4\text{Cl}$  and extracted with EtOAc. The organic layer was separated, dried over  $\text{Na}_2\text{SO}_4$ , and concentrated to dryness. The residue was chromatographed ( $\text{SiO}_2$ , hexanes/EtOAc 2:1, then 3:1). A second column ( $\text{SiO}_2$ , hexanes/EtOAc 1:1, then only EtOAc).was needed to obtain the pure product as a tan solid (10 mg, 11%):  $^1\text{H}$  NMR  $\delta$  3.90 (s, 3H), 7.59–7.68 (m, 3H), 7.70–7.77 (m, 2H), 7.81 (s, 1H), 8.24 (s, 1H).

**6,6,8,8-Tetramethyl-7-undecanol (27).** An oven-dried 2-necked round bottom flask was sealed under a septum-capped addition funnel and a jacketed condenser w/bubbler. The vessel was flushed with argon for 20 min, and then charged with NaH (4.32 g, 0.18 mol), diethyl ether (30 mL), and a magnetic stirring bar. The flask was placed in a water bath at room temperature, and then a mixture of iodomethane (15.0 mL, 34.1 g, 0.24 mol) and 7-undecanone (6.14 mL, 5.10 g, 30 mmol) was slowly added. After the addition of all liquid reagents, slow evolution of gas was observed from the reaction, and the water bath had cooled to 19 °C. The water in the bath was exchanged for warm water from the tap (28 °C). Over 40 min, the temperature of the water bath was increased to 40 °C and the rate of

gas evolution had increased slightly. By 1 h, the water bath was increased to 45 °C, but bubbling had stopped. It seemed that the ether had exited the vessel, so THF (40 mL) was added. Slow bubbling was again observed in the flask. After overnight heating and stirring at 55 °C, the volume of the mixture had decreased, and a white gelatinous solid had appeared. A removed sample showed no significant reactivity to water, so the vessel was opened and the reaction mixture was removed and extracted with water and ether. The ether layer was dried over MgSO<sub>4</sub> and analyzed by GCMS: trimethylated ketone appeared to be the predominant product (~83%). The residue (5.88 g) was concentrated and submitted to a second alkylation reaction: A 25 mL round bottom flask charged with a magnetic stirring bar, and sealed with a septum. THF (10 mL) was added, and the vessel was immersed in a acetone bath kept close to -78 °C with liquid nitrogen (no dry ice available at the time). A sample of the methylated ketone residue (424 mg, ~ 2 mmol trimethylated ketone) was added, and the mixture was allowed to slowly warm to room temperature. Then iodomethane (375 µL, 852 mg, 6.0 mmol) was added, and the mixture was allowed to stir overnight. The mixture was then extracted with water and hexanes, and the hexanes layer was dried over MgSO<sub>4</sub> and concentrated. GCMS of the residue showed a major peak at 226 m/z (tetramethylketone). <sup>1</sup>H NMR showed a singlet at 1.21 ppm corresponding to the methyl groups. IR analysis still showed a band corresponding to the C=O stretch at 1680 cm<sup>-1</sup>. Therefore the residue of the second reaction was added to a mixture of dry THF (5 mL) and dry MeOH) and treated with NaBH<sub>4</sub> (1.68 g, 44 mmol) in portions over 4 h and allowed to stir overnight. The reaction mixture was then extracted with water and hexanes, and the hexanes layer was dried over MgSO<sub>4</sub>, concentrated, and chromatographed (SiO<sub>2</sub>, hexanes with 1% ethyl acetate) to give the product as a colorless oil: <sup>1</sup>H NMR δ 0.90 (t, *J* = 7.2 Hz,

6H), 0.97 (s, 6H), 0.99 (s, 6H), 1.16–1.24 (m, 10H), 1.44–1.56 (m, 2H), 3.17 (s, 1H);  $^{13}\text{C}$  NMR  $\delta$  14.5, 24.0, 25.8, 26.1, 26.6, 40.0, 42.3, 82.2.

**4,5-Dicyano-1-methylimidazole (28).** A 5 mL round bottom flask was charged with dicyanoimidazole (118 mg, 1.0 mmol), NMP (1.0 mL), and a magnetic stirring bar. The solid material dissolved at room temperature. DBU (149  $\mu\text{L}$ , 152 mg, 1.0 mmol) was added, and 1 min later iodomethane (62  $\mu\text{L}$ , 142 mg, 1.0 mmol) was added. After 15 min, TLC analysis ( $\text{SiO}_2$ ,  $\text{CH}_2\text{Cl}_2$  w/3% ethyl acetate) indicated that much of the imidazole had reacted. The reaction mixture was extracted with water and  $\text{CH}_2\text{Cl}_2$ , and the organic layer was dried and concentrated. Chromatography ( $\text{SiO}_2$ ,  $\text{CH}_2\text{Cl}_2$  w/3% ethyl acetate) gave the product as a tan solid (52 mg, 39%):  $^1\text{H}$  NMR  $\delta$  3.87 (s, 3H), 7.91 (s, 1H).

**4,5-Dicyano-1-undec-7-yl-imidazole (29).** A 5 mL conical reaction was charged with dicyanoimidazole (472 mg, 4.0 mmol), DMF (1.0 mL), and a magnetic stirring bar. The vial was placed in an oil bath heated to 153 °C. Then DBU (608 mg, 4.0 mmol) was added. After 30 s, 7-bromoundecane (1.05 g, 4.0 mmol) was added. After stirring for 1 h, the mixture was cooled to room temperature and put directly to a silica gel column packed in hexanes and eluted (hexanes/ethyl acetate 4:1). Fraction containing the product were concentrated, to give a colorless oil (633 mg, 53%):  $^1\text{H}$  NMR  $\delta$  0.87 (t,  $J$  = 6.9 Hz, 6H), 1.00–1.38 (m, 16H), 1.84–1.96 (m, 4H), 4.11–4.33 (m, 1H), 7.64 (s, 1H);  $^{13}\text{C}$  NMR  $\delta$  14.2, 22.7, 26.1, 28.8, 31.6, 35.7, 61.8, 108.5, 111.8, 112.0, 123.3, 139.9.

## K. References:

- (1) (a) Kudrik, E. V.; Shaposhnikov, G. P. *Mendeleev Commun.* **1999**, 85–86; (b) Kudrik, E. V.; Shaposhnikov, G. P.; Balakirev, A. E. *Russ. J. Gen. Chem.* **1999**, 69, 1321–1324; (c) Balakirev, A. E., Kudrik, E. V.; Shaposhnikov, G. P. *Russ. J. Gen. Chem.* **2002**, 72, 1616–1619.
- (2) For syntheses leading to the starting material used in ref 1, see: (a) Zharnikova, M. A.; Balakirev, A. E.; Maizlish, V. E.; Kudrik, E. V.; Shaposhnikov, G. P. *Russ. J. Gen. Chem.* **1999**, 69, 1870–1871; (b) Shishkina, O. V.; Maizlish, V. E.; Shaposhnikov, G. P.; Lyubimtsev, A. V.; Smirnov, R. P.; Baran'ski, A. *Russ. J. Gen. Chem.* **1997**, 67, 842–845; (c) Elvidge, J. A.; Golden, J. H.; Linstead, R. P. *J. Chem. Soc.* **1957**, 2466–2469; (d) Levy, L. F.; Stephen, H. *J. Chem. Soc.* **1931**, 79–82.
- (3) Pardo, C.; Yuste, M.; Elguero, J. *J. Porphyrins Phthalocyanines* **2000**, 4, 505–509.
- (4) (a) Cheeseman, G. W. H. *J. Chem. Soc.* **1962**, 1170–1176; (b) Acheson, R. M. *J. Chem. Soc.* **1956**, 4731–4735; (c) Elderfield, R. C.; Meyer, V. B. *J. Am. Chem. Soc.* **1954**, 1887–1891; (d) Mørkved, E. H.; Neset, S. M.; Bjørlo, O.; Kjøsen, H.; Hvistendahl, G.; Mo, F. *Acta Chem. Scand.* **1995**, 49, 658–662.
- (5) Grimmett, M. R. *Imidazole and Benzimidazole Synthesis*, Academic Press, 1997, pp 71–94.
- (6) Weidenhagen, R. *Chem. Ber.* **1936**, 69, 2263–2272; Weidenhagen, R.; Weedon, U. *Chem. Ber.* **1938**, 71, 2347–2360.
- (7) (a) use of lead tetraacetate: Stephens, F. F.; Bower, J. D. *J. Chem. Soc.* **1949**, 2971–2972; (b) use of manganese dioxide: Bhatnagar, I.; George, M. V. *Tetrahedron* **1968**, 24, 1293–1298.

- (8) (a) Dubey, P. K.; Ratnam, C. V. *Ind. J. Chem.* **1979**, *18B*, 428–431; (b) Yadagiri, B.; Lown, J. W. *Synth. Comm.* **1990**, *20*, 955–963; (c) Rangarajan, M.; Kim, J. S.; Sim, S.-P.; Liu, A.; Liu, L. F.; LaVoie, E. J. *Bioorg. Med. Chem.* **2000**, *8*, 2591–2600.
- (9) Smith, J. G.; Ho, I. *Tetrahedron Lett.* **1971**, *38*, 3541–3544.
- (10) (a) Langhals, H.; Demmig, S.; Potrawa, T. *J. Prakt. Chem.* **1991**, *333*, 733–748; (b) Langhals, H.; Karolin, J.; Johansson, L. B.-A. *J. Chem. Soc., Faraday Trans.* **1998**, 2919–2922; Langhals, H.; Ismael, R.; Yürük, O. *Tetrahedron* **2000**, *56*, 5435–5441.
- (11) Kato, M.; Komoda, K.; Namera, A.; Sakai, Y.; Okada, S.; Yamada, A.; Yokoyama, K.; Migita, E.; Minobe, Y.; Tani, T. *Chem. Pharm. Bull.* **1997**, *45*, 1767–1776.
- (12) Guida, W. C.; Mathre, D. J. *J. Org. Chem.* **1980**, *45*, 3172–3176.
- (13) (a) Fitton, P.; Rick, E. A. *J. Organometal. Chem.* **1971**, *28*, 287–291; (b) Diercks, R.; Vollhardt, K. P. C. *Angew. Chem. Int. Ed. Engl.* **1986**, *25*, 266–267; (c) Höger, S.; Meckenstock, A.-D.; Müller, S. *Chem. Eur. J.* **1998**, *4*, 2423–2434.
- (14) (a) Tomoda, H.; Saito, S.; Ogawa, S.; Shiraishi, S. *Chem. Lett.* **1980**, 1277–1280; (b) Tomoda, H.; Saito, S.; Shiraishi, S. *Chem. Lett.* **1983**, 313–316.
- (15) Liu, W.; Lee, C.-H.; Chan, H.-S., Mak, T. C. W.; Ng, D. K. P. *Eur. J. Inorg. Chem.* **2004**, 286–292.
- (16) House, H. O.; Fischer Jr., W. F. *J. Org. Chem.* **1969**, *34*, 3626–3627.
- (17) Zanon, J.; Klapars, A.; Buchwald, S. L. *J. Am. Chem. Soc.* **2003**, *125*, 2890–2891.
- (18) Forsyth, R.; Nimkar, V. K.; Pyman, F. L. *J. Chem. Soc.* **1926**, 800–808.
- (19) (a) Gould, I. R.; Zimmt, M. B.; Turro, N. J.; Baretz, B. H.; Lehr, G. F. *J. Am. Chem. Soc.* **1985**, *107*, 4607–4612; (b) Dyllick-Brenzinger, R. A.; Patel, V.; Rampersad, M.

- B.; Stother, J. B.; Thomas, S. E. *Can. J. Chem.* **1990**, *68*, 1106–1115; (c) Valgimigli, L.; Banks, J. T.; Lusztyk, J.; Ingold, K. U. *J. Org. Chem.* **1999**, *64*, 3181–3183.
- (20) Gilchrist, T. L. *Heterocyclic Chemistry*, Addison Wesley Longman Limited: Essex, England, 1997, pg 297.
- (21) Stuzhin, P. A.; Ercolani, C. Unpublished results, cited in *The Porphyrin Handbook*; Kadish, K. M., Smith, K. M., Guilard, R., Eds.; Academic Press: San Diego, 2003; Vol. 15, pg 275.

## Chapter 4

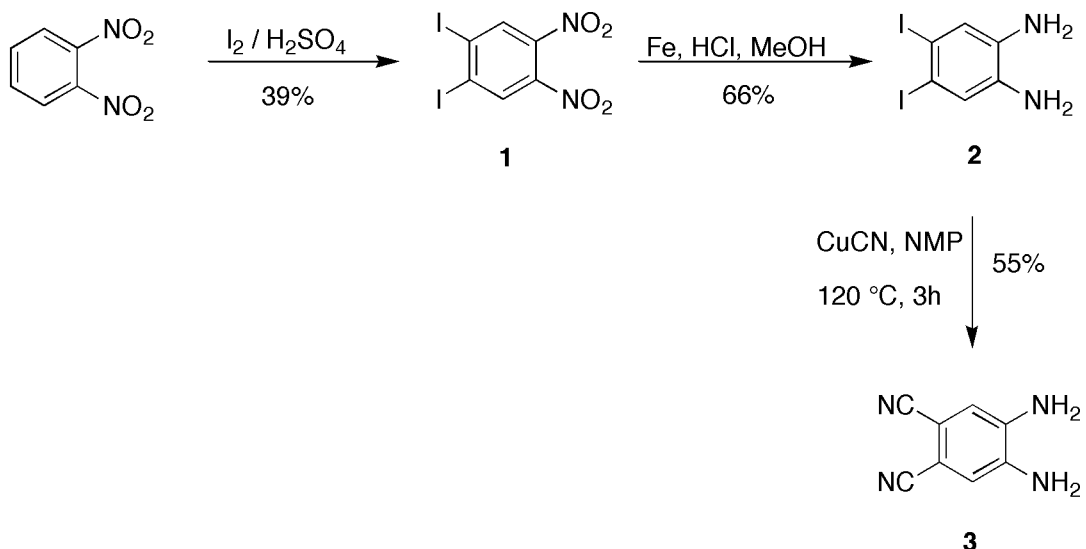
This chapter describes the synthesis of a linear, *trans*-substituted phthalocyanine analogue, based on the benzimidazoporphyrazine scaffold. The development of new synthetic methodology for benzimidazoporphyrazines (BzImPAs) is presented as a stepping-stone toward the desired *trans*-BzImPA(s). The structural properties and photochemical behavior have been compared with those of well-known phthalocyanines.

### A. Synthesis.

All of the published reports of benzimidazoporphyrazines have employed 5,6-dicyanobenzimidazoles as the key building blocks.<sup>1,2</sup> Kudrik and coworkers showed the utility of dicyanophenylenediamine **3** (Scheme 4.1) as a precursor to 2-alkyl-5,6-dicyanobenzimidazoles.<sup>2</sup> Their synthesis of **3** required seven steps, with an overall yield of ~7%.<sup>2,3</sup> The preparation of **3** by Mitzel and coworkers, with a 14% yield over four steps, is the best reported route to date.<sup>4,5</sup> Scheme 4.1 shows a new synthesis of **3**, with a 14% yield over three steps.

The iodination of dinitrobenzene uses  $I_3^+$ , formed by mixture of iodine with oleum.<sup>6</sup> The reconstitution of  $I_2$  as a product of the ensuing iodination reaction allows the  $I_3^+$  intermediate to reform continuously, and thus makes atom-economic use of the halogen starting material. However, even this efficiency does not explain the original reported yield of 56% for diiodination when using only a half-equivalent of  $I_2$ . Attempts to repeat the reaction as reported consistently gave yields of 19-20%. The yield was improved to 39% by lowering the temperature of the reaction from 180 °C to 120 °C, shortening the time to 75

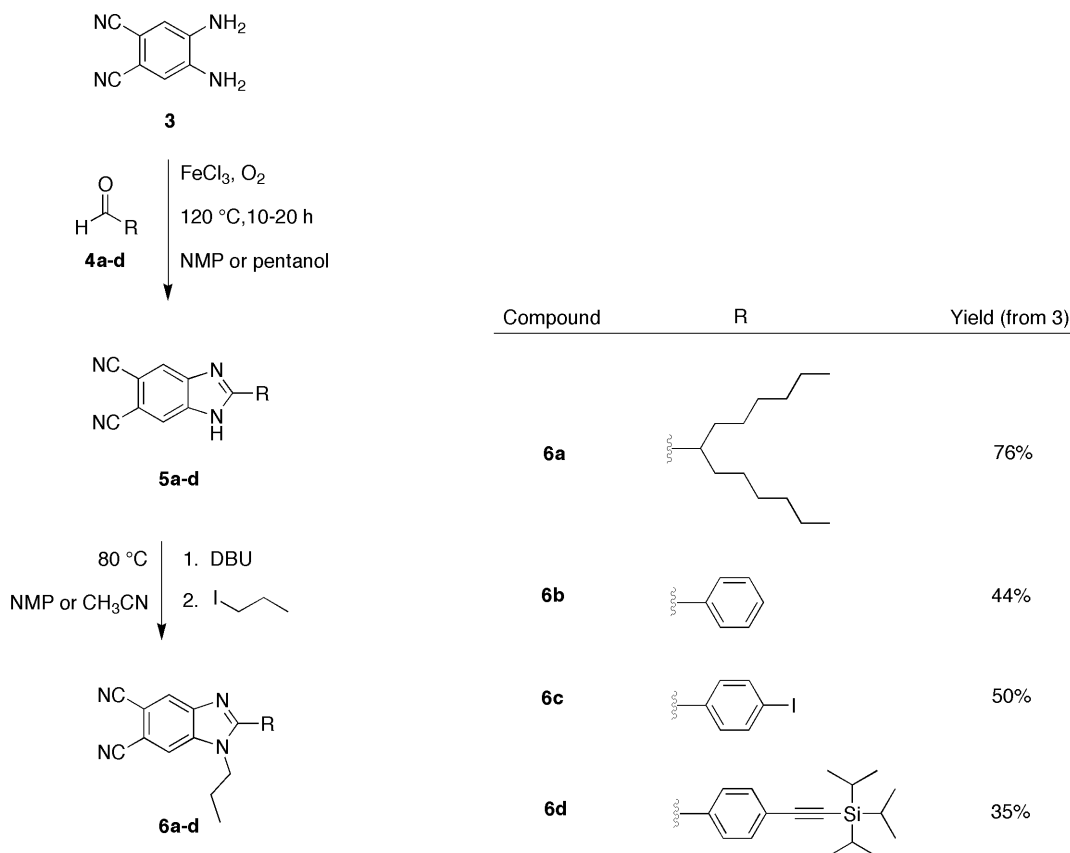
min, and increasing the iodine to the stoichiometric requirement (1 equiv of I<sub>2</sub> for diiodination). The low yield of the reaction is compensated by its amenity to high scale.



Scheme 4.1

The reduction of **1** to the corresponding diamino compound **2** using Sn/HCl has been reported by Whitesides and coworkers, although no specific procedure or yield was provided.<sup>7</sup> The use of Fe/HCl gave the compound in 66% yield and avoids the voluminous tin salts which are typical of Sn reductions. The diamine **2** complexes readily with the iron salts formed from the reaction, requiring treatment of the hot mixture with an aqueous solution of EDTA to recover the product. The cyanation of **2** proceeds at lower temperature (120 vs. 140 °C) more quickly (3 vs. 15 h) and in greater yield (55 vs. 25%) than for the corresponding dibromophenylenediamine.<sup>4</sup> Complexation of the product with the copper salts left over at the end of the reaction is again avoided by treatment of the hot crude mixture with an aqueous solution of EDTA.

Dicyanobenzimidazoles have previously been prepared from **3** and carboxylic acids.<sup>2</sup> However, in these reports, the carboxylic acids have been of low molecular weight (e.g., formic to hexanoic acid) and were used neat, thereby serving as reagent, solvent, and Brönsted acid catalyst. In contrast, benzimidazole syntheses using substituted benzoic acids with *o*-phenylenediamine have typically employed strong hygroscopic acids such as conc. HCl and polyphosphoric acid as the solvent/catalyst.<sup>8</sup> The oxidative cyclization yielding benzimidazoles from phenylenediamines and aldehydes is a milder technique. Originally developed by Weidenhagen using Cu(OAc)<sub>2</sub>,<sup>9</sup> this method has evolved in recent years to the more environmentally benign use of O<sub>2</sub>, with FeCl<sub>3</sub> as a catalytic oxidant.<sup>10,11</sup> Scheme 4.2 shows the oxidative cyclizations using **3** and selected aldehydes **4a-d**.



Scheme 4.2.

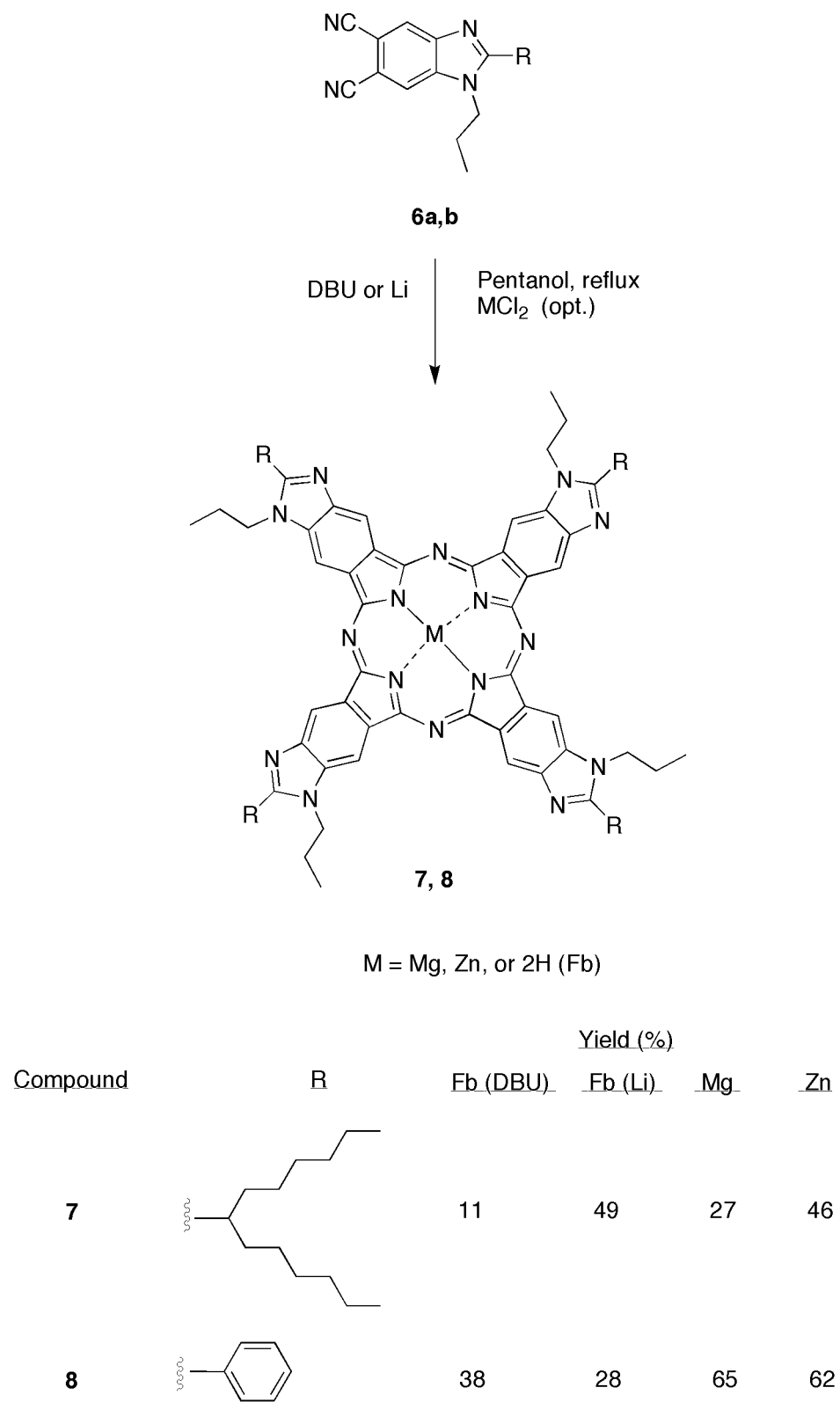
Yields of 58% and 81% were obtained for benzimidazoles **5a** and **5d**, respectively. The reactions required longer times than those previously reported, perhaps due to the more electron-poor quality of **3** compared to *o*-phenylenediamine. Benzimidazole **5d** was also prepared directly from **2**, taking advantage of the copper salts left over from the cyanation reaction (Scheme 1), by adding aldehyde **4c** and bubbling O<sub>2</sub> through the crude reaction mixture containing **3**. This procedure was considerably faster than the FeCl<sub>3</sub> method, due to the large quantity of copper salts present, and gave **5d** in 41% yield. It was however, not successful for **5a**. Due to the poor solubility of compounds **5b** and **5c**, the cyclization reaction mixture was carried forward to the alkylation at the 1-position, giving **6b** and **6c**.

Alkylation of the 1-position of these dicyanobenzimidazoles with the relatively small propyl group was predicated on the intent to use the resulting benzimidazoporphyrazines as components in materials where the macrocycles would be closely packed. Larger alkyl groups, although perhaps helpful for the solubility of the benzimidazoporphyrazines, would prohibit the close packing of the macrocycles. Benzimidazoles **5a** and **5d** proved unreactive to iodopropane in the absence of a base, even at elevated temperature. Deprotonation could be effected with DBU, and subsequent alkylation with iodopropane (bp 101 °C) succeeds at 80 °C in acetonitrile or NMP (*N*-methyl pyrrolidinone). The initial yield of the alkylation reaction is low, but by using successive rounds of addition of the base and electrophile in the reaction, acceptable yields were obtained. The use of excess base did not raise the yield of the reaction. Propyl-dicyanobenzimidazoles **6a-d** were obtained in 35-76% yield from diamine **3** (Scheme 4.2). The swallowtail benzimidazole **5a** gave better results in the

alkylation reaction (94%) compared to the 2-arylbenzimidazoles, suggesting some influence of the 2-substituent on the basicity/nucleophilicity of the benzimidazole.

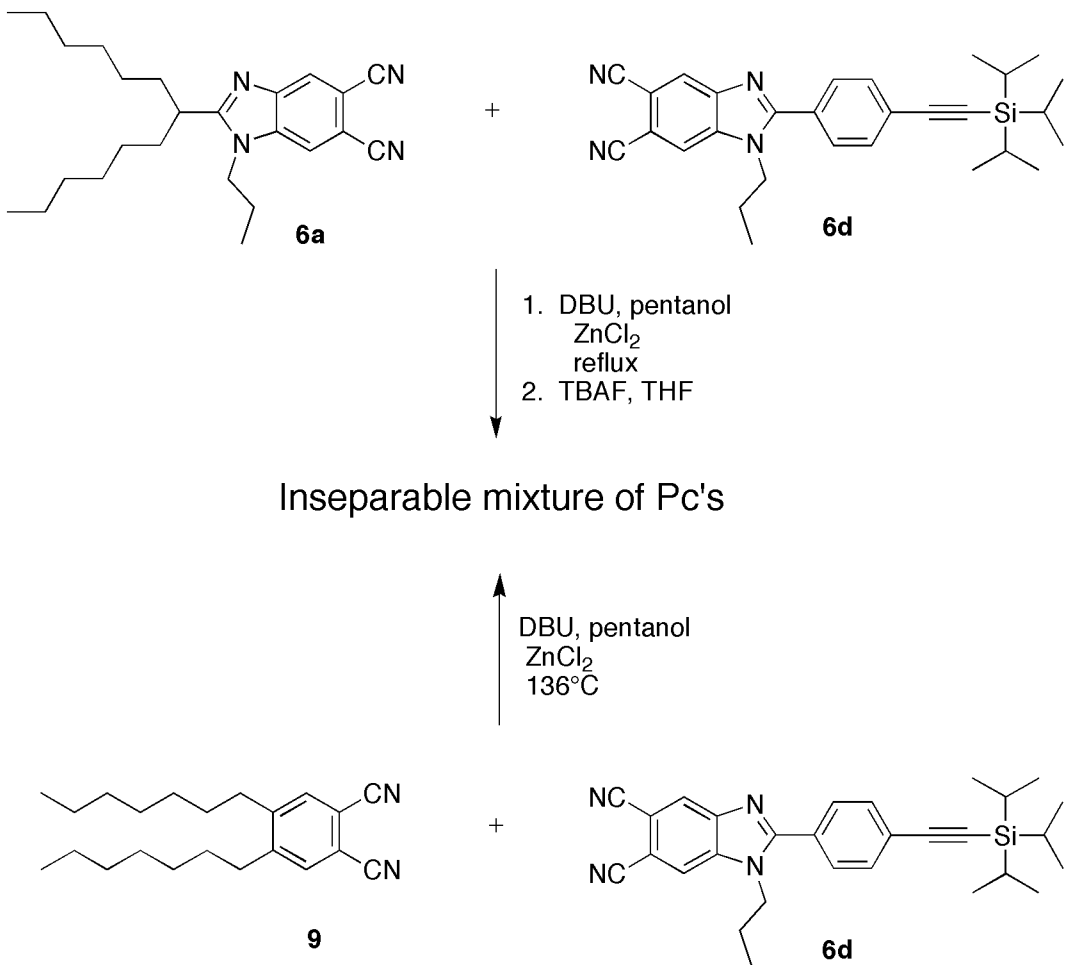
The swallowtail- and phenyl-benzimidazoles **6a** and **6b** were chosen as benchmark motifs for 2-alkyl- and 2-aryl-5,6-benzimidazoporphyrazines, respectively. In principle, a wide variety of aldehyde-bearing groups can be installed at the 2-position. This versatility is limited by the stability of a given aldehyde-bearing group under the conditions of the oxidative cyclization and alkylation reactions. Groups that might interfere with or be affected by these two steps, such as ferrocenyl or pyridyl, can be transformed to dicyanobenzimidazoles by cross-coupling to the *p*-iodophenyl-benzimidazole **6c**. The protected ethynylphenyl-benzimidazole **6d** was prepared as a building block for *trans*-diethynyl-benzimidazoporphyrazines.

The previous reports of A<sub>4</sub>-type benzimidazoporphyrazines report UV-Vis absorption spectra in DMF and sulfuric acid.<sup>1,2</sup> Benzimidazoporphyrazines **7** and **8** (Scheme 4.3), as well as the corresponding zinc and magnesium chelates, were prepared to investigate the photochemical properties of these macrocycles ( $\epsilon$ ,  $\lambda_{\text{abs}}$ ,  $\lambda_{\text{em}}$ ,  $\Phi_f$ ) in common organic solvents. This allows a comparison of the effects of the extra-annular imidazole ring with the corresponding benzo rings of naphthalocyanine (vide infra), without the complicating effects of low symmetry in the target *trans*-substituted macrocycle.



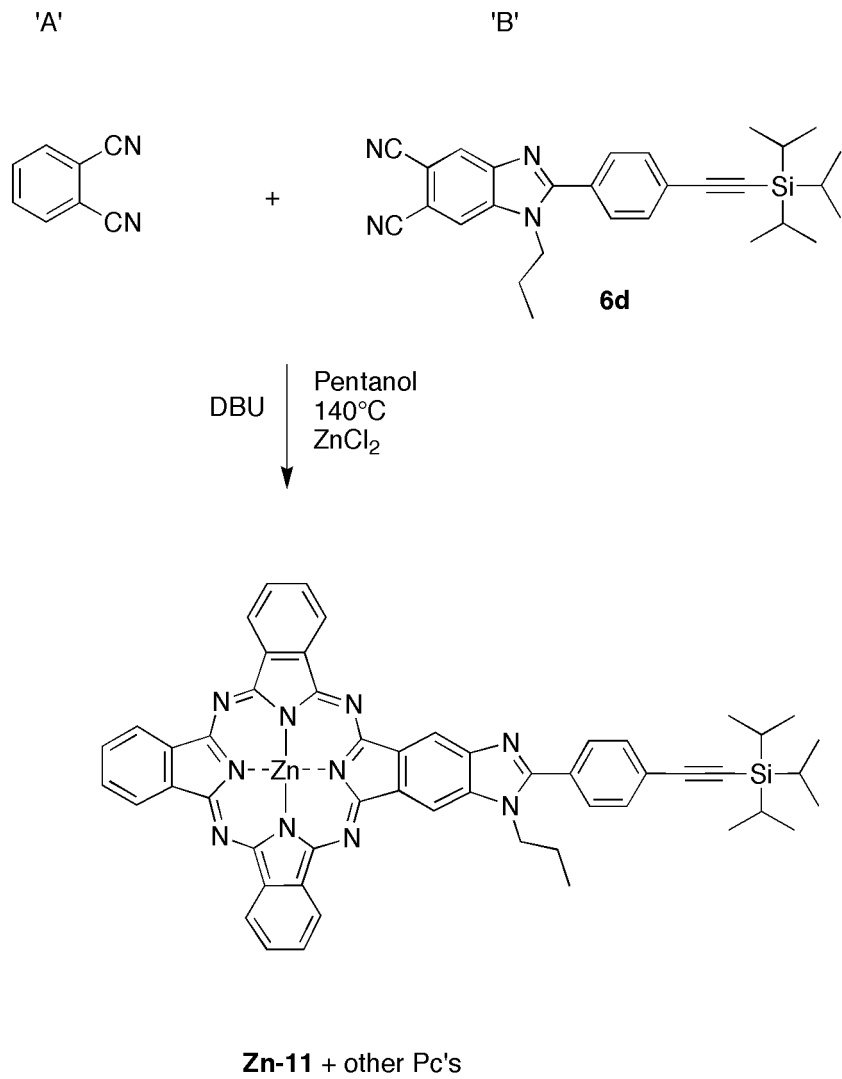
Scheme 4.3.

The yields of the DBU-mediated reactions of **6a** increase according to the presence and type of metal salt in the order Fb<Mg<Zn, in accord with known results for phthalocyanine formation using DBU with and without metal salts.<sup>12</sup> The corresponding reactions with **6b** do show an improvement in the yields for the metallo-derivatives compared to the free base, but the DBU-mediated reaction was slightly better than that using lithium pentoxide, and the yields of **Mg-8** and **Zn-8** are within experimental variation. The <sup>1</sup>H NMR spectrum of **Fb-8** shows the usual evidence of the aromatic ring current, with the core protons found at -3.13 ppm, whereas in **Fb-7** the core protons are found at 0.30–0.50 ppm. Whether this latter result is due to a steric or electronic effect is not known. The general structure shown in Scheme 3 depicts a macrocycle have C<sub>4h</sub> symmetry, but the A<sub>4</sub> benzimidazoporphyrazines can have up to four regioisomers resulting from the placement of the propyl groups. As a result, the <sup>1</sup>H NMR spectra of the zinc and free base forms of **7** and **8** exhibited broad signals for most of the expected resonances. However, the <sup>1</sup>H NMR signatures for **Mg-7** and **Mg-8** were far less complex, indicating a possibly monodisperse product. The effect of metal templating on the distribution of regioisomers in phthalocyanine-forming reactions has been previously detailed.<sup>13</sup> All of the A<sub>4</sub> benzimidazoporphyrazines are green in solid form as well as in solution.



Scheme 4.4.

Initial attempts to prepare a *trans*-diethynyl-benzimidazoporphyrazine from macrocyclization of mixtures of dicyanobenzimidazoles were plagued by the inseparability of the resulting products. Analysis of the product mixture from the reaction of **6a** and **6d** (Scheme 4.4) by laser desorption mass spectrometry (LD-MS) indicated that all possible products had been formed, but no successful separation could be effected by either adsorption chromatography (silica or alumina) or size exclusion chromatography. The same circumstances were encountered for the reaction between **6d** and diheptylphthalonitrile **10**.



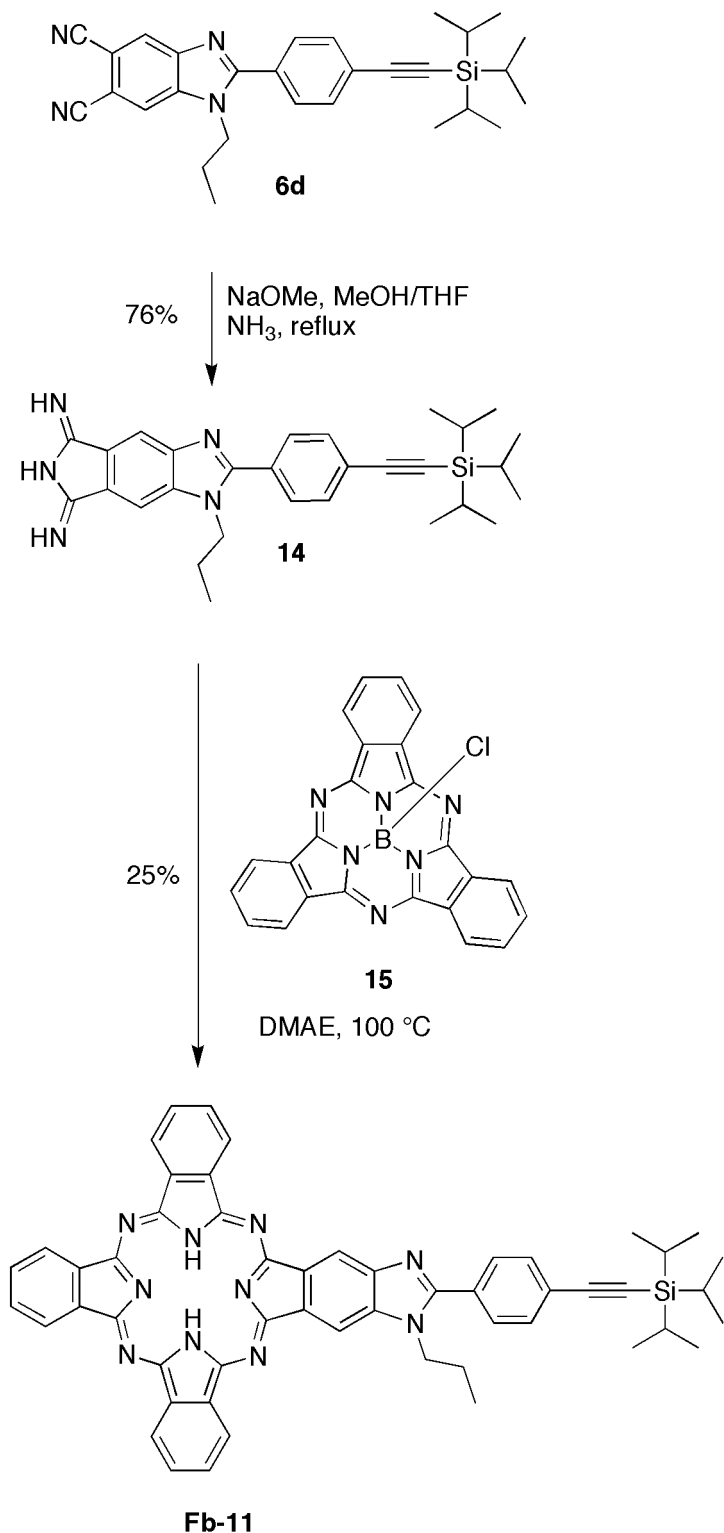
Pc	Compound	Yield
A <sub>4</sub>	<b>Zn-10</b>	4%
A <sub>3</sub> B	<b>Zn-11</b>	22%
A <sub>2</sub> B <sub>2</sub> - <i>cis</i>	<b>Zn-12</b>	14%
A <sub>2</sub> B <sub>2</sub> - <i>trans</i>	<b>Zn-13</b>	1%

Scheme 4.5.

The reaction of **6d** with dicyanobenzene (Scheme 4.5) was a more successful, mixed-macrocyclization, allowing the separation of the smaller macrocyclic products (A<sub>4</sub>, A<sub>3</sub>B, and

$A_2B_2$ ) from the larger ones ( $AB_3$  and  $B_4$ ) by size exclusion chromatography. The smaller macrocycles were then further separated by adsorption chromatography. The larger macrocycles were not isolated. Compound **6b** appeared to be slightly more reactive than 1,2-dicyanobenzene, and a 1:1 ratio of the two reactants (respectively) gave a product mixture favoring the  $AB_3$  and  $B_4$  products. A corresponding ratio of 1:1.5 gave a more even mixture of the possible products. The recovered samples of the *trans*-diethynylbenzimidazoporphyrazine **Zn-13** and the *cis*-isomer **Zn-12** displayed similar  $^1H$  NMR spectra, but were easily distinguished by their respective UV-Vis absorption spectra (vide infra). **Zn-11** was easily separated in the initial size exclusion column. This compound is a blue solid, but takes on a blue-green color in solution. The  $A_2B_2$  compounds are also blue solids, but appear green in solution.

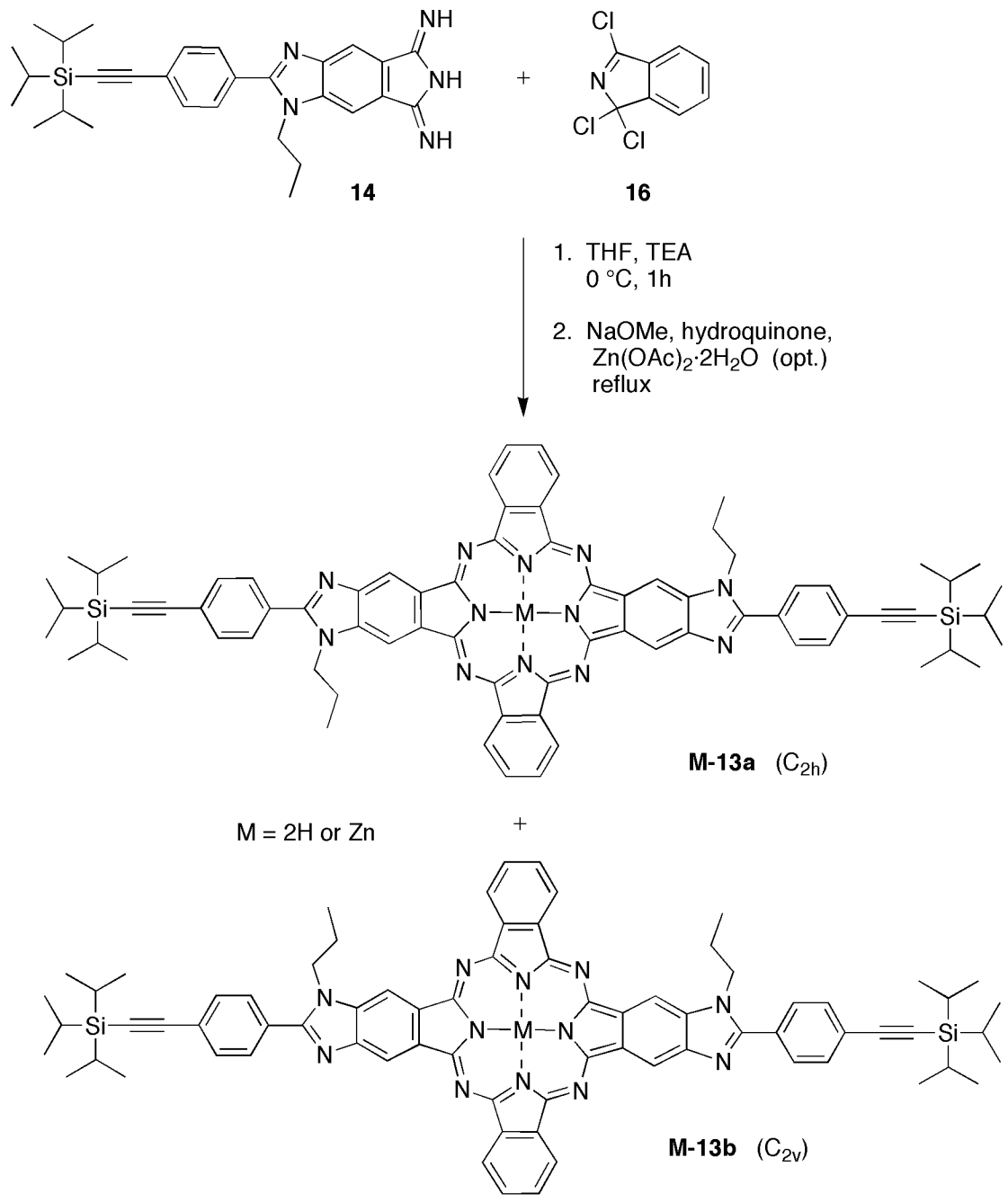
Dicyanobenzimidazole **6d** was transformed into the corresponding diiminoisoindoline **14** in 76% yield using a well-known procedure (Scheme 4.6).<sup>14</sup> The product did not fully crystallize from the reaction as is usually reported, but the quantity of recovered solid could be amplified by concentrating the mixture using a stream of argon. The crystals obtained were greenish-white needles that turned deep green upon melting. The melted sample was recovered from the capillary and was found to exhibit a UV-Vis absorption profile analogous to that of **Fb-8**.



Scheme 4.6.

Diiminoisoindoline **14** was reacted with boron-subphthalocyanine (**15**) to prepare the A<sub>3</sub>B compound **Fb-11** (Scheme 4.6). Due to the reactivity of **14**, the subPc **15** had to be employed at four times the stoichiometric ratio in order to suppress the formation of products having more than one benzimidazole moiety. The reaction yield was highest when conducted at 100 °C. Higher temperatures gave the product more quickly but in lower yield, whereas lower temperatures were ineffective. **Fb-11** exhibits poor solubility, but is marginally more soluble than the large quantity of unsubstituted phthalocyanine that is also formed. The desired product could be largely separated from the unsubstituted phthalocyanine by Soxhlet extraction of the solid residue of the reaction using chloroform, followed by size-exclusion chromatography. Although the yield is modest (25%), the alternative route to **Fb-11** would be the demetalation of **Zn-11**, which is not possible under mild conditions. (Zinc-porphyrins can be demetalated in the presence of TFA at room temperature, but this is ineffective for zinc phthalocyanines.) There is no published report of the demetalation of a zinc-phthalocyanine. **Fb-11** was colored very similarly to **Zn-11**, blue in solid form and slightly more greenish blue in solution.

The *trans*-diethynyl-benzimidazoporphyrazine **Fb-13** was prepared in 9% yield by cross-condensation of diiminoisoindoline **14** with trichloroisooindolenine **16** (Scheme 4.7), following the procedure reported by Young and Onyebuagu.<sup>15</sup> A trace quantity of an AB<sub>3</sub> byproduct was formed in the reaction, as previously observed.<sup>16</sup> The yield of the *trans*-A<sub>2</sub>B<sub>2</sub> product dropped to 4% when ZnCl<sub>2</sub> was used as a templating agent in the reaction. The compound **Zn-13** was more accessible by metalation of **Fb-13** using Zn(OAc)<sub>2</sub>·2H<sub>2</sub>O.



Compound	Yield
<b>Fb-13 (a + b)</b>	9%
<b>Zn-13 (a + b)</b>	4% $Zn(OAc)_2 \cdot 2H_2O$ , dioxane/DMF, reflux (90%)

Scheme 4.7.

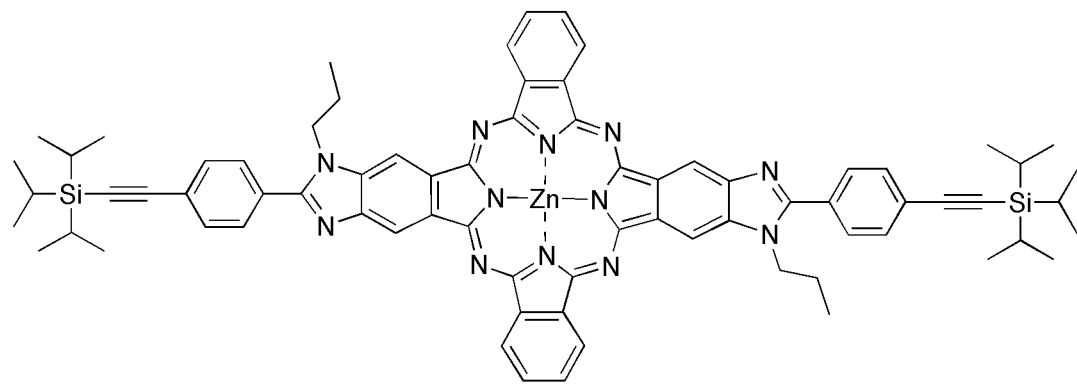
There are two possible regioisomers of the *trans*-A<sub>2</sub>B<sub>2</sub> structure, of C<sub>2v</sub> and C<sub>2h</sub> symmetries, owing to the position of the respective N<sub>imidazo</sub> substituents. For **Fb-13** these regioisomers were not separable by chromatography on silica gel. The <sup>1</sup>H NMR spectra of the isolated sample of **Fb-13** had duplicate signals for each expected resonance, including the protons within the macrocycle. This result is similar to the <sup>1</sup>H NMR spectra for the free base and zinc metalated A<sub>4</sub> benzimidazoporphyrazines. Compound **Fb-8** has a slightly broadened signal for the inner protons, but not the twinned peaks that are seen for **Fb-13**. Hanack and coworkers attributed the split appearance of the inner proton resonance to the different environments encountered by the NH protons in the tautomers of their *trans*-A<sub>2</sub>B<sub>2</sub> structure.<sup>16</sup> A variable temperature <sup>1</sup>H NMR experiment in d<sub>8</sub>-THF showed that the signals for the various duplicated resonances of **Fb-13** did approach one another at high temperatures (up to 55 °C), but the signals never merged, and the usual broadening associated with exchange-equilibrium behavior was not observed. Given the rather low temperature limit of the solvent, this result is not conclusive as to the origin of the twinned resonances.

The <sup>1</sup>H NMR spectrum of a sample of **Zn-13** having both regioisomers was far less complex than the corresponding signature of the free base compound. Only the aromatic region showed more complexity than would be expected for a monodisperse sample. Although this supports the hypothesis that the duplicate set of signals observed for **Fb-13** is the result of tautomerism, the simplicity of the spectrum of **Zn-13** can also be interpreted as the coincidental overlapping of several signatures. Fortunately, the regioisomers of **Zn-13** were separable by chromatography on silica gel, and exhibited distinct patterns in the aromatic region of the <sup>1</sup>H NMR spectrum, enabling assignment. The first eluting species, **Zn-13a**, exhibits an ABCD splitting pattern for the protons on the benzo rings, consistent

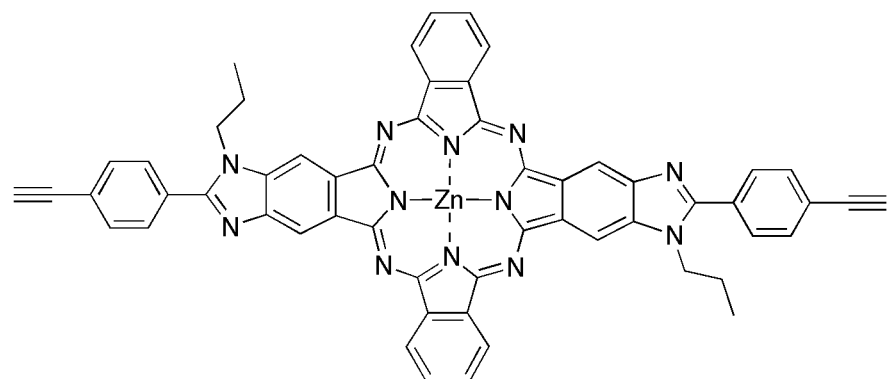
with the assignment of  $C_{2h}$  symmetry. The second eluting species, **Zn-13b**, shows multiplets that resemble typical AA'BB' splitting patterns, corresponding to the structure assigned to  $C_{2v}$  symmetry. COSY NMR analyses were performed to confirm the coupling patterns that support these assignments of the regioisomers. As with the  $A_2B_2$  products from the reaction of **6d** with dicyanobenzene, all of the *trans*- $A_2B_2$  compounds were blue in solid form but deeply green in solution.

The deprotection of **Zn-13a** and **Zn-13b** proceeded smoothly using TBAF in dichloromethane, but the compounds proved to be surprisingly polar during chromatography (Scheme 4.8). Loss of the triisopropylsilyl groups also adversely affected the solubility of the resulting diethynyl compounds. Whereas **Zn-13a/b** are soluble in chlorinated solvents and very soluble in THF, the products **Zn-17a/b** slowly precipitated from the eluent upon exiting the chromatography column, and are then only weakly soluble in chlorinated solvents, and moderately soluble in THF. This low solubility makes the prospect of chemical (e.g., Pd mediated) polymerization of the diethynyl monomer more challenging. Other polymerization options exist, such as the recently investigated thermal polymerization of diethynyl porphyrins.<sup>17</sup>

The procedures developed for this route typically gave moderate to low yields, but are each amenable to higher scale. The biggest losses are incurred at the initial synthesis of compound **1** and the cross-condensation synthesis of **Fb-13**. The quantities of the isolated diethynyl-*trans*-benzimidazoporphyrazines are small (<10 mg), but sufficient for their full characterization and testing in exploratory polymerizations.



TBAF, THF



Zn-17a (87%)



Scheme 4.8.

## B. Photochemistry.

The absorption and emission spectra of compounds **Fb-7**, **Zn-7**, and **Mg-7** are shown in Figure 4.1. The spectra for the phenyl-substituted **M-8** series are closely matching to those of the alkyl series **M-7**, but are red-shifted by 2-4 nm (Table 1). The general appearance of the spectra is typical of phthalocyanines, with broad B bands in the 300-400 nm region, and sharper Q bands providing strong absorbance in the red/near-IR portion of the spectrum. Of all the benzimidazoporphyrazines in this study, only **Fb-8** does not obey the Beer-Lambert law. For the others, no significant change is observed in the UV-Vis absorbance profile between solutions having maximal absorbance in the range 0.02–2.0 absorbance units. **Fb-8** showed a 15% decrease in the ratio of the B band to the Q band between solutions at 0.02 and 2.0 absorbance units. The extinction coefficients are somewhat higher than the reported values for unsubstituted phthalocyanines and even the more soluble tetra-*tert*-butylphthalocyanines,<sup>18</sup> but this may simply be an effect of the narrowness of the Q band maxima for the BzImPAs.

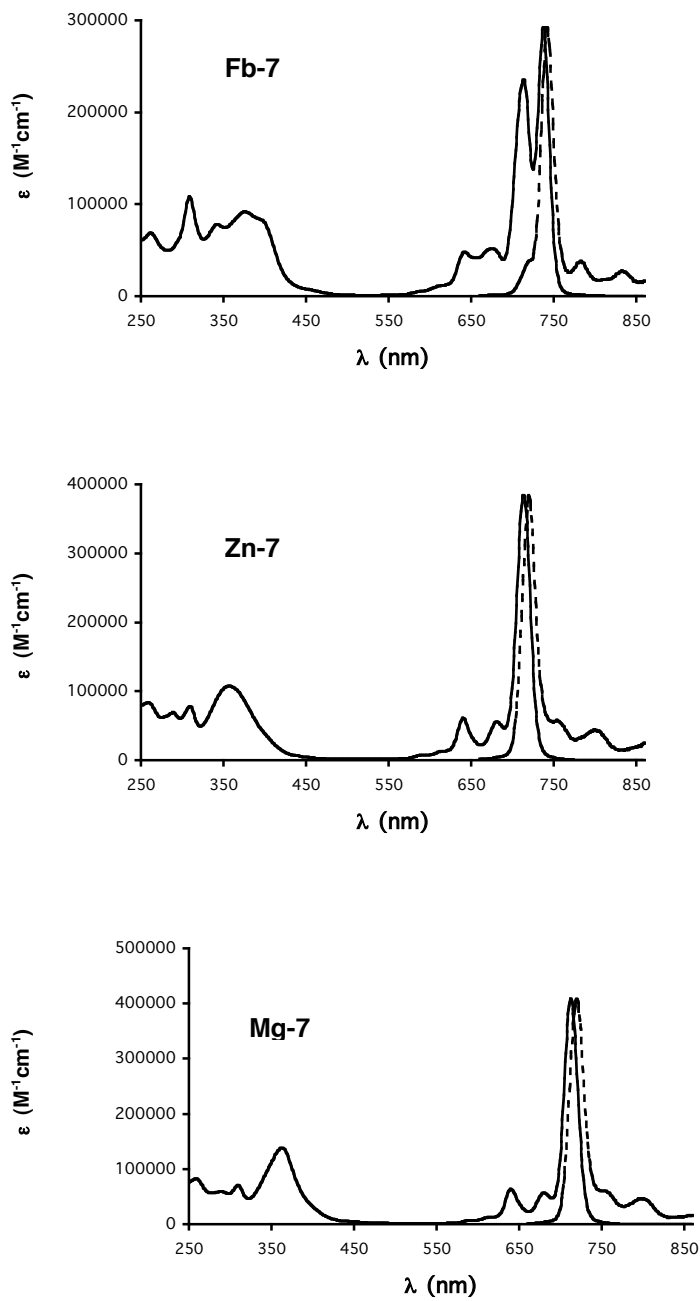


Figure 4.1. Absorption and emission spectra for tetrasubstituted benzimidazoporphyrazines.

Table 4.1. Photochemical data for benzimidazoporphyrazines.

Compound	B band $\lambda_{\text{abs}}$ (nm) [ $\varepsilon_{\log 10}$ ]	Q bands $\lambda_{\text{abs}}$ (nm) [ $\varepsilon_{\log 10}$ ]	Q/B <sup>a</sup>	$\lambda_{\text{em}}$ (nm)	$\Phi_f^b$
<b>Fb-7</b>	376 [4.96]	713 [5.37], 738 [5.47]	3.2	742	0.59
<b>Fb-8</b>	382 [4.96]	718 [5.31], 740 [5.38]	2.6	744	0.70
<b>Fb-11</b>	337 [4.89]	669 [4.98], 695 [4.98]	1.2	700, 714 <sup>c</sup>	0.68
<b>Fb-13</b>	340 [5.13]	662 [4.99], 681 [4.99] 703 [5.18], 732 [4.94]	1.1	711, 739 <sup>c</sup>	0.66
<b>Zn-7</b>	357 [5.03]	713 [5.58]	3.6	720	0.47
<b>Zn-8</b>	357 [5.08]	717 [5.59]	3.2	724	0.43
<b>Zn-11</b>	340 [5.10]	674 [5.43]	2.2	692	0.47
<b>Zn-12</b>	340 [4.95]	693 [5.31]	2.3	701	0.44
<b>Zn-13a</b>	338 [5.12]	679 [5.37], 709 [5.21]	1.75	717	0.32
<b>Zn-13b</b>	338 [5.11]	679 [5.36], 709 [5.19]	1.78	717	0.26
<b>Mg-7</b>	363 [5.14]	713 [5.61]	3.0	720	0.69
<b>Mg-8</b>	364 [5.12]	717 [5.53]	2.6	724	0.84

<sup>a</sup>Ratios of intensities were calculated from absorbance data. Q value was chosen from the most intense Q band for a given compound.

<sup>b</sup>The method for quantum yield determination is described in the Experimental Section.

<sup>c</sup>The fluorescence profile of the sample was dependent upon the wavelength of excitation.

The Q bands of the A<sub>4</sub> BzImPAs are red-shifted by ~35-50 nm compared to the corresponding free base or metallophthalocyanines.<sup>18</sup> The Q band maxima for various phthalocyanine species in THF are as follows: zinc phthalocyanine (**ZnPc**, 665 nm),<sup>19</sup> **Zn-7** (713 nm), and zinc naphthalocyanine (**ZnNc**, 756 nm).<sup>19</sup> Thus, the difference between the excited-state energy gap of **ZnPc** and **ZnNc** is 1820 cm<sup>-1</sup>; the excited-state energy gap of **Zn-7** is 1015 cm<sup>-1</sup> greater than that of **ZnPc**, and 805 cm<sup>-1</sup> less than that of **ZnNc**. This is not

surprising given the relative extent of  $\pi$ -conjugation in each species: **ZnPc** has a total of 42  $\pi$  electrons, spread over 36 nuclei, while **ZnNc** has 54  $\pi$  electrons that are spread out over 48 nuclei; the  $\pi$ -system of **Zn-7** has the same number of electrons as **ZnNc**, but four fewer nuclei. This translates to four fewer molecular orbitals via the LCAO formalism, and explains why the BzImPAs are blue-shifted compared to naphthalocyanines. Another distinction of the imidazole annulation is that the moderate red-shift of the phthalocyanine electronic transitions comes without any sacrifice in the fluorescence quantum yield. Whereas the  $\Phi_f$  of **ZnNc** (0.13)<sup>45</sup> is reduced from that of **ZnPc** (0.32),<sup>19</sup> the  $\Phi_f$  of **Zn-7** is higher (0.47).

The lower symmetry of free base macrocycles **Fb-11** ( $A_3B$ ) and **Fb-13** (*trans*- $A_2B_2$ ) results in very different behavior from the  $A_4$  BzImPAs. Figure 4.2 shows the absorption and emission profiles of the  $A_3B$  and *trans*- $A_2B_2$  compounds. The Q band maxima are more complex, the Q band intensity is dropped to roughly the same as the B band, and the fluorescence behavior shows dependence on the wavelength of excitation. The altered Q/B ratio is not the result of aggregation, as no difference was observed in the absorption profile between solutions having maximal absorptions of 0.02 and 2.0 absorbance units (a 100-fold change in concentration).

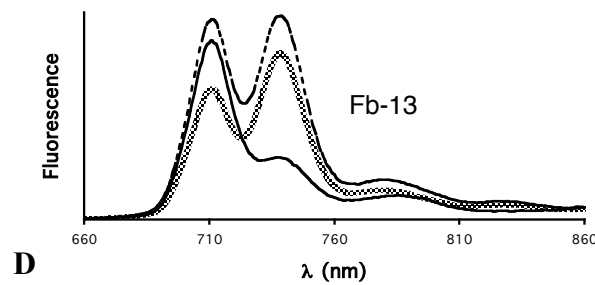
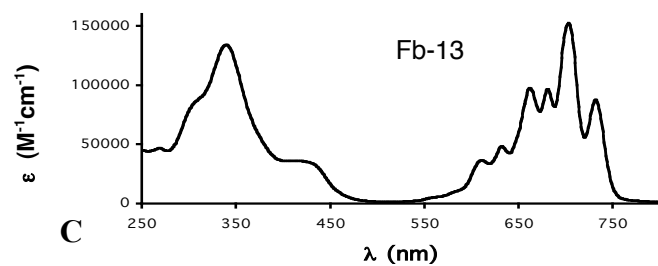
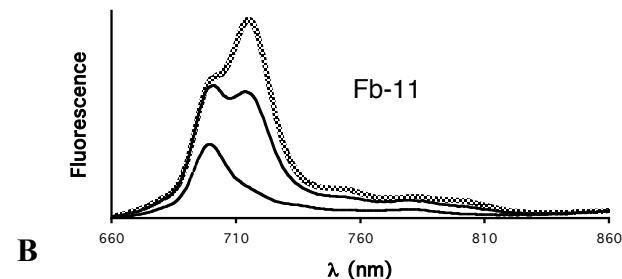
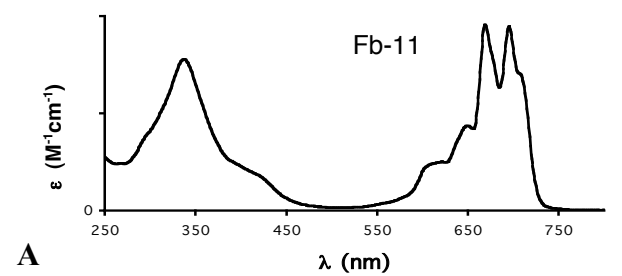


Figure 4.2. (A) Absorption spectra for **Fb-11**. (B) Emission spectra for **Fb-11** (excitation at 435, 600, and 630 nm). (C) Absorption spectra for **Fb-13**. (D) Emission spectra for **Fb-13** (excitation at 435, 630, and 640 nm).

There are two transition dipole moments, one along the short axis of the molecule and one along the long axis of the molecule. In addition, for the free base A<sub>3</sub>B and *trans*-A<sub>2</sub>B<sub>2</sub> BzImPAs, tautomerism of the inner NH protons can result in either N-N or NH-NH along the short axis, and NH-NH or N-N along the long axis. (By contrast, the standard free base phthalocyanine system also two distinct transition dipole moments owing to the N-N and NH-NH axes. The two transition dipole moments, normally labeled as Q<sub>x</sub> and Q<sub>y</sub>, respectively, give rise to the two sets of peaks normally observed.) For the free base A<sub>3</sub>B and *trans*-A<sub>2</sub>B<sub>2</sub> BzImPAs, the tautomerism of the core protons may give result in two photochemically distinct species, as the Q<sub>x</sub> and Q<sub>y</sub> dipoles will each give rise to distinct electronic transitions depending on their placement on the short or elongated axis of the macrocycle.

This hypothesis is supported by the fluorescence behavior of **Fb-11** and **Fb-13**: each compound appears to have two strong fluorescence maxima and more than two accompanying vibronic bands at longer wavelengths. The two tautomers of a given low symmetry free base macrocycle may each be responsible for one emission maximum and accompanying vibronic bands. Thus the complex absorption profiles are not indicative of a single set of electronic transitions, but rather are each an overlay of the bands due to two photochemically distinct species. If these complex absorption and emission profiles were indeed the result of individual photochemical species, then the compounds would be in violation of Kasha's rule, which states that excited chromophores must always pass through the same lowest singlet excited-state before returning to the ground-state.

The zinc chelates **Zn-11**, **Zn-12**, and **Zn-13**, each show a single emission maximum (Figure 4.3). For **Zn-12** (*cis*-A<sub>2</sub>B<sub>2</sub> architecture) this is no surprise, as the two axes of the phthalocyanine are identical with respect to their extent of annulation. **Zn-13** (*trans*-A<sub>2</sub>B<sub>2</sub>) shows the type of double Q band manifold normally expected for a free base BzImPA, due to the pronounced difference in the length of the two axes. **Zn-11** has a tall shoulder on the longer wavelength side of the band, and may have two distinct transition dipole moments as in **Zn-13**, but the two dipole moments may overlap so extensively as to appear to be one band. The two regioisomers of **Zn-13**, of C<sub>2h</sub> and C<sub>2v</sub> symmetry, show almost identical spectra. The extinction coefficients of **Zn-13b** are minutely smaller than those of **Zn-13a**, and the ratio of the intensity of the two Q bands to one another in **Zn-13a** is slightly lower (3%) than the corresponding ratio of Q bands in **Zn-13b**. The fluorescence quantum yields are slightly different, but both are still in an acceptable range for zinc phthalocyanine-type compounds. These two diethynyl constructs are essentially equivalent and their deprotected derivatives **Zn-16a** and **Zn-16b** should be of equal utility as polymerizable extra-annulated phthalocyanines.

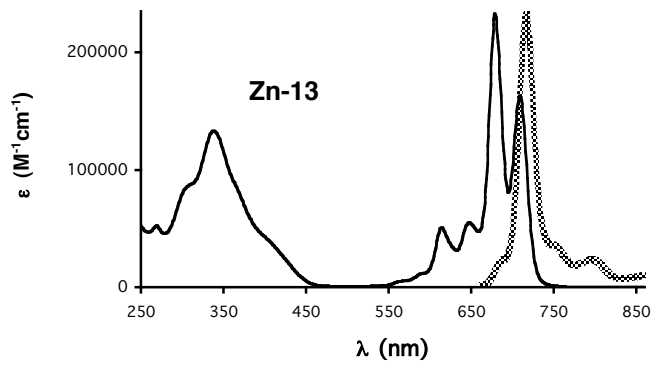
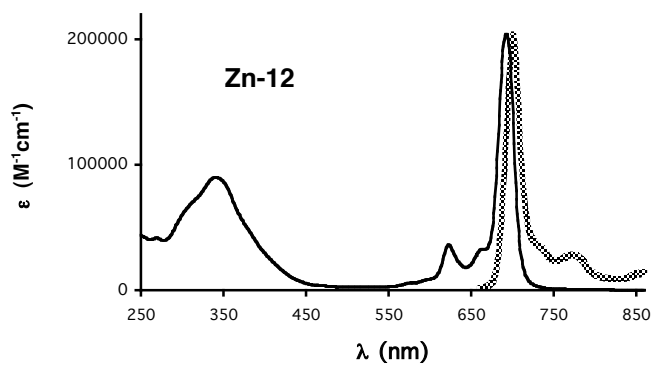
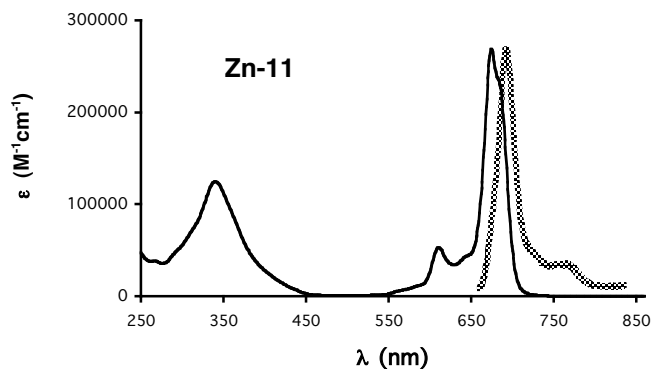


Figure 4.3. Absorption and emission spectra for low symmetry zinc-benzimidazoporphyrazines.

### C. Conclusion.

A new basic route to benzimidazoporphyrnazines has been developed, and the photochemical characteristics of some generic examples have been detailed. Benzimidazoporphyrnazines exhibit absorption spectra that are slightly red-shifted with respect to that of typical phthalocyanines, and have large extinction coefficients and high fluorescence quantum yields. The free base and zinc chelate forms of an axially oriented A<sub>3</sub>B macrocycle have been prepared. A regioisomeric pair of linear, *trans*-diethynyl-benzimidazoporphyrnazines has been prepared as precursors for polymerization studies. These compounds, although of lowered symmetry (C<sub>2v</sub>, C<sub>2h</sub>), are essentially phthalocyanine-like in their photochemical behavior.

## D. Experimental Section.

**General.**  $^1\text{H}$  (400 MHz) and  $^{13}\text{C}$  (100 MHz) NMR spectra were obtained in  $\text{CDCl}_3$  unless noted otherwise. Silica gel (Scientific Adsorbents, 40  $\mu\text{m}$  average particle size) was used for column chromatography. Anhydrous  $\text{CH}_2\text{Cl}_2$  was purchased from Aldrich. Aldehydes **4b** and **4c** were purchased from Aldrich and used as received. All other chemicals were reagent grade and were used as received. Benzimidazoles **5b** and **5c** were not isolated but were carried forward to the corresponding products **6b** and **6c**. Photochemical data were measured using THF as solvent. Fluorescence quantum yields were measured by comparison to tetra-*tert*-butylphthalocyanine, which was itself measured in both THF and  $\text{CHCl}_3$  set at  $\Phi_f = 0.70$  in THF (by comparison to the reported  $\Phi_f$  of 0.77 for tetra-*tert*-butylphthalocyanine in  $\text{CHCl}_3$  with correction for the indices of refraction of the different samples).<sup>18a</sup>

**Noncommercial Compounds:** Compounds **4a**,<sup>20</sup> **4d**,<sup>21</sup> **9**,<sup>22,23</sup> **15**,<sup>24</sup> and **16**<sup>25</sup> were prepared according to the literature.

**1,2-Diido-4,5-dinitrobenzene (1).** A three-necked 100 mL round-bottom flask was charged with oleum (38 mL of a 20% solution, 0.18 mol  $\text{SO}_3$ ), and a magnetic stirring bar. The flask was fitted with a condenser and a bubbler and the spare necks were closed with glass stoppers. The flask was placed in an oil bath heated to 120 °C. Iodine (6.86 g, 27.0 mmol) was added to the flask. After 20 min, *o*-dinitrobenzene (4.54 g, 27.0 mmol) was added to the reaction vessel, and the reaction was heated for 75 min, and then removed from heat and immediately poured into a 1 L conical flask filled with ice. The crude mixture was quenched with NaOH pellets until it was slightly alkaline to pH paper, with more ice added to keep the mixture cold. The mixture was then filtered through filter paper and the filtrate

was extracted with CHCl<sub>3</sub>. The organic layer of the extraction was washed with aqueous Na<sub>2</sub>S<sub>2</sub>O<sub>5</sub>, water, and brine, dried over Na<sub>2</sub>SO<sub>4</sub>, filtered, and concentrated to dryness. The dark brown filter cake was stirred with 200 mL of hot water to which Na<sub>2</sub>S<sub>2</sub>O<sub>5</sub> was added until no further bubbling was observed. The mixture was then filtered and the filtrate was discarded. The filter cake and the residue from the extraction were recrystallized (EtOH/water) yielding dark brown crystals (4.47 g, 39%): mp 183–184 °C (lit.<sup>33</sup> mp 184 °C); <sup>1</sup>H NMR δ 8.31 (s, 2H); <sup>13</sup>C NMR δ 114.6, 134.8; Anal. Calcd for C<sub>6</sub>H<sub>2</sub>I<sub>2</sub>N<sub>2</sub>O<sub>4</sub>: C, 17.16; H, 0.48; N, 6.67; Found: C, 17.44; H, 0.41, 6.61.

*Scale-up:* The above procedure was followed with the following quantities of reagents: oleum (200 mL), iodine (37.80 g), *o*-dinitrobenzene (25.0 g). To quench the large volume of SO<sub>2</sub> produced by the reaction, the evolved gas was bubbled through a solution of aqueous NaOH (5 M, 1 L), which was later used to quench the acidic crude reaction mixture over ice, along with an additional 125 g of NaOH, followed by Na<sub>2</sub>S<sub>2</sub>O<sub>5</sub> (18.5 g). The CHCl<sub>3</sub> extraction of the initial crude filtrate was omitted. Yield: 32%. Characterization data were consistent with the smaller scale reaction.

**1,2-Diamino-4,5-diiiodobenzene (2).** Following a literature procedure,<sup>26</sup> a sample of **1** (17.42 g, 41.5 mmol) and a magnetic stirring bar were added to a 500 mL conical flask fitted with a jacketed condenser. EtOH (95%, 150 mL) and conc. aqueous HCl (68.6 mL, 0.83 mol) were added, and the mixture was stirred and heated to boiling. Fe (18.59 g, 0.332 mol) was added in portions, resulting in foaming of the mixture and accelerated refluxing of the EtOH, which would subside within a few minutes of each addition. The reaction was heated for an additional 45 min beyond the final addition of Fe. A hot solution of EDTA (156 g, 0.411 mol, in 300 mL H<sub>2</sub>O) was added to the reaction mixture, and KOH pellets were

added until the solution was alkaline to pH paper. The hot mixture was extracted twice with ethyl acetate and the extracts were combined, washed with water, followed by brine, dried over Na<sub>2</sub>SO<sub>4</sub>, filtered and concentrated to dryness. The residue was recrystallized (EtOH/water), giving tan needles (9.92 g, 66%): mp 135–136 °C; <sup>1</sup>H NMR (d<sub>8</sub>-THF) δ 4.21 (brs, 4H), 7.03 (s, 2H); <sup>13</sup>C NMR (d<sub>8</sub>-THF) δ 91.1, 124.5, 137.6; Anal. Calcd for C<sub>6</sub>H<sub>6</sub>I<sub>2</sub>N<sub>2</sub>: C, 20.02; H, 1.68; N, 7.78; Found: C, 20.19; H, 1.59, 7.71.

**1,2-Diamino-4,5-dicyanobenzene (3).** A 50 mL round-bottom flask was charged with **2** (6.94 g, 19.3 mmol), and CuCN (6.91 g, 77.2 mmol, 4 eq), and a magnetic stirring bar. The vessel was capped with a septum and flushed with Ar for 10 min, and NMP (20 mL) was added. The vessel was heated to 120 °C for 3 h, then diluted with DMF (20 mL) and added to a hot aqueous solution of EDTA (88 g, 232 mmol, in 500 mL H<sub>2</sub>O) in a 1 L conical flask. Oxygen was bubbled through the mixture as it was stirred and heated for 2 h. After 2 h of this treatment, the dark heterogeneous mixture turned to a homogeneous green solution. The hot green solution was extracted twice with ethyl acetate, and the extracts were washed with water, followed by brine, dried over Na<sub>2</sub>SO<sub>4</sub>, filtered, and concentrated to dryness. The residue was recrystallized (EtOH/water), giving tiny tan needles (1.66 g, 55%): mp 262–264 °C (lit. mp 193–195<sup>29b</sup> or 272–275<sup>31</sup> °C); <sup>1</sup>H NMR (d<sub>6</sub>-acetone) δ 5.40 (br s, 4H), 7.04 (s, 2H); <sup>13</sup>C NMR (d<sub>6</sub>-acetone) δ 103.8, 117.1, 117.4, 139.4; FAB-MS obsd 158.0591, calcd 158.0592 (C<sub>6</sub>H<sub>6</sub>N<sub>4</sub>).

**5,6-Dicyano-2-(undec-7-yl)benzimidazole (5a).** A 100 mL round-bottom flask was charged with **3** (1.32 g, 8.37 mmol), pentanol (42 mL), 2-hexyl-1-octanal<sup>20</sup> (1.77 g, 8.37 mmol), and a magnetic stirring bar. The flask was fitted with a Hickman still and placed in an oil bath heated to 120 °C. NMP (4.0 mL) was added to fully dissolve the solid material.

The mixture was heated and stirred for 2 h. Then  $\text{FeCl}_3 \cdot 6\text{H}_2\text{O}$  (113 mg, 0.42 mmol) was added to the reaction vessel and oxygen was bubbled through the mixture as it was heated and stirred for an additional 12 h. The reaction mixture was then removed from heat and added to 200 mL diethyl ether. The ether solution was washed three times with water, then washed with brine, dried over  $\text{Na}_2\text{SO}_4$ , filtered, and concentrated to dryness. The residue was chromatographed (silica,  $\text{CHCl}_3$ ), yielding a tan solid (2.37 g, 81%): mp 148–149 °C;  $^1\text{H}$  NMR  $\delta$  0.82 (t,  $J = 7.6$  Hz, 6H), 1.10–1.30 (m, 16H), 1.77–1.87 (m, 2H), 2.90–3.04 (m, 1H), 8.07 (br s, 2H), 10.36 (br s, 1H);  $^{13}\text{C}$  NMR  $\delta$  14.2, 22.8, 27.7, 29.4, 31.8, 34.9, 41.3, 108.4, 117.0, 165.3; FAB-MS obsd 351.2551, calcd 351.2549 ( $\text{C}_{22}\text{H}_{30}\text{N}_4$ ).

**5,6-Dicyano-2-(4-(triisopropylsilylethynyl)phenyl)benzimidazole (5d).** A 25 mL round-bottom flask was charged with **3** (468 mg, 2.96 mmol), NMP (15 mL), **4d**<sup>21</sup> (847 mg, 2.96 mmol), and a magnetic stirring bar. The flask was fitted with a Hickman still, placed in an oil bath heated to 120 °C, and stirred for 1 h. Then  $\text{FeCl}_3 \cdot 6\text{H}_2\text{O}$  (296  $\mu\text{L}$  of a 100 mM solution, 30  $\mu\text{mol}$ ) was added to the reaction vessel and oxygen was bubbled through the mixture as it was heated and stirred for an additional 20 h. The reaction mixture was then removed from heat and added to ethyl acetate. The ethyl acetate solution was washed three times with water, then washed with brine, dried over  $\text{Na}_2\text{SO}_4$ , filtered, and concentrated to dryness. The residue was chromatographed (silica,  $\text{CHCl}_3$ , 2% ethyl acetate), yielding a colorless solid (732 mg, 58%). mp 347–348 °C;  $^1\text{H}$  NMR ( $d_6$ -acetone)  $\delta$  1.15–1.18 (m, 21H), 7.05 (d,  $J = 8.4$  Hz, 2H), 8.24–8.28 (m, 4H);  $^{13}\text{C}$  NMR ( $d_6$ -acetone)  $\delta$  11.5, 18.5, 93.5, 106.7, 108.4, 116.7, 118.4, 122.1 (br), 126.3, 127.6, 128.7, 132.7, 142.0 (br), 156.4; FAB-MS obsd 425.2161, calcd 425.2083 [ $(\text{M} + \text{H})$ ,  $\text{M} = \text{C}_{26}\text{H}_{28}\text{N}_4\text{Si}$ ].

**Synthesis of 5d directly from 2:** A 2-necked 25 mL flask was charged with **2** (577 mg, 1.60 mmol), CuCN (573 mg, 6.40 mmol), and NMP (2 mL). The vessel was fitted with a bubbler and the sidearm was capped with a septum. The mixture was heated at 120 °C for 2 h, and then more NMP (8 mL) and **4d**<sup>21</sup> (458 mg, 1.60 mmol) were added and O<sub>2</sub> was bubbled through the mixture. After 40 min, TLC (silica, CHCl<sub>3</sub>, 4% isopropanol) showed the desired product and no remaining **3** or **4d**, so the mixture was transferred to a 500 mL conical flask containing a hot solution of aqueous EDTA (4.87 g, 12.8 mmol, in 200 mL) and the mixture was heated and stirred for 30 min, and then filtered. The filter cake was dried in vacuo and chromatographed (silica, CH<sub>2</sub>Cl<sub>2</sub>, 2% ethyl acetate), giving a colorless solid (280 mg, 41%). Characterization data were identical with the preparation from **3** above.

**5,6-Dicyano-1-propyl-2-(undec-7-yl)benzimidazole (6a).** A 10 mL round-bottom flask was charged with **5a** (743 mg, 2.12 mmol), and CH<sub>3</sub>CN (2.0 mL). The flask was capped with a septum and placed in an oil bath heated to 80 °C. DBU (317 µL, 2.12 mmol) was added, and the mixture was stirred for 2 min. Then iodopropane (207 µL, 2.12 mmol) was added and the mixture was stirred for 20 min. A second dose of DBU (317 µL, 2.12 mmol), followed by iodopropane (207 µL, 2.12 mmol), was added, and 20 min later, a third identical round of DBU and iodopropane was again added. HPLC analysis of the reaction mixture (C-18 reverse phase, CH<sub>3</sub>CN as isocratic eluent) indicated that the yields of the reaction after the first, second, and third round of reagents were 60%, 78%, and 97%, respectively. After the third round of reagents was added and the mixture was stirred for 20 min, the reaction mixture was removed from heat and added to 200 mL diethyl ether. The ether solution was washed three times with water, then washed with brine, dried over Na<sub>2</sub>SO<sub>4</sub>, filtered, and concentrated to dryness. The residue was chromatographed (silica,

hexanes/ethyl acetate 7:1, then hexanes/ethyl acetate 6:1), yielding a tan solid (786 mg, 94%): mp 52–53 °C; <sup>1</sup>H NMR δ 0.81 (t, *J* = 6.8 Hz, 6H), 1.02 (t, *J* = 7.2 Hz, 3H), 1.05–1.13 (m, 16H), 1.72–1.82 (m, 6H), 2.88–2.98 (m, 1H), 4.15 (t, *J* = 7.6 Hz, 2H); <sup>13</sup>C NMR δ 11.6, 14.2, 14.2, 22.8, 23.8, 27.8, 29.5, 31.8, 35.2, 38.3, 45.9, 107.8, 108.4, 116.2, 116.9, 117.0, 125.8, 137.0, 145.3, 165.5; Anal. Calcd for C<sub>25</sub>H<sub>36</sub>N<sub>4</sub>: C, 76.49; H, 9.24; N, 14.27; Found C, 17.38; H, 9.36; N, 14.18.

**5,6-Dicyano-2-phenyl-1-propylbenzimidazole (6b).** A 25 mL round-bottom flask was charged with **3** (316 mg, 2.00 mmol), NMP (10 mL), benzaldehyde, (202 μL, 2.00 mmol), and a magnetic stirring bar. The flask was fitted with a Hickman still, placed in an oil bath heated to 120 °C, and stirred for 1 h. Then FeCl<sub>3</sub>·6H<sub>2</sub>O (27 mg, 0.10 mmol) was added to the reaction vessel and oxygen was bubbled through the mixture as it was heated and stirred for an additional 20 h. The reaction mixture was then removed from heat and added to ethyl acetate. The ethyl acetate solution was washed three times with water, then washed with brine, dried over Na<sub>2</sub>SO<sub>4</sub>, filtered, and concentrated to dryness. The residue (458 mg, 1.88 mmol) was dissolved in NMP (2 mL) and heated to 80 °C. Then DBU (280 μL, 1.88 μmol) was added and the mixture was stirred for 2 min, and iodopropane (183 μL, 1.88 mmol) was added. After 20 min, the mixture was treated with a second round of DBU and iodopropane, and after an additional 20 min, a third round of reagents was added. After a final 20 min of heating, the mixture was transferred to ethyl acetate and washed three times with water, followed by brine. After drying the organic layer over Na<sub>2</sub>SO<sub>4</sub>, the mixture was filtered, concentrated to dryness, and chromatographed (silica, CH<sub>2</sub>Cl<sub>2</sub>, 3% ethyl acetate, 1% isopropanol), yielding an off-white solid (253 mg, 44%): mp 183–185 °C; <sup>1</sup>H NMR (CDCl<sub>3</sub>) δ 0.90 (t, *J* = 7.6 Hz, 2H), 1.81–1.92 (m, 2H), 4.29 (t, *J* = 7.6 Hz, 2H), 7.56–7.62 (m, 3H),

7.70–7.73 (m, 2H), 7.89 (s, 1H), 8.20 (s, 1H);  $^{13}\text{C}$  NMR ( $\text{CDCl}_3$ )  $\delta$  11.4, 23.5, 47.3, 108.7, 109.0, 116.7, 116.8, 116.9, 126.6, 128.8, 129.5, 129.5, 131.4, 137.8, 145.4, 159.5; FAB-MS obsd 287.1302, calcd 287.1297 [ $(\text{M}+\text{H})^+$ ;  $\text{M} = \text{C}_{18}\text{H}_{14}\text{N}_4$ ].

**5,6-Dicyano-2-(4-iodophenyl)-1-propylbenzimidazole (6c).** A 25 mL round-bottom flask was charged with **3** (340 mg, 2.15 mmol), NMP (10 mL), 4-iodobenzaldehyde, (499 mg, 2.15 mmol), and a magnetic stirring bar. The flask was fitted with a Hickman still, placed in an oil bath heated to 120 °C, and stirred for 1 h. Then  $\text{FeCl}_3 \cdot 6\text{H}_2\text{O}$  (29 mg, 0.11 mmol) was added to the reaction vessel and oxygen was bubbled through the mixture as it was heated and stirred for an additional 24 h. The reaction mixture was then removed from heat and added to ethyl acetate. The ethyl acetate solution was washed three times with water, then washed with brine, dried over  $\text{Na}_2\text{SO}_4$ , filtered, and concentrated to dryness. The residue (603 mg, 1.63 mmol) was suspended in  $\text{CH}_3\text{CN}$  and heated to 80 °C. Then DBU (243  $\mu\text{L}$ , 1.63  $\mu\text{mol}$ ) was added and the mixture was stirred for 2 min, and iodopropane (159  $\mu\text{L}$ , 1.63 mmol) was added. After 20 min, the mixture was treated with a second round of DBU and iodopropane, and after an additional 20 min, a third round of reagents was added. After a final 20 min of heating, the mixture was transferred to ethyl acetate and washed three times with water, followed by brine. After drying the organic layer over  $\text{Na}_2\text{SO}_4$ , the mixture was filtered, concentrated to dryness, and chromatographed (silica,  $\text{CHCl}_3$ , 5% ethyl acetate), giving a white solid (440 mg, 50%): mp 208–209 °C;  $^1\text{H}$  NMR ( $\text{CDCl}_3$ )  $\delta$  0.91 (t,  $J = 7.6$  Hz, 3H), 1.80–1.91 (m, 2H) 4.26 (t,  $J = 7.6$  Hz, 2H), 7.46 (d,  $J = 8.0$  Hz, 2H), 7.87 (s, 1H), 7.95 (d,  $J = 8.0$  Hz, 2H), 8.22 (s, 1H);  $^{13}\text{C}$  NMR ( $\text{CDCl}_3$ )  $\delta$  11.4, 23.6, 47.4, 98.4, 109.0, 109.3, 116.55, 116.62, 116.9, 126.7, 128.2, 130.9, 137.8, 138.7, 145.3, 158.4; Anal. Calcd for  $\text{C}_{18}\text{H}_{13}\text{IN}_4$ : C, 52.45; H, 3.18; N, 13.59; Found: C, 52.40; H, 3.06; N, 13.40.

**5,6-Dicyano-2-(4-(triisopropylsilylethynyl)phenyl)-1-propylbenzimidazole (6d).**

A 20 mL vial was charged with **5d** (763 mg, 1.79 mmol), and NMP (10 mL). The vial was capped with a septum and placed in an oil bath heated to 120 °C. DBU (267 µL, 1.79 mmol) was added, and the mixture was stirred for 2 min. Then iodopropane (175 µL, 1.79 mmol) was added and the mixture was stirred for 20 min. A second dose of DBU (267 µL, 1.79 mmol), followed by iodopropane (175 µL, 1.79 mmol), was added, and 20 min later, a third identical round of DBU and iodopropane was again added. After the third round of reagents was added and the mixture was stirred for 20 min, the reaction mixture was removed from heat and added to ethyl acetate. The solution was washed three times with water, then washed with brine, dried over Na<sub>2</sub>SO<sub>4</sub>, filtered, and concentrated to dryness. The residue was chromatographed (silica, CHCl<sub>3</sub>), yielding a colorless solid (506 mg, 61%): mp 242–243 °C; <sup>1</sup>H NMR (d<sub>6</sub>-acetone) δ 0.89 (t, *J* = 7.2 Hz, 3H), 1.17–1.19 (m, 21H), 1.86–1.96 (m, 2H), 4.53 (t, *J* = 7.6 Hz, 2H), 7.75 (d, *J* = 8.0 Hz, 2H), 7.91 (d, *J* = 8.0 Hz, 2H), 8.36 (s, 1H), 8.50 (s, 1H); <sup>13</sup>C NMR (d<sub>6</sub>-acetone) δ 10.5, 11.3, 18.4, 23.2, 47.1, 93.1, 106.6, 108.1, 108.3, 116.8, 116.9, 118.3, 125.8, 126.3, 129.6, 129.9, 132.5, 138.5, 145.4, 158.4; Anal. Calcd for C<sub>29</sub>H<sub>34</sub>N<sub>4</sub>Si: C, 74.63; H, 7.34; N, 12.01; Found: C, 74.75; H, 7.32; N, 12.01.

**Tetrakis(2-tridec-7-yl-1-propylbenzimidazo[5,6-*b*:5',6'-*g*:5'',6''-*l*:5''',6''''-*q*])porphyrazine (Fb-7).** A 5 mL reaction vial was charged with **6a** (150 mg, 382 µmol), pentanol (1.90 mL), and a magnetic stirring bar. The vial was capped and heated in a heating block set at 145 °C and then DBU (57 µL, 382 µmol) was added. Heating and stirring continued for 18 h. The vial was then removed from heat, and upon cooling to room temperature, the mixture was diluted with 18 mL of MeOH, and then centrifuged. The supernatant was removed and the pellet was resuspended in MeOH and centrifuged again.

After removing the supernatant the second time, the pellet was redissolved in THF (2 mL) and precipitated by addition of MeOH (18 mL). The mixture was centrifuged, and upon removal of the supernatant, the pellet was dried in vacuo, revealing a green solid (17 mg, 11%):  $^1\text{H}$  NMR ( $\text{d}_8$ -THF)  $\delta$  0.30–0.50 (br s, 2H), 0.80–1.00 (m, 24H), 1.17–1.60 (m, 76H), 1.80–2.10 (m, 8H), 2.10–2.42 (m, 16H), 3.10–3.25 (m, 2H), 3.30–3.40 (m, 2H), 4.30–4.50 (m, 4H), 4.70–4.84 (m, 4H), 9.30–9.70 (m, 8H); LD-MS obsd 1570.8; FAB-MS obsd 1571.2178, calcd 1571.1916 ( $\text{C}_{100}\text{H}_{146}\text{N}_{16}$ );  $\lambda_{\text{abs}}$  (nm) 309, 342, 376, 640, 676, 713, 737;  $\lambda_{\text{em}}$  742 nm;  $\Phi_f = 0.59$ .

**Preparation of Fb-7 using Lithium pentoxide:** A 5 mL reaction vial was charged with a magnetic stirring bar, pentanol (1.0 mL), and Li ribbon (23 mg, 3.3 mmol). The vial was capped, vented and warmed to 90 °C. After all of the Li was consumed (40 min) the vial was removed from heat and allowed to cool to room temperature. Then a pentanol solution of **6a** (150 mg, 0.382 mmol, in 1.0 mL) was added, and the vial was capped and heated to 140 °C for 4 h. The vial was then removed from heat and, upon cooling to room temperature, the reaction mixture was diluted into 18 mL of MeOH (2%  $\text{CH}_3\text{CO}_2\text{H}$ ). The mixture was centrifuged, and the supernatant was removed. The supernatant was removed and the pellet was resuspended in MeOH and centrifuged again. After removing the supernatant the second time, the pellet was redissolved in THF (2 mL) and precipitated by addition of MeOH (18 mL). The mixture was centrifuged, and upon removal of the supernatant, the pellet was dried in vacuo, giving a green solid (74 mg, 49%). Characterization data were consistent with the material produced from the DBU-mediated reaction (vide supra).

**Tetrakis(2-tridec-7-yl-1-propylbenzimidazo[5,6-*b*:5',6'-*g*:5'',6''-*l*:5''',6'''-*q*])porphyrzinatomagnesium(II) (**Mg-7**).** A 5 mL reaction vial was charged with **6a** (150 mg, 382  $\mu$ mol), MgCl<sub>2</sub> (13 mg, 96  $\mu$ mol), pentanol (1.90 mL), and a magnetic stirring bar. The vial was capped and heated in a heating block set at 145 °C and then DBU (57  $\mu$ L, 382  $\mu$ mol) was added. Heating and stirring continued for 18 h. The vial was then removed from heat, and upon cooling to room temperature, the mixture was diluted with 16 mL of MeOH and 2 mL of water, and then centrifuged. The supernatant was removed and the pellet was resuspended in MeOH/water (8:1), and centrifuged again. After removing the supernatant the second time, the pellet was redissolved in THF (2 mL) and precipitated by addition of MeOH (16 mL) and water (2 mL). The mixture was centrifuged, and upon removal of the supernatant, the pellet was dried in vacuo, giving a green solid (41 mg, 27%): <sup>1</sup>H NMR (d<sub>8</sub>-THF)  $\delta$  0.82–0.96 (m, 24H), 1.16–1.58 (m, 76H), 1.87–2.02 (m, 8H), 2.18–2.36 (m, 16H), 3.24–3.34 (m, 4H), 4.66–4.74 (m, 8H), 9.40 (s, 2H), 9.47 (s, 2H), 9.65 (s, 2H), 9.68 (s, 2H); LD-MS obsd 1592.7; FAB-MS obsd 1593.1650, calcd 1593.1610 (C<sub>100</sub>H<sub>144</sub>MgN<sub>16</sub>);  $\lambda_{\text{abs}}$  (nm) 310, 363, 640, 680, 713;  $\lambda_{\text{em}}$  720 nm;  $\Phi_f$  = 0.69.

**Tetrakis(2-tridec-7-yl-1-propylbenzimidazo[5,6-*b*:5',6'-*g*:5'',6''-*l*:5''',6'''-*q*])porphyrzinatozinc(II) (**Zn-7**).** A 5 mL reaction vial was charged with **6a** (150 mg, 382  $\mu$ mol) and a magnetic stirring bar. The vial was then introduced into a glovebox under Argon atmosphere and ZnCl<sub>2</sub> (13 mg, 96  $\mu$ mol) was added. The vial was capped and removed from the glove box, and pentanol (1.90 mL) was added. The vial was heated to 140 °C in a heating block and then DBU (57  $\mu$ L, 382  $\mu$ mol) was added. The temperature of the heating block was raised to 145 °C and continued for 18 h. The vial was then removed from heat, and upon cooling to room temperature, the mixture was diluted with 16 mL of MeOH

and 2 mL of water, and then centrifuged. The supernatant was removed and the pellet was resuspended in MeOH and centrifuged again. After removing the supernatant the second time, the pellet was redissolved in THF (2 mL) and precipitated by addition of MeOH (16 mL) and water (2 mL). The mixture was centrifuged, and upon removal of the supernatant, the pellet was dried in vacuo, giving a green solid (72 mg, 46%):  $^1\text{H}$  NMR ( $\text{d}_8$ -THF)  $\delta$  0.82–0.95 (m, 24H), 1.20–1.60 (m, 76H), 1.88–2.05 (m, 8H), 2.17–2.35 (m, 16H), 3.20–3.35 (m, 4H), 4.60–4.80 (m, 8H), 9.45 (s, 2H), 9.50 (s, 2H), 9.64–9.74 (m, 4H); LD-MS obsd 1633.0; FAB-MS obsd 1633.1111, calcd 1633.1051 ( $\text{C}_{100}\text{H}_{144}\text{N}_{16}\text{Zn}$ );  $\lambda_{\text{abs}}$  (nm) 309, 357, 640, 681, 713;  $\lambda_{\text{em}}$  724 nm;  $\Phi_f = 0.47$ .

**Tetrakis(2-phenyl-1-propylbenzimidazo[5,6-*b*:5',6'-*g*:5'',6''-*l*:5''',6'''-*q*])porphyrazine (Fb-8).** A 5 mL reaction vial was charged with **6b** (50.0 mg, 0.175  $\mu\text{mol}$ ), pentanol (875  $\mu\text{L}$ ) and a magnetic stirring bar. The vial was capped and heated in a heating block set to 145 °C and then DBU (26  $\mu\text{L}$ , 175  $\mu\text{mol}$ ) was added. Heating and stirring continued for 18 h. The vial was then removed from heat, and upon cooling to room temperature, the mixture was diluted with 18 mL of MeOH, and then centrifuged. The supernatant was removed and the pellet was resuspended in MeOH and centrifuged again. This suspension-centrifugation procedure was repeated a third time. After removing the supernatant the third time, the pellet was redissolved in THF (4 mL) and precipitated by addition of MeOH (15 mL) and water (0.5 mL). The mixture was centrifuged, and upon removal of the supernatant, the pellet was dried in vacuo, giving a green solid (19 mg, 38%). The sample was found to be a regioisomeric mixture of products, which resulted in some  $^1\text{H}$  NMR resonances having non-integer integrations:  $^1\text{H}$  NMR ( $\text{d}_8$ -THF)  $\delta$  -3.13 (br s, 2H), 1.02–1.25 (m, 12H), 2.04–2.34 (m, 8H), 4.18–4.56 (m, 8H), 7.50–7.70 (m 12H), 7.90–8.08

(m, 8H), 8.12–8.22 (br s, 1H), 8.28–8.77 (m, 5H), 8.90–8.96 (m, 0.5H), 9.00–9.12 (m, 1.5H); LD-MS obsd, 1146.7; FAB-MS obsd 1147.5127, calcd 1147.5109 [(M+H)<sup>+</sup>; M = C<sub>72</sub>H<sub>58</sub>N<sub>16</sub>];  $\lambda_{\text{abs}}$  (nm) 316, 382, 648, 679, 718, 740;  $\lambda_{\text{em}}$  744 nm;  $\Phi_f$  = 0.70.

**Preparation of Fb-8 using Lithium pentoxide:** A 5 mL reaction vial was charged with a magnetic stirring bar, pentanol (875  $\mu$ L), and Li ribbon (10.0 mg, 1.44 mmol). The vial was capped, vented and warmed to 90 °C. After all of the Li was consumed (1 h) the vial was removed from heat and allowed to cool to room temperature. Then **6b** (50 mg, 175  $\mu$ mol) was added, and the vial was heated in a heating block set to 145 °C for 18 h. The vial was then removed from heat and, upon cooling to room temperature, the reaction mixture was diluted into 18 mL of MeOH (2% CH<sub>3</sub>CO<sub>2</sub>H). The mixture was centrifuged, and the supernatant was removed. The supernatant was removed and the pellet was resuspended in MeOH and centrifuged again. This suspension-centrifugation procedure was repeated a third time. After removing the supernatant the third time, the pellet was redissolved in THF (4 mL) and precipitated by addition of MeOH (15 mL) and water (0.5 mL). The mixture was centrifuged again, and upon removal of the supernatant, the pellet was dried in vacuo, giving a green solid (14 mg, 28%). Characterization data were consistent with the material produced from the DBU-mediated reaction (vide supra).

**Tetrakis(2-phenyl-1-propylbenzimidazo[5,6-*b*:5',6'-*g*:5'',6''-*l*:5''',6''''-*q*])porphyrazinatomagnesium(II) (**Mg-8**).** A 5 mL reaction vial was charged with **6b** (50.0 mg, 0.175  $\mu$ mol), MgCl<sub>2</sub> (4.2 mg, 44  $\mu$ mol), pentanol (875  $\mu$ L) and a magnetic stirring bar. The vial was capped and heated in a heating block set to 145 °C and then DBU (26  $\mu$ L, 175  $\mu$ mol) was added. Heating and stirring continued for 18 h. The vial was then removed from heat, and upon cooling to room temperature, the mixture was diluted with 18 mL of MeOH,

and then centrifuged. The supernatant was removed and the pellet was resuspended in MeOH and centrifuged again. This suspension-centrifugation procedure was repeated a third time. After removing the supernatant the third time, the pellet was redissolved in THF (4 mL) and precipitated by addition of MeOH (15 mL) and water (0.5 mL). The mixture was centrifuged, and upon removal of the supernatant, the pellet was dried in vacuo, giving a green solid (33 mg, 65%):  $^1\text{H}$  NMR ( $\text{d}_8$ -THF)  $\delta$  1.12–1.22 (m, 12H), 2.22–2.34 (m, 8H), 4.83–4.92 (m, 8H), 7.59–7.72 (m, 12H), 8.06–8.12 (m, 8H), 9.55 (br s, 2H), 9.63 (br s, 2H), 9.76–9.84 (m, 4H); LD-MS obsd, 1168.8; FAB-MS obsd 1168.4695, calcd 1168.4724 ( $\text{C}_{72}\text{H}_{56}\text{MgN}_{16}$ );  $\lambda_{\text{abs}}$  (nm) 314, 364, 643, 684, 717;  $\lambda_{\text{em}}$  724 nm;  $\Phi_f = 0.84$ .

**Tetrakis(2-phenyl-1-propylbenzimidazo[5,6-*b*:5',6'-*g*:5'',6''-*l*:5''',6'''-*q*])porphyrazinatozinc(II) (Zn-8).**

A 5 mL reaction vial was charged with **6b** (50.0 mg, 0.175  $\mu\text{mol}$ ), and a magnetic stirring bar. The vial was then introduced into a glovebox under an argon atmosphere and  $\text{ZnCl}_2$  (6.0 mg, 44  $\mu\text{mol}$ ) was added. The vial was capped and removed from the glove box, and pentanol (875  $\mu\text{L}$ ) was added. The vial was capped and heated in a heating block set to 145 °C and then DBU (26  $\mu\text{L}$ , 175  $\mu\text{mol}$ ) was added. Heating and stirring continued for 18 h. The vial was then removed from heat, and upon cooling to room temperature, the mixture was diluted with 18 mL of MeOH, and then centrifuged. The supernatant was removed and the pellet was resuspended in MeOH and centrifuged again. This suspension-centrifugation procedure was repeated a third time. After removing the supernatant the third time, the pellet was redissolved in THF (4 mL) and precipitated by addition of MeOH (15 mL) and water (0.5 mL). The mixture was centrifuged, and upon removal of the supernatant, the pellet was dried in vacuo, giving a green solid (33 mg, 62%). The sample was found to be a regiosomeric mixture of products,

which resulted in some  $^1\text{H}$  NMR resonances having non-integer integrations:  $^1\text{H}$  NMR ( $\text{d}_8$ -THF)  $\delta$  1.11–1.21 (m, 12H), 2.20–2.33 (m, 8H), 4.72–4.86 (m, 8H), 7.60–7.71 (m, 12H), 8.05–8.12 (m, 8H), 9.30–9.43 (m, 4H), 9.49 (s, 0.5H), 9.59, (br s, 1.5H), 9.66 (s, 0.5H), 9.71–9.74 (m, 1.5H); LD-MS obsd, 1208.6; FAB-MS obsd 1208.4205, calcd 1208.4165 ( $\text{C}_{72}\text{H}_{56}\text{N}_{16}\text{Zn}$ );  $\lambda_{\text{abs}}$  (nm) 315, 357, 643, 685, 717;  $\lambda_{\text{em}}$  724 nm;  $\Phi_f = 0.43$ .

**Preparative-scale macrocyclization reaction using **6d** and 1,2-dicyanobenzene:**

A 2-necked 25 mL round-bottom flask was charged with **6d** (317 mg, 0.679 mmol), dicyanobenzene (130 mg, 1.02 mmol, 1.5 equiv), and a magnetic stirring bar. The flask was fitted with a condenser and a bubbler, and a septum for the second neck. The apparatus was flushed for 20 min with a stream of argon, and then briefly opened to add  $\text{ZnCl}_2$  (58 mg, 0.43 mmol). Then pentanol (8.5 mL) and the mixture was gradually heated to reflux. When the mixture was homogeneous, DBU (254  $\mu\text{L}$ , 1.70 mmol) was added. Heating and stirring at reflux temperature was continued overnight (12 h). The mixture was then cooled to room temperature, and diluted into MeOH (300 mL) and water (50 mL). The resulting precipitate was filtered, rinsed with EtOH, and dried in vacuo. The residue was then dissolved in THF and eluted through a short plug of silica gel in THF, and chromatographed over a column of Bio-Beads SX-3 in THF. The mixture separated into three bands. The first band (green) appeared (by HPLC-SEC analysis) to contain compounds containing two and more-than-two benzimidazoles. The second band (blue) contained **Zn-11**. The third band (blue) contained **Zn-10**. The fractions containing **Zn-10** and **Zn-11** were set aside, and the first band of green material was reconcentrated and chromatographed over a column of Bio-Beads SX-1. The mixture separated into two broad green bands. The first band, containing pigments having three and four benzimidazoles, could not be further purified by any chromatographic method,

and was therefore discarded. The second green band contained a mixture of **Zn-12** and **Zn-13**. The mixture was separated by chromatography (silica, CHCl<sub>3</sub>, 2% isopropanol).

**Zinc Phthalocyanine (Zn-10, A<sub>4</sub>).** The compound was isolated as a blue band from chromatography on Bio-Beads SX-3 (vide supra). The THF solution was concentrated and the residue was chromatographed over a short column (silica, CHCl<sub>3</sub>, 2% isopropanol). Fractions containing the product were concentrated, giving a blue solid (10 mg, 4%): <sup>1</sup>H NMR (d<sub>8</sub>-THF) δ 8.17–8.23 (m, 8H), 9.45–9.50 (m, 8H); LD-MS obsd, 576.3; FABMS obsd 576.0813, calcd 576.0789 (C<sub>32</sub>H<sub>16</sub>N<sub>8</sub>Zn); λ<sub>abs</sub> 666 nm.

**Tribenzo[*g,l,q*]-{2-(4-(2-triisopropylsilyl)ethynyl)phenyl}-1-propylbenzimidazo[5,6-*b*]porphyrazinatozinc(II) (Zn-11, A<sub>3</sub>B).** The compound was isolated as a blue band from chromatography on Bio-Beads SX-3 (vide supra). The THF solution was concentrated and the residue was chromatographed over a short column (silica, CHCl<sub>3</sub>, 2% isopropanol). Fractions containing the product were concentrated, giving a blue solid (86 mg, 22%): <sup>1</sup>H NMR (d<sub>8</sub>-THF) δ 1.14 (t, *J* = 7.2 Hz, 3H), 1.27 (s, 21H), 2.16–2.26 (m, 2H), 4.75 (t, *J* = 7.6 Hz, 2H), 7.82 (d, *J* = 8.0 Hz, 2H), 8.00–8.15 (m, 8H), 9.09 (s, 1H), 9.13 (d, *J* = 7.6 Hz, 1H), 9.22–9.34 (m, 5H), 9.37 (s, 1H); LD-MS obsd, 914.7; FAB-MS obsd 914.2986, calcd 914.2968 (C<sub>53</sub>H<sub>46</sub>N<sub>10</sub>SiZn); λ<sub>abs</sub> (nm): 340, 611, 674; λ<sub>em</sub> 692 nm; Φ<sub>f</sub> = 0.47.

**Dibenzo[*l,q*]-{2-(4-(2-triisopropylsilyl)ethynyl)phenyl}-1-propylbenzimidazo[5,6-*b*:5',6'-*g*]porphyrazinatozinc(II) (Zn-12, cis-A<sub>2</sub>B<sub>2</sub>).** The compound was isolated from silica gel chromatography (vide supra) as the first green band and concentrated to give a green solid (74 mg, 14%): <sup>1</sup>H NMR (d<sub>8</sub>-THF) δ 1.09–1.20 (m, 6H), 2.15–2.30 (m, 4H), 4.81 (t, *J* = 7.6 Hz, 4H), 7.76–7.84 (m, 4H), 8.06–8.19 (m, 8H), 9.12–9.50 (m, 5H), 9.63 (s, 1H),

9.70 (s, 1H); LD-MS obsd 1252.5; FAB-MS obsd 1252.5148, calcd 1252.5146 ( $C_{74}H_{76}N_{12}Si_2Zn$ );  $\lambda_{abs}$  (nm): 340, 623, 693;  $\lambda_{em}$  701 nm;  $\Phi_f = 0.44$ .

**Dibenzo[*g,q*]-(*2*-{4-(2-triisopropylsilyl)ethynyl}phenyl)-1-propylbenzimidazo[5,6-*b*:5',6'-*I*]porphyrazinatozinc(II)-C<sub>2v</sub> (**Zn-13b**, *trans*-A<sub>2</sub>B<sub>2</sub>).** The compound was isolated from chromatography as the second green band and concentrated to give a green solid (4 mg, 1%). Characterization data were consistent with the compound **Zn-13b** isolated from the metallation of **Fb-13** (vide infra): <sup>1</sup>H NMR (d<sub>8</sub>-THF)  $\delta$  1.15 (t, *J* = 7.2 Hz, 6H), 1.25 (s, 42H), 2.20–2.28 (m, 4H), 4.81 (t, *J* = 7.2 Hz, 4H), 7.79 (d, *J* = 8.4 Hz, 4H), 8.09 (d, *J* = 8.4 Hz, 4H), 8.12–8.17 (m, 2H), 8.17–8.22 (m, 2H), 9.37 (s, 2H), 9.37–9.42 (m, 2H), 9.43–9.48 (m, 2H), 9.60 (s, 2H); LD-MS obsd 1252.6, calcd 1252.5 ( $C_{74}H_{76}N_{12}Si_2Zn$ );  $\lambda_{abs}$  (nm): 335, 679, 708; FAB-MS and fluorescence data were not separately obtained for this sample, but were obtained for the sample reported from the metallation of **Fb-13**.

**Tribenzo[*g,l,q*]-(*2*-{4-(2-triisopropylsilyl)ethynyl}phenyl)-1-propylbenzimidazo[5,6-*b*]porphyrazine (**Fb-11**, A<sub>3</sub>B).** A 20 mL reaction vial was charged with **14a** (40.0 mg, 83  $\mu$ mol), boron subphthalocyanine **15**<sup>24</sup> (143 mg, 332  $\mu$ mol, 4 equiv), DMAE (4 mL), and a magnetic stirring bar. The vial was capped and heated in an oil bath maintained at 100 °C. Periodically, a few microliters of the reaction mixture were removed, diluted into THF, and analyzed by UV-Vis spectroscopy. After the reaction had proceeded for 10 h, **15** could not be observed in the UV-Vis spectrum. The reaction was then cooled to room temperature and diluted with MeOH (50 mL) and water (30 mL). The mixture was filtered through paper, and the solid residue was rinsed with MeOH and air-dried. The filter paper containing the solid residue was then loaded into a Soxhlet thimble and the thimble was extracted with CHCl<sub>3</sub> for 20 h. Upon cooling the apparatus, most of the

extracted pigment precipitated out of the filtrate. The solvent was removed from the filtrate under reduced pressure and the solid material was resuspended in THF (20 mL) with sonication. The mixture was filtered through a cotton-plugged pipette and chromatographed over a column of Bio-Beads SX-3 in THF. The desired compound was recovered from the column as a dark blue-green band that eluted just after a faint green band and before a purple band. The faint green band was identified by UV-Vis as a mixture of benzimidazoporphyrazines having more than one benzimidazole, and was discarded. The purple band was identified by UV-Vis as a mixture of trace remaining subPc **15** and unsubstituted phthalocyanine and was discarded. The fractions containing the desired compound were concentrated and chromatographed over silica gel ( $\text{CH}_2\text{Cl}_2$ , 2% isopropanol, 2.5% THF, 2.5% ethyl acetate). Fractions containing the desired compound were concentrated, giving a blue solid (18 mg, 25%):  $^1\text{H}$  NMR  $\delta$  -3.29 (br s, 2H), 1.17 (t,  $J$  = 7.6 Hz, 3H), 1.32 (s, 21H), 2.10–2.25 (m, 2H), 4.45–4.60 (m, 2H), 7.68 (t,  $J$  = 7.2 Hz, 1H), 7.75–7.94 (m, 4H), 7.87 (d,  $J$  = 8.0 Hz, 4H), 8.11 (d,  $J$  = 8.0 Hz, 4H), 8.24–8.32 (m, 1H), 8.52–8.66 (m, 3H), 8.68–8.82 (m, 4H); LD-MS obsd 852.5; FAB-MS obsd 853.3945, calcd 853.3911 [(M+H) $^+$ ; M = C<sub>53</sub>H<sub>48</sub>N<sub>10</sub>Si];  $\lambda_{\text{abs}}$  (nm) 337, 622, 649, 669, 695;  $\lambda_{\text{em}}$  (nm) 700, 714;  $\Phi_f$  = 0.68.

**Dibenzo[*g,q*]-{(2-{4-(2-triisopropylsilyl ethynyl)phenyl}-1-propylbenzimidazo[5,6-*b*:5',6'-*I*])porphyrazine (Fb-13, *trans*-A<sub>2</sub>B<sub>2</sub>)**. An oven-dried three-necked 300 mL round bottom flask was charged with **14** (465 mg, 0.96 mmol), and a magnetic stirring bar. The vessel was flushed with argon for 10 min and immersed in an ice bath. Freshly dried THF (70 mL) and freshly dried TEA (269  $\mu$ L, 1.92 mmol, 2 equiv.) were added to the flask. A sample of **17** (212 mg, 0.96 mmol) was dissolved in dry THF (10 mL) and slowly added to

the reaction vessel. The mixture was kept at 0–5 °C for 1 h, and then allowed to warm to room temperature overnight. Then the triethylammonium salt that had formed was removed by filtration of the mixture into an oven-dried two-necked 250 mL round bottom flask. The vessel was flushed with argon for 5 min and a solution of hydroquinone (106 mg, 0.96 mmol) in THF (10 mL) was added, followed by NaOMe (658 µL of a 25 wt% solution in MeOH, 2.88 mmol, 3 equiv). The mixture was refluxed for 6 h, then cooled to room temperature and poured into MeOH (20 mL), to which water (100 mL) was added. After standing for 1 h, the mixture was filtered and the solid residue was air dried, dissolved in CH<sub>2</sub>Cl<sub>2</sub>, and chromatographed (silica, CH<sub>2</sub>Cl<sub>2</sub>, 1% isopropanol, 5% ethyl acetate, 5% THF). The first green band (faint) was identified by LD-MS as the AB<sub>3</sub> macrocycle (LD-MS *m/z* 1526.0). The product was collected as the second (dark) green band (49 mg, 9%): <sup>1</sup>H NMR δ -4.32 (br s, 1H), -4.22 (br s, 1H), 1.02 (t, *J* = 6.8 Hz, 3H), 1.10 (t, *J* = 6.8 Hz, 3H), 1.34 (s, 42H), 1.82–2.10 (m, 4H), 4.10–4.38 (m, 4H), 7.29–7.37 (m, 1H), 7.47–7.64 (m, 4H), 7.74–7.83 (m, 4H), 7.83–7.90 (m, 1H), 7.91 (d, *J* = 7.6 Hz, 2H), 7.95 (d, *J* = 8.4 Hz, 2H), 7.99–8.15 (m, 4H), 8.17–8.24 (m, 1H), 8.29–8.47 (m, 1H); LDMS obsd 1190.7; FABMS obsd 1190.6040, calcd 1190.6011 (C<sub>74</sub>H<sub>78</sub>N<sub>12</sub>Si<sub>2</sub>);  $\lambda_{\text{abs}}$  (nm): 340, 610, 631, 662, 681, 703, 732;  $\lambda_{\text{em}}$  (nm): 711, 739;  $\Phi_f$  = 0.66.

**Dibenzo[*g,q*]-{(2-{4-(2-triisopropylsilyl ethynyl)phenyl}-1-propylbenzimidazo[5,6-*b*:5',6'-*I*])porphyrazinatozinc(II) (Zn-13, *trans*-A<sub>2</sub>B<sub>2</sub>)}. From cross-condensation reaction:**

An oven-dried 20 mL reaction vial was charged with **14** (48 mg, 99 µmol), and a magnetic stirring bar. The vial was capped with a septum flushed with argon for 10 min and immersed in an ice bath. Freshly dried THF (8 mL) and freshly dried TEA (28 µL, 0.20 mmol, 2 equiv.) were added to the vial. A sample of **17** (22 mg, 99 µmol) was dissolved in dry THF

(2 mL) and slowly added to the reaction vial. The mixture was kept at 0–5 °C for 1 h, and then allowed to warm to room temperature overnight. Then the triethylammonium salt that had formed was removed by filtration of the mixture into an oven-dried 25 mL round bottom flask. Hydroquinone (11 mg) was added and the vessel was flushed with argon for 5 min and NaOMe (69 µL of a 25 wt% solution in MeOH, 0.30 mmol, 3 equiv) was added. The mixture was refluxed for 6 h, then cooled to room temperature and poured into MeOH (50 mL), to which water (2 mL) was added. After standing for 1 h, the mixture was filtered and the solid residue was air dried, dissolved in CH<sub>2</sub>Cl<sub>2</sub>, and chromatographed (silica, CH<sub>2</sub>Cl<sub>2</sub>, 1% isopropanol, 2.5% ethyl acetate, 2.5% THF). The first green band (faint) was identified by LD-MS as the ZnAB<sub>3</sub> macrocycle (LD-MS m/e 1591.0). The product was collected as the second (dark) green band (5.0 mg, 4%): <sup>1</sup>H NMR δ 1.15 (t, *J* = 7.6 Hz, 6H), 1.28 (s, 42H), 2.13–2.25 (m, 4H), 4.69 (t, *J* = 7.6 Hz, 4H), 7.80 (d, *J* = 8.0 Hz, 4H), 8.02–8.20 (m, 4H), 8.09 (d, *J* = 8.0 Hz, 4H), 9.06–9.13 (m, 1H), 9.18–9.24 (m, 2H), 9.29–9.43 (m, 5H); LD-MS obsd 1252.5; FAB-MS obsd 1252.5242, calcd 1252.5146 (C<sub>74</sub>H<sub>76</sub>N<sub>12</sub>Si<sub>2</sub>Zn); λ<sub>abs</sub> (nm): 338, 614, 648, 679, 709. Fluorescence data were not collected from this sample, but were collected for the separate regioisomers (*vide infra*).

*From zinc-metallation of **Fb-13**:* A 20 mL reaction vial was charged with **Fb-13** (20 mg, 17 µmol), Zn(OAc)<sub>2</sub>·2H<sub>2</sub>O (7.4 mg, 34 µmol, 2 equiv), dioxane (2.0 mL), DMF (0.5 mL), and a magnetic stirring bar. The vial was kept in an oil bath heated to 100 °C for 2 h, upon which the UV-Vis absorbance analysis of a removed sample showed a spectrum for **Zn-13** with no evidence of remaining starting material. The reaction mixture was cooled and diluted to 20 mL with MeOH. The mixture was filtered and the solid was air dried, then dissolved through the filter with THF, and concentrated to dryness. The residue was

chromatographed (silica, toluene, 10% THF) to separate a trace of remaining **Fb-13** that was too small to be detected in the mixture by UV-Vis analysis. The product eluted as the first (dark) green band (19 mg, 90%). A second chromatography (silica, CH<sub>2</sub>Cl<sub>2</sub>, 1% isopropanol, 5% ethyl acetate, 5% THF) separated the two regioisomeric products. The first green band was assigned as **Zn-13a**. Fractions containing the second green band were rechromatographed twice to separate all trace of the first eluting isomer. The second eluting species was assigned as **Zn-13b**. These two isomers, **Zn-13a** and **Zn-13b**, were determined by their COSY NMR data to be the C<sub>2h</sub> and C<sub>2v</sub> symmetric structures, respectively (see Results and Discussion). Data for **Zn-13a (C<sub>2h</sub>)**: yield = 10.0 mg (47%); <sup>1</sup>H NMR δ 1.16 (t, J = 8.0 Hz, 6H), 1.28 (s, 42H), 2.14–2.26 (m, 4H), 4.71 (t, J = 8.0 Hz, 4H), 7.81 (d, J = 8.0 Hz, 4H), 8.02–8.14 (m, 4H), 8.08 (d, J = 8.0 Hz, 4H), 8.88 (s, 2H), 9.13 (d, J = 7.2 Hz, 2H), 9.22 (s, 2H), 9.23 (d, J = 7.2 Hz, 2H); LD-MS obsd 1252.5; FAB-MS obsd 1252.5214, calcd 1252.5146 (C<sub>74</sub>H<sub>76</sub>N<sub>12</sub>Si<sub>2</sub>Zn); λ<sub>abs</sub> (nm): 338, 614, 648, 679, 709; λ<sub>em</sub> 717 nm; Φ<sub>f</sub> = 0.32  
Data for **Zn-13b (C<sub>2v</sub>)**: yield = 9.0 mg (43%); <sup>1</sup>H NMR δ 1.15 (t, J = 7.6 Hz, 6H), 1.28 (s, 42H), 2.13–2.25 (m, 4H), 4.69 (t, J = 7.6 Hz, 4H), 7.79 (d, J = 7.6 Hz, 4H), 8.13 (d, J = 7.6 Hz, 6H), 8.10–8.19 (m, 2H), 8.95 (s, 2H), 9.09–9.20 (m, 2H), 9.21–9.35 (m, 4H); LD-MS obsd 1252.6; FAB-MS 1252.5172, calcd 1252.5146 (C<sub>74</sub>H<sub>76</sub>N<sub>12</sub>Si<sub>2</sub>Zn); λ<sub>abs</sub> (nm): 338, 614, 648, 679, 709; λ<sub>em</sub> 717 nm; Φ<sub>f</sub> = 0.26.

**2-(4-(2-(Triisopropylsilyl)ethynyl)phenyl)-1-propylimidazo[4,5-*f*]isoindole-1,3-diimine (14).** Following a literature procedure,<sup>14</sup> a 25 mL round bottom flask was charged with **6d** (606 mg, 1.30 mmol) and a magnetic stirring bar. The vessel was sealed with a condenser, a bubbler, and a septum for the second neck. The apparatus was flushed with argon for 15 min, and then anhydrous MeOH (14 mL), freshly dried THF (7 mL), and

NaOMe (30  $\mu$ L of a 25 wt% solution in MeOH, 130  $\mu$ mol) were added. The reaction flask was heated in an oil bath at 70 °C, and the mixture became homogeneous. The argon line was removed and ammonia gas was bubbled through the mixture as it refluxed for 6 h. The flask was then removed from heat and allowed to cool under ammonia atmosphere. When the mixture reached room temperature, the ammonia gas flow was stopped and the mixture was allowed to stand overnight under a slowly flowing stream of argon, during which time some greenish-white crystals formed in the vessel. The supernatant was drained off with a pipette and the crystals were washed with a few milliliters of anhydrous MeOH, and then dried in vacuo. Yield: 479 mg, 76%; mp 248–250 °C, upon which the sample melted and turned deep green – the melting capillary was broken and the residue taken up in THF and analyzed by UV-Vis spectroscopy, which showed a spectrum similar to that of **Fb-8**; Due to the presence of tautomeric forms of the product, the NH signals do not all integrate to integers:  $^1\text{H}$  NMR ( $d_8$ -THF)  $\delta$  0.86 (t,  $J$  = 7.2 Hz, 3H), 1.19 (s, 21H), 1.80–1.92 (m, 2H), 3.14 (br s, 0.5H), 4.30–4.44 (m, 2H), 7.48 (br s, 0.5H), 7.65 (d,  $J$  = 8.0 Hz, 2H), 7.83 (d,  $J$  = 8.0 Hz, 2H), 7.80–8.60 (m, 4H); Due to poor solubility,  $^{13}\text{C}$  NMR spectroscopy was not performed; IR (film): 3260, 3201, 2941, 2861, 2161, 1666, 1547, 1460, 1410, 1345, 1144, 1109, 1081, 1054, 994, 916, 882; Anal. Calcd for  $\text{C}_{29}\text{H}_{37}\text{N}_5\text{Si}$ : C, 72.01; H, 7.71; N, 14.48; Found: C, 69.90; H, 7.86; N, 13.91 (consistent with crystal inclusion of one molecule MeOH per molecule compound; FAB-MS obsd 484.2876, calcd 484.2896  $[(\text{M} + \text{H})^+]$ ; M =  $\text{C}_{29}\text{H}_{37}\text{N}_5\text{Si}$ ].

**Dibenzo[*g,q*]-{(2-{4-ethynylphenyl}-1-propylbenzimidazo[5,6-*b*:5',6'-*I*])porphyrazinatozinc(II)-C<sub>2h</sub> (Zn-17a, *trans*-A<sub>2</sub>B<sub>2</sub>)**. A 20 mL vial was charged with **Zn-13a** (9.5 mg, 7.6  $\mu$ mol), CH<sub>2</sub>Cl<sub>2</sub> (4 mL), and a magnetic stirring bar. Then TBAF (17  $\mu$ L of

a 1 M solution in THF, 17  $\mu$ mol) was added, and the mixture was stirred at room temperature for 1.5 h. TLC analysis (silica,  $\text{CH}_2\text{Cl}_2$ , 1% isopropanol, 5% ethyl acetate, 5% THF) indicated that neither starting material nor intermediate remained, so the mixture was directly added to a short (15 cm) silica gel column packed in  $\text{CH}_2\text{Cl}_2$ . The product proved to be very polar, and the eluent ( $\text{CH}_2\text{Cl}_2$ , 1% isopropanol, 5% ethyl acetate, 5% THF) was changed to increasing amounts of THF (final eluent:  $\text{CH}_2\text{Cl}_2$ / THF, 1:4) to elute the product as a dark blue-green band (6.2 mg, 87%):  $^1\text{H}$  NMR ( $d_8$ -THF)  $\delta$  1.17 (t,  $J$  = 7.2 Hz, 6H), 2.18–2.28 (m, 4H), 3.84 (s, 2H), 4.74 (t,  $J$  = 8.0 Hz, 4H), 7.70 (d,  $J$  = 8.4 Hz, 4H), 8.02–8.12 (m, 4H), 8.05 (d,  $J$  = 8.4 Hz, 2H), 9.04 (br s, 2H), 9.21 (d,  $J$  = 6.4 Hz, 2H), 9.26–9.32 (m, 4H); LD-MS obsd 940.8; FAB-MS obsd 940.2510, calcd 940.2477 ( $\text{C}_{56}\text{H}_{36}\text{N}_{12}\text{Zn}$ ).

**Dibenzo[*g,q*]-(*2*-{4-ethynylphenyl}-1-propylbenzimidazo[5,6-*b*:5',6'-*I*])porphyrazinatozinc(II)-C<sub>2v</sub> (**Zn-17b, trans-A<sub>2</sub>B<sub>2</sub>**).** The same procedure was followed as for **Zn-17a**, with the following quantities: **Zn-13b** (8.2 mg, 6.5  $\mu$ mol),  $\text{CH}_2\text{Cl}_2$  (4 mL), and TBAF (14  $\mu$ L of a 1 M solution in THF, 14  $\mu$ mol). The chromatography procedure was followed similarly (final eluent:  $\text{CH}_2\text{Cl}_2$ , 30% THF), and the product eluted as a dark blue-green band (4.4 mg, 72%):  $^1\text{H}$  NMR ( $d_8$ -THF)  $\delta$  1.15 (t,  $J$  = 6.8 Hz, 6H), 2.16–2.27 (m, 4H), 3.85 (s, 2H), 4.72 (t,  $J$  = 7.6 Hz, 4H), 7.77 (d,  $J$  = 7.6 Hz, 4H), 8.04 (d,  $J$  = 7.6 Hz, 6H), 8.12–8.17 (m, 2H), 9.04 (s, 2H), 9.16–9.22 (m, 2H), 9.29–9.35 (m, 4H); LD-MS obsd 940.9; FAB-MS obsd 940.2490, calcd 940.2477 ( $\text{C}_{56}\text{H}_{36}\text{N}_{12}\text{Zn}$ ).

## E. References:

- (1) Pardo, C.; Yuste, M.; Elguero, J. *J. J. Porphyrins Phthalocyanines* **2000**, *4*, 505–509.
- (2) (a) Kudrik, E. V.; Shaposhnikov, G. P. *Mendeleev Commun.* **1999**, 85–86. (b) Kudrik, E. V.; Shaposhnikov, G. P.; Balakirev, A. E. *Russ. J. Gen. Chem.* **1999**, *69*, 1321–1324. (c) Balakirev, A. E.; Kudrik, E. V.; Shaposhnikov, G. P. *Russ. J. Gen. Chem.* **2002**, *72*, 1616–1619.
- (3) For syntheses leading to the starting material **3** used in ref 29, see: (a) Zharnikova, M. A.; Balakirev, A. E.; Maizlish, V. E.; Kudrik, E. V.; Shaposhnikov, G. P. *Russ. J. Gen. Chem.* **1999**, *69*, 1870–1871. (b) Shishkina, O. V.; Maizlish, V. E.; Shaposhnikov, G. P.; Lyubimtsev, A. V.; Smirnov, R. P.; Baran'ski, A. *Russ. J. Gen. Chem.* **1997**, *67*, 842–845. (c) Elvidge, J. A.; Golden, J. H.; Linstead, R. P. *J. Chem. Soc.* **1957**, 2466–2469; Levy, L. F.; Stephen, H. *J. Chem. Soc.* **1931**, 79–82.
- (4) Mitzel, F.; Fitzgerald, S.; Beeby, A.; Faust, R. *Chem. Eur. J.* **2003**, *9*, 1233–1241.
- (5) For syntheses leading to the starting material used in ref 31, see: (a) Cheeseman, G. W. *H. J. Chem. Soc.* **1962**, 1170–1176. (b) Acheson, R. M. *J. Chem. Soc.* **1956**, 4731–4735; Elderfield, R. C.; Meyer, V. B. *J. Am. Chem. Soc.* **1954**, 1887–1891. (c) Mørkved, E. H.; Næset, S. M.; Bjørlo, O.; Kjøsen, H.; Hvistendahl, G.; Mo, F. *Acta Chem. Scand.* **1995**, *49*, 658–662.
- (6) Arotsky, J.; Butler, R.; Darby, A. C. *J. Chem. Soc. (C)* **1970**, 1480–1485.
- (7) Schwiebert K. E.; Chin, D. N.; MacDonald, J. C.; Whitesides, G. M. *J. Am. Chem. Soc.* **1996**, *118*, 4018–4029.
- (8) Grimmett, M. R. *Imidazole and Benzimidazole Synthesis*, Academic Press, 1997, pp 71–94.

- (9) (a) Weidenhagen, R. *Chem. Ber.* **1936**, *69*, 2263–2272. (b) Weidenhagen, R.; Weedon, U. *Chem. Ber.* **1938**, *71*, 2347–2360.
- (10) Coville, N. J.; Neuse, E. W. *J. Org. Chem.* **1977**, *42*, 3485–491.
- (11) Singh, M. P.; Sasmal, S.; Lu, W.; Chatterjee, M. N. *Synthesis* **2000**, 1380–1390.
- (12) (a) Tomoda, H.; Saito, S.; Ogawa, S.; Shiraishi, S. *Chem. Lett.* **1980**, 1277–1280. (b) Tomoda, H.; Saito, S.; Shiraishi, S. *Chem. Lett.* **1983**, 313–316.
- (13) Rager, C.; Schmid, G.; Hanack, M. *Chem. Eur. J.* **1999**, *5*, 280–288.
- (14) Brach, P. J.; Grammatica, S. J.; Ossanna, O. A.; Weinberger, L. *J. Heterocyc. Chem.* **1970**, *7*, 1403–1405.
- (15) Young, J. G.; Onyebuagu, W. *J. Org. Chem.* **1990**, *55*, 2155–2159.
- (16) Stihler, P.; Hauschel, B.; Hanack, M. *Chem. Ber.* **1997**, *130*, 801–806.
- (17) Liu, Z.; Schmidt, I.; Thamyongkit, P.; Loewe, R. S.; Syomin, D.; Diers, J. R.; Zhao, Q.; Misra, V.; Lindsey, J. S., Bocian, D. F. *Chem. Mater.* **2005**, in press.
- (18) (a) data for (*t*-Bu)<sub>4</sub>H<sub>2</sub>Pc and (*t*-Bu)<sub>4</sub>MgPc: Teuchner, K.; Pfarrherr, A.; Stiel, H.; Freyer, W.; Leupold, D. *Photochem. Photobiol.* **1993**, *57*, 465–471. (b) additional data for (*t*-Bu)<sub>4</sub>MgPc: Freyer, W.; Dähne, S.; Minh, L. Q.; Teuchner, K. Z. *Chem.* **1986**, *26*, 334–336. (c) data for (*t*-Bu)<sub>4</sub>ZnPc: Tran-Thi, T.-H.; Desforge, C.; Thiec, C.; Gaspard, S. *J. Phys. Chem.* **1989**, *93*, 1226–1233.
- (19) Kobayashi, N.; Mack, J.; Ishii, K.; Stillman, M. J. *Inorg. Chem.* **2002**, *41*, 5350–5363.
- (20) Kato, M.; Komoda, K.; Namera, A.; Sakai, Y.; Okada, S.; Yamada, A.; Yokoyama, K.; Migita, E.; Minobe, Y.; Tani, T. *Chem. Pharm. Bull.* **1997**, *45*, 1767–1776.
- (21) Rao, P. D.; Dhanalekshmi, S.; Littler, B. J.; Lindsey, J. S. *J. Org. Chem.* **2000**, *65*, 7323–7344.

- (22) Nishi, H.; Azuma, N.; Kitahara, K. *J. Heterocyclic Chem.* **1992**, *29*, 475–477.
- (23) Hanack, M.; Haisch, P.; Lehmann, H.; Subramanian, L. R. *Synthesis* **1993**, 387–390.
- (24) Claessens C. G.; Gonzalez-Rodriguez D.; del Rey B.; Torres T.; Mark G.; Schuchmann H. P.; von Sonntag C.; MacDonald J. G.; Nohr R. S. *Eur. J. Org. Chem.* **2003**, *14*, 2547–2551.
- (25) Farbenfabriken Bayer, U. S. Patent 2,701,252; Feb. 1, 1955.
- (26) Griffiths, J.; Roozpeikar, B. *J. Chem. Soc., Perkin Trans. I* **1976**, 42–45.

## **Chapter 5**

This chapter presents a triple-decker lanthanide sandwich coordination compound bearing a compact all-carbon tripod for attachment to an electroactive surface. The triple decker contains two cerium atoms and a substituted phthalocyanine sandwiched between two molecules of *meso*-tetra-*p*-tolylporphyrin. The phthalocyanine is an A<sub>3</sub>B-type where three benzo groups bear no substituents and one benzo group incorporates an annulated imidazo entity. The tripodal tether is a compact, triallyl unit attached via an intervening *p*-phenylene unit. The resulting triple-decker architecture is centered on the tripod. The molecular design provides the triple decker with small molecular footprint, and thereby high density coverage, upon attachment to an electroactive surface. The triple decker affords several cationic oxidation states over a low potential range.

### **A. Background.**

Porphyrinic macrocycles combine with lanthanide atoms to form double-decker and triple-decker sandwich complexes.<sup>1-3</sup> The triple deckers exhibit a large number of oxidation states within a relatively narrow electrochemical window. Owing to the facile redox-active properties, triple deckers have been considered for use as charge-storage components in a variety of applications, including molecular batteries and molecular information storage media. Triple deckers also are of interest as components of optoelectronic displays owing to the rich color changes that accompany the redox processes. Such applications typically require attachment of the triple decker to an electroactive surface. The requirement for a covalent tether poses constraints on the type of triple decker employed.

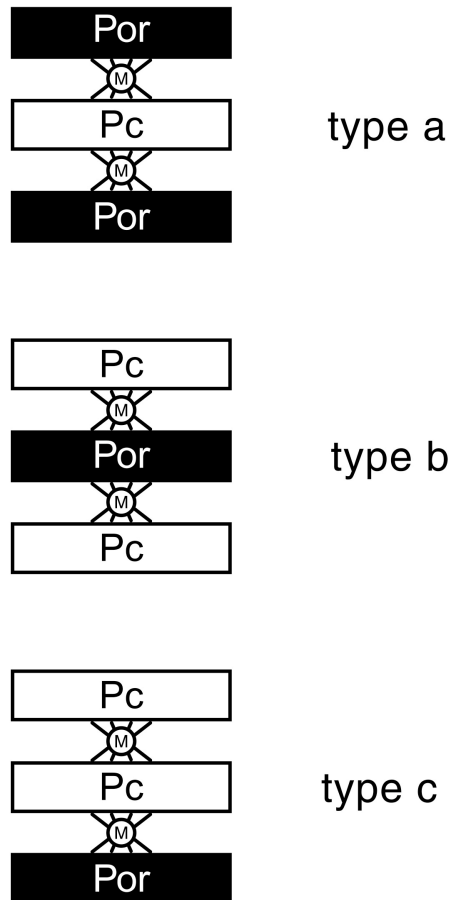


Chart 5.1. Structures of three known types of heteroleptic triple decker lanthanide sandwich complexes.

Three types of heteroleptic triple deckers composed of porphyrins and phthalocyanines are shown in Chart 5.1. Type-c  $[(\text{Pc})\text{Ln}(\text{Pc})\text{Ln}(\text{Por})]$ , type-b  $[(\text{Pc})\text{Ln}(\text{Por})\text{Ln}(\text{Pc})]$  and type-a  $[(\text{Por})\text{Ln}(\text{Pc})\text{Ln}(\text{Por})]$  triple deckers differ in the number and layered arrangement of the respective porphyrin and phthalocyanine ligands. The term (Por) or (Pc) refers to the dianion of a generic porphyrin or phthalocyanine entity, respectively, in a sandwich architecture without regard to the nature of the substituents. Rational routes exist

for the synthesis of type-a and type-c triple deckers,<sup>4</sup> whereas type-b triple deckers are only available by statistical reactions.<sup>2,5</sup>

Given the greater sophistication of synthetic control in porphyrin versus phthalocyanine chemistry,<sup>6</sup> we have almost exclusively employed type-c triple deckers in studies of molecular information storage. Indeed, 14 type-c triple deckers bearing tethers attached to the porphyrin ligand have been prepared.<sup>5,7-11</sup> The generic design is shown in Figure 5.1. Dyads and oligomers also have been prepared bearing one or two surface attachment groups.<sup>5,8,9</sup> For the monomeric complexes illustrated in Figure 5.1, the surface attachment groups have included aryl-SAc,<sup>5,7</sup> benzyl-SAc,<sup>8,9</sup> thiocyanate,<sup>7</sup> benzyl alcohol,<sup>10</sup> and tripodal benzyl-SAc.<sup>11</sup> The alcohol groups enable attachment to Si, whereas the thioacetate groups (which undergo deprotection *in situ*) enable attachment to Au or Si.

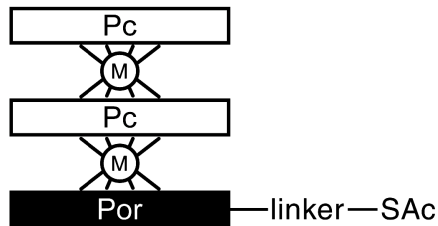


Figure 5.1. A type-c triple decker bearing a tether for surface attachment.

The triple decker monomers exhibited a rather low surface coverage ( $2.5 \times 10^{-11}$  mol·cm<sup>-2</sup>), corresponding to a large molecular footprint (~670 Å<sup>2</sup>).<sup>9</sup> Such a large area diminishes the surface charge density from the theoretical maximum. Achieving high surface charge density is a key objective of the molecular information storage approach. Because the tether is attached to the porphyrin, the triple decker in principle could rotate like a camshaft, sweeping out a large area (Figure 5.2). In addition, the triple decker can tilt

significantly on the surface. We felt that both the tilting and camshaft motions are the source of the substantial increase in molecular footprint and thereby diminished surface charge density.

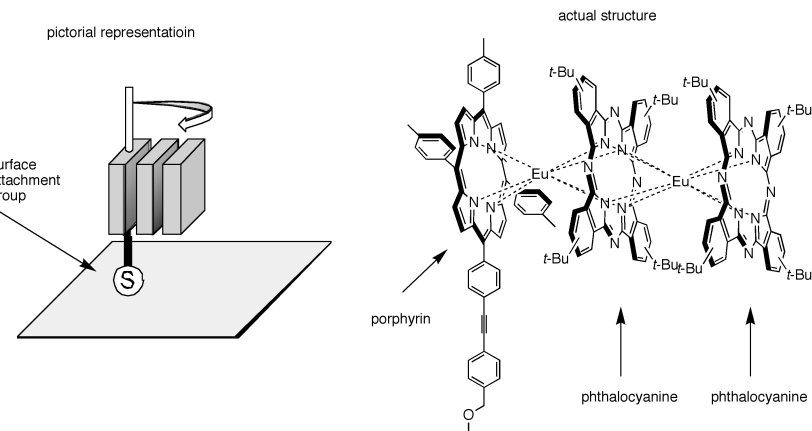


Figure 5.2. Camshaft rotation of a type-c triple decker tethered to a surface (via a surface attachment group, denoted by “S”).

In an effort to enforce an upright orientation of the triple decker, we prepared two triple deckers wherein each bears a tripodal tether.<sup>11</sup> The tripodal-substituted triple deckers are shown in Figure 5.3. The two triple deckers exhibited surface coverages of  $\sim 1 \times 10^{-11}$  mol·cm<sup>-2</sup>, which are still less dense than possible upon close packing. A chief problem remained that the type-c triple decker could sweep out a large surface area by rotation about the tether axis.

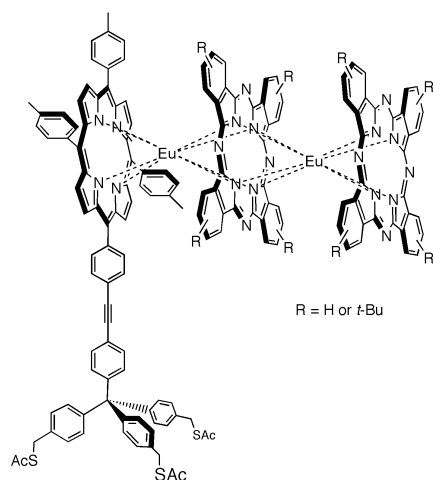


Figure 5.3. Architectures containing a type-c triple decker bearing a tripodal thiol tether.

We also prepared a phthalocyanine bearing the same tri-thiol tether, as shown in Figure 5.4.<sup>11</sup> The phthalocyanine was substituted at one of the  $\beta$ -positions via an ethynyl unit. In this architecture, the cant angle of the phthalocyanine (see pg 13) causes the macrocycle to sweep out a larger area than would be desirable.

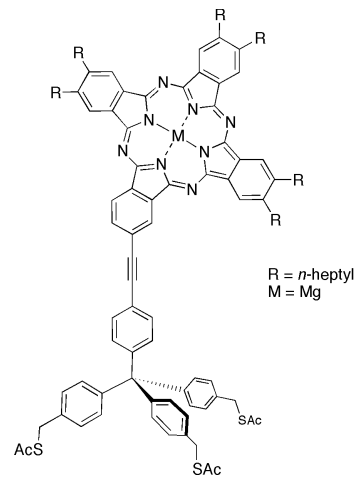


Figure 5.4. A phthalocyanine attached to a tripodal thiol tether. Note the cant angle of the tripodal axis with respect to the N-N axis of the phthalocyanine.

To eliminate the cant angle, a phthalocyanine architecture is needed that has peripheral substituents that are aligned with one of the N-N axes of the macrocycle (bisecting two opposite benzo rings and two inner nitrogen atoms). Phthalocyanines having such a diametrically aligned substitution geometry would facilitate information storage studies by enabling higher packing density in the monolayers. In this regard, we recently developed new methodology for the preparation of a known type of phthalocyanine analogue, called benzimidazoporphyrazines (Figure 5.5 – see Chapter 4).<sup>12</sup> Each imidazo unit has two substituents: one *N*-imidazo substituent and a substituent at the 2-position. The 2-position is aligned along an N-N axis of the phthalocyanine.

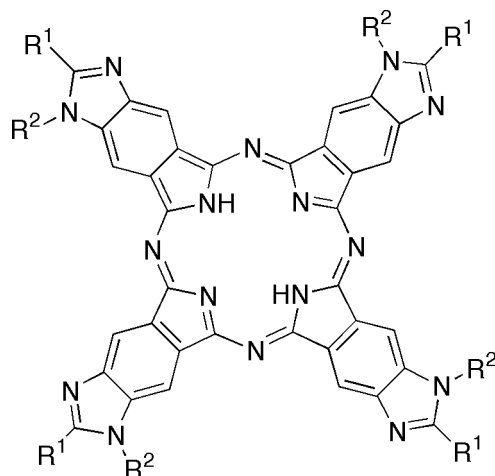


Figure 5.5. Generic structure of A<sub>4</sub> benzimidazoporphyrazines.

We report herein the synthesis of a phthalocyanine containing one annulated imidazo group and three unsubstituted benzo units (i.e., a benzimidazoporphyrazine), and conversion of the phthalocyanine to a type-a triple decker, where the phthalocyanine (1) is sandwiched by two tetra-*p*-tolylporphyrin molecules and two cerium atoms, and (2) bears a compact all-carbon (“triallyl”) tether. The triple decker lanthanide sandwich complex is centrally

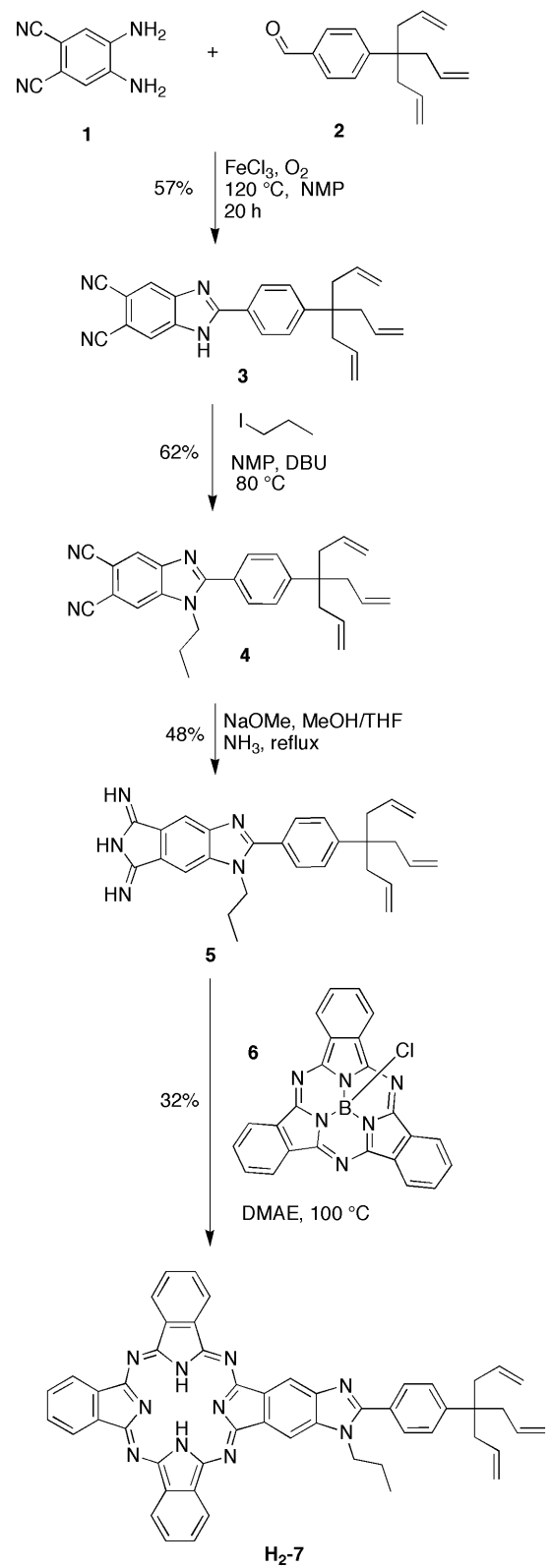
positioned on the tripod. The all-carbon tether has been employed with metalloporphyrins, affording high surface coverage upon attachment to Si(100).<sup>13</sup> This approach provides straightforward access to triple-decker architectures for high density surface coverage upon attachment to an electroactive surface.

## B. Synthesis: strategy and results.

Lanthanide triple decker sandwich coordination compounds generally afford four cationic oxidation states.<sup>1</sup> Cerium was chosen as the lanthanide metal in both layers of the triple decker because each cerium undergoes a further oxidation ( $\text{Ce}^{3+}/\text{Ce}^{4+}$ ), affording a total of six cationic oxidation states.<sup>14</sup> The availability of six oxidation states is attractive for multibit storage in a given memory cell. Although we have prepared such homonuclear cerium-containing triple deckers,<sup>15</sup> all of the tethered triple deckers prepared to date have contained europium or europium/cerium. The synthesis of the type-a triple decker is achieved by reaction of a dilithio-phthalocyanine and a porphyrin.<sup>15</sup> The synthesis of the imidazophthalocyanine bearing the tether at the 2-imidazo position and no substituents at the other benzo rings is best achieved by a ring-expansion reaction<sup>16-20</sup> of a sub-phthalocyanine and the benzimidazo-diiminoisoindoline. We sought to construct the phthalocyanine bearing a compact all-carbon tether via a *p*-phenylene unit to the 2-position of the imidazo unit. This design required introduction of the tether at the earliest stage in the route to the diiminoisoindoline.

We recently developed a new synthesis of dicyanophenylenediamine **1**<sup>12</sup> (Scheme 5.1), which upon reaction with a variety of aldehydes afforded the corresponding dicyanobenzimidazoles.<sup>12</sup> A *p*-substituted benzaldehyde bearing the all-carbon tether (**2**),

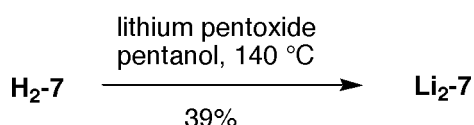
obtained from the commercially available *p*-trifluoromethylaniline, was used in the synthesis of tripodal-tethered metalloporphyrins.<sup>13</sup> The reaction of **1** and **2** proceeded via oxidative cyclization to form benzimidazole **3** in 57% yield, a yield consistent with our previous results for 2-aryl-dicyanobenzimidazoles.<sup>12</sup> The alkylation of **3** with 1-iodopropane proceeded cleanly but incompletely, affording **4** in 62% yield accompanied by unreacted starting material (31% yield). The cyclization of **4** was performed according to a previously published report,<sup>21</sup> affording diiminoisoindoline **5** in 48% yield. Although this procedure typically affords yields >90%, the lower yield of **5** is attributed to incomplete recovery from the cooled methanolic reaction mixture.



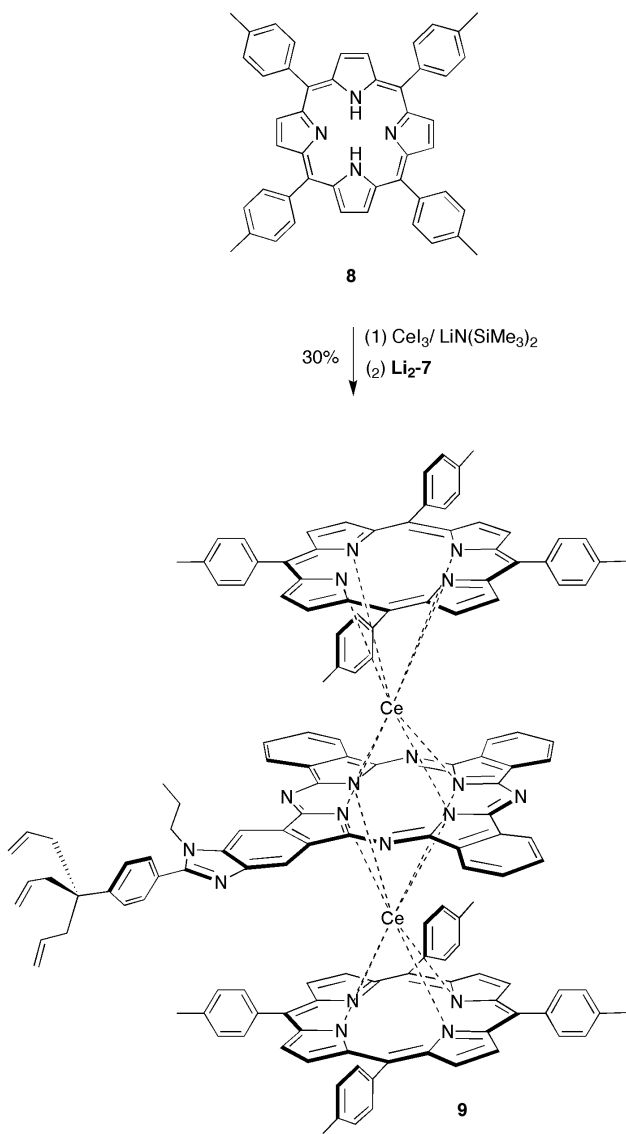
Scheme 5.1.

The ring expansion reaction of subphthalocyanines such as **6**<sup>22</sup> has been reported under various procedures.<sup>16-20</sup> We chose a procedure using the polar, reducing solvent 2-dimethylaminoethanol (DMAE).<sup>18</sup> Due to the good reactivity of **5**, four equivalents of **6** were required to suppress the formation of products bearing more than one imidazo moiety. After 8 h of reaction, the presence of reactant **6** was no longer evident and a substantial amount of unsubstituted phthalocyanine was formed in addition to the desired imidazophthalocyanine **H<sub>2</sub>-7**. The macrocycles were separated from the DMAE by precipitation with MeOH. **H<sub>2</sub>-7** is sufficiently more soluble than the unsubstituted phthalocyanine to be largely separated by Soxhlet extraction using CH<sub>2</sub>Cl<sub>2</sub>. Complete purification required size exclusion chromatography and adsorption chromatography.

The lithiation of **H<sub>2</sub>-7** (Scheme 5.2) was followed by UV-Vis spectroscopy, and the formation of **Li<sub>2</sub>-7** was evident within 15 min. The product **Li<sub>2</sub>-7** has greatly improved solubility compared to the free base **H<sub>2</sub>-7**, similar to the previous observation for lithium phthalocyanine,<sup>23</sup> and was isolated by extraction of the reaction residue with dry acetone. The material thereby obtained was used directly without characterization.



Scheme 5.2.



Scheme 5.3.

The preparation of triple decker **9** (Scheme 5.3) was performed according to a procedure we previously reported.<sup>15</sup> Thus,  $\text{CeI}_3$  in bis(2-methoxyethyl) ether was treated with  $\text{LiN}(\text{SiMe}_3)_2$  at reflux, affording the putative  $\text{I-Ce}[\text{N}(\text{SiMe}_3)_2]_2$ . The addition of tetra-*p*-tolylporphyrin (**8**)<sup>24</sup> afforded the corresponding Ce-porphyrin half-sandwich complex, which was then treated with **Li<sub>2</sub>-7** at reflux for 10 h. Analytical SEC showed the absence of starting

materials and the presence of the target type-a triple decker **9**. The good solubility of **9** allowed for purification by standard adsorption chromatography, and **9** was isolated in 30% yield. The <sup>1</sup>H NMR analysis of **9** produced a complex signature due to the effects of the cerium atoms, with most of the resonances being broadened and located at unexpected chemical shifts, but the resonances corresponding to the triallyl moiety were clearly defined and found in the same portion of the spectrum as for **H<sub>2</sub>-7**. LDMS analysis of **9** gave a clear signal at the expected mass range. In summary, the synthesis of triple decker **9** proceeded in a straightforward manner. The overall yield from the dicyanophenylenediamine **1** was low (0.6%), but valuable intermediates could be recovered from two of the intervening synthetic steps.

### C. Characterization of surface monolayers.

Silicon electrodes were coated with monolayers of **9** and studied by infra-red (IR) spectroscopy and by electrochemical measurements at the laboratories of the research group of Professor David Bocian (University of California at Riverside). As a point of disclosure, I should indicate here that I participated in the characterization studies described in this section, but I did not design the electrochemical or surface IR experiments, nor did I set up the instrumentation or fabricate the Si electrodes used in these studies. My participation included the preparation (cutting, chemical etching/cleaning) of the Si electrodes, coating of the electrodes with **H<sub>2</sub>-7** and **9**, observing the electrochemical experiments, and collecting the standard IR data. The electrochemical experiments on surface monolayers were conducted by Lingyun Wei, a graduate student in the Bocian group.

Surface monolayers of **H<sub>2</sub>-7** and **9** were prepared on electrodes comprised of silicon (100) wafers that were each coated with a mask of SiO<sub>2</sub> on the upper surface, leaving a small area of Si(100) exposed in the center of the mask. The electrodes are prepared on a silicon disc, approximately the same size as a standard commercial compact disc used for storing data or music. Many electrodes can be fabricated onto one disk, and each is separated from the disc by applying point-pressure along straight lines: the crystallinity of the Si(100) allows for its facile cleavage in this manner. A schematic for the deposition of the SiO<sub>2</sub> mask is shown in Figure 5.6. The active area of each square silicon electrode wafer corresponds to an area in black in the Photo Mask. The chemical etch step removes the SiO<sub>2</sub> at the exposed region. The chemical clean step removes the photosensitive polymer used as the photoresist.

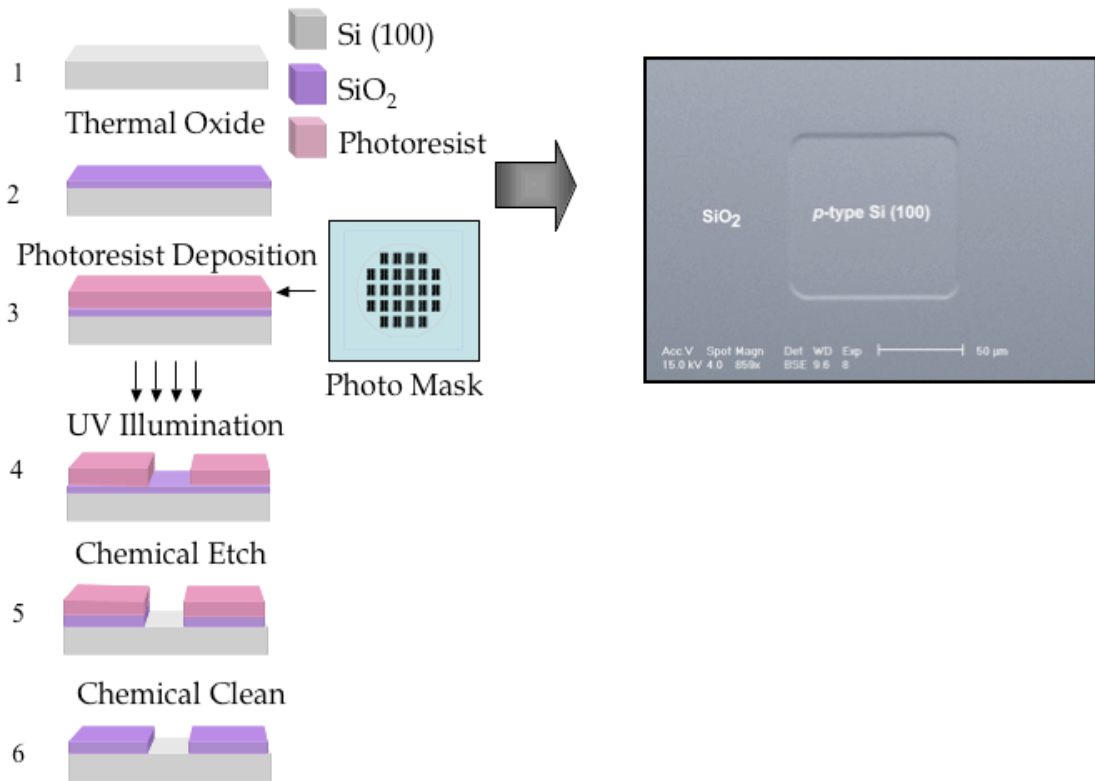


Figure 5.6. Schematic of Si electrode fabrication. (figure courtesy of Lingyun Wei).

Samples of **H<sub>2</sub>-7** and **9** were examined by IR spectroscopy as KBr pellets, and then a monolayer of **9** on a Si electrode was examined by Gallium-attenuated total reflectance IR spectroscopy. The IR spectra serve to assess the transformation of the allyl groups that are the binding elements of the compounds. The IR spectra from KBr pellets are shown in Figures 5.7 and 5.8 (upper portion). The characteristic C=C stretching of the allyl groups is seen at 1610 and 1638 cm<sup>-1</sup>. These bands are greatly diminished, if not altogether missing, in the IR spectrum of the monolayer. The absence of such bonds is consistent with all three allyl groups binding covalently to the Si(100) surface. Any stretches of the carbons that were

in the allyl group is longer than the same frequency. It is apparent in the spectrum of the monolayer that the carbon-hydrogen stretching in the 2800-3200  $\text{cm}^{-1}$  region is also missing. This is an artifact due to the difficulty in establishing a good blank spectrum. The blanks are electrodes heated with neat THF and have highly variable signal strength at the high frequency region.

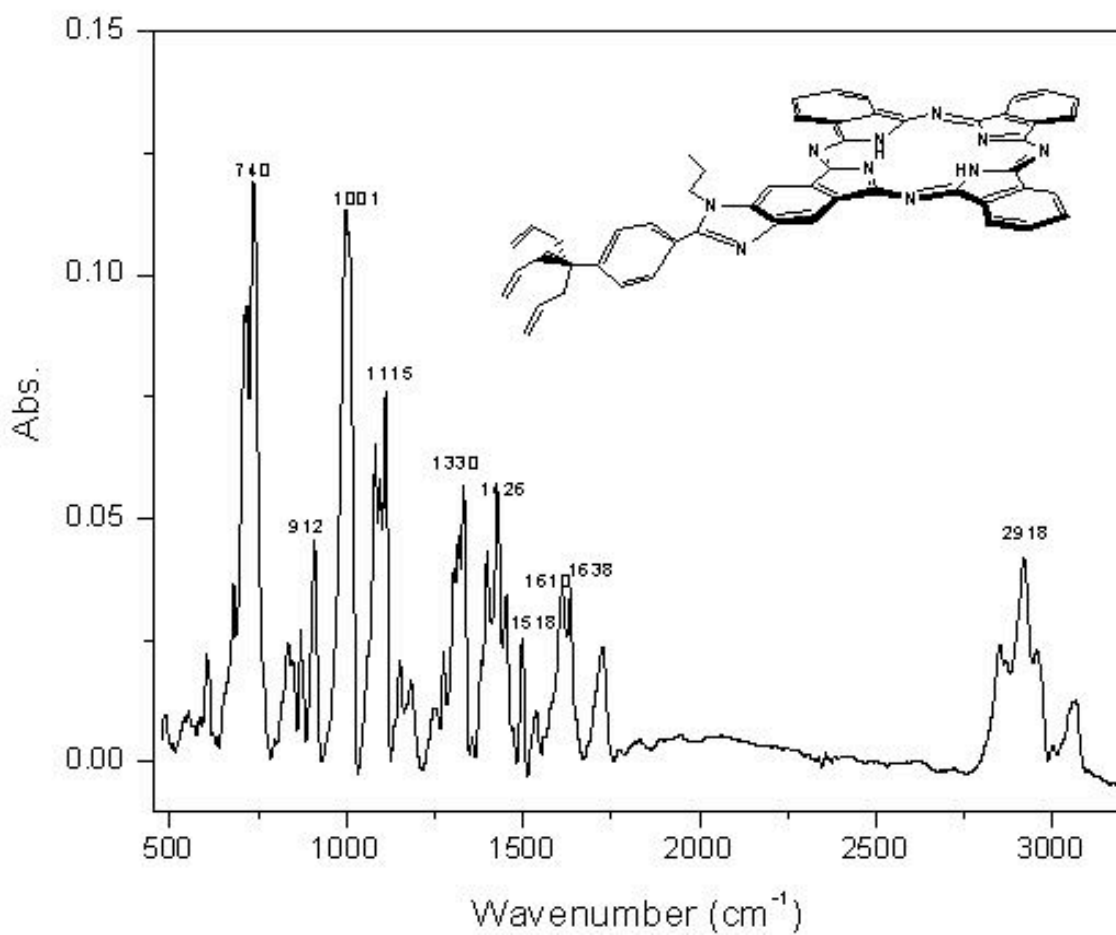


Figure 5.7. IR spectrum of **H<sub>2</sub>-7** [KBr pellet] (figure courtesy of Lingyun Wei).

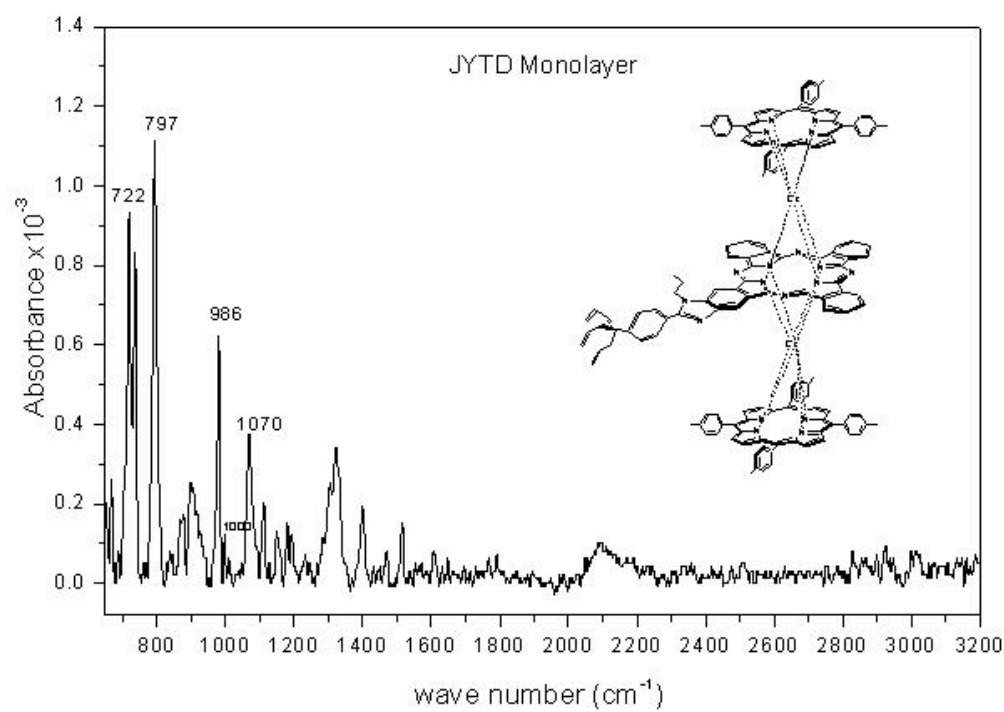
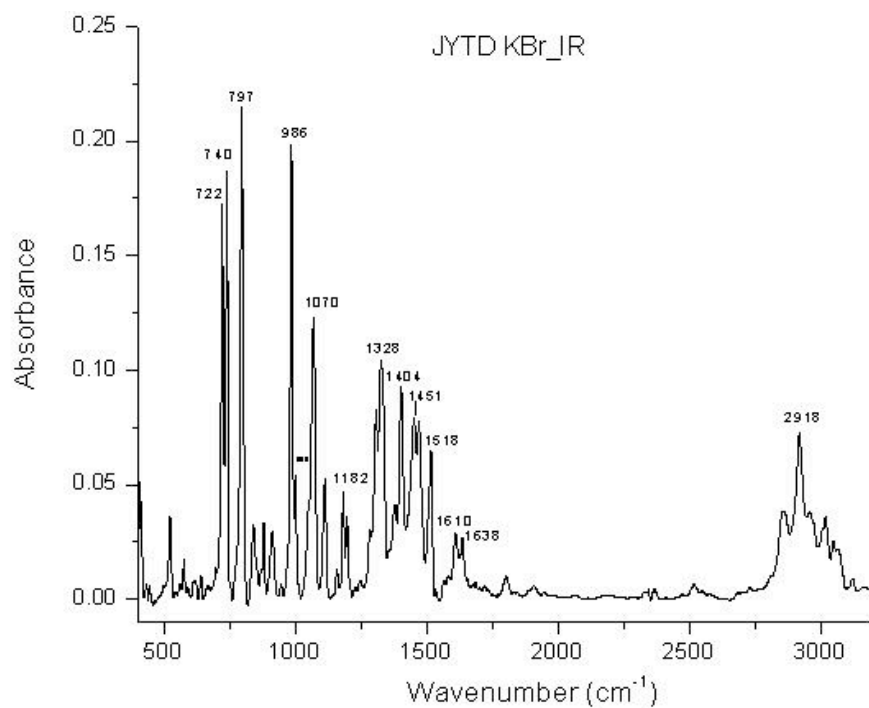


Figure 5.8. IR spectra of compound **9** in KBr (upper) and in a monolayer (lower) (figure courtesy of Lingyun Wei).

The apparatus of the electrochemical experiment is shown in Figure 5.9. This is a two electrode setup wherein the reference electrode is used as the counter electrode. The two electrode setup is useful only for measurements that use very small current. The electrodes lead to a potentiostat device which is controlled by a computer.

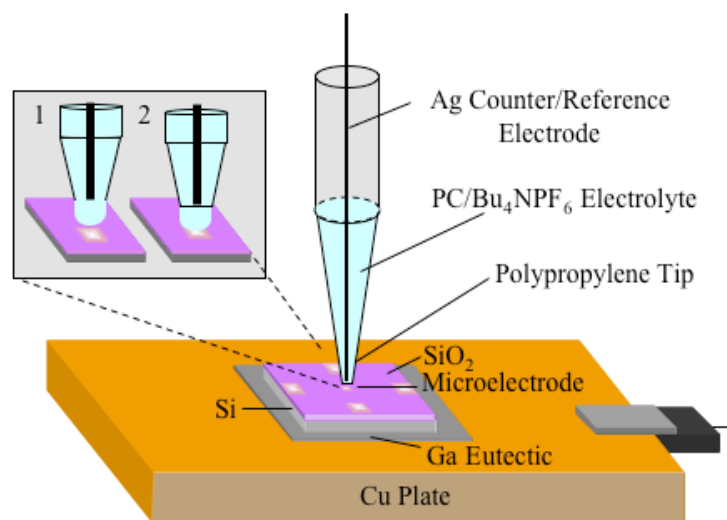


Figure 5.9. Apparatus used in electrochemical measurements of electrodes coated with **H<sub>2</sub>-7** or **9** (figure courtesy of Lingyun Wei).

A cyclic voltammogram of compound **9** is shown in Figure 5.10. Three oxidation states are observed in the range 0.0–0.9 V (vs. Ag/Ag<sup>+</sup>). The type-a triple decker is expected to have six distinct oxidation states. The electrochemical response for monolayers of **9** degraded rapidly when scanned at more positive voltage, so the full six oxidation states were not seen for this compound. The signal degradation is attributed to some decomposition or reorganization of the triple deckers in the monolayer. In Figure 5.10, the surface packing

density of  $1.5 \times 10^{-10}$  mol/cm<sup>2</sup> is an order of magnitude greater than the values for the previous triple deckers bearing tripodal linkers (vide infra). This density corresponds to a molecular footprint of  $\sim 110$  Å<sup>2</sup> (see Chapter 2 for equations relating to footprint calculations). The surface packing densities of the prepared electrodes varied in the range of  $\sim 1 \times 10^{-10}$  to  $1 \times 10^{-11}$  mol/cm<sup>-1</sup>. This variability was dependent on the quantity of compound **9** used in the coating (concentration of **9** in THF) and the temperature of the coating. The best values were obtained at a coating temperature of 450 °C. The concentration of the coating solution was not rigorously controlled, so exact quantities of **9** used in the coating are unknown. The quantity of **9** needed to prepare a solution for coating several electrodes is too small (micrograms) to weigh on a standard analytical balance.

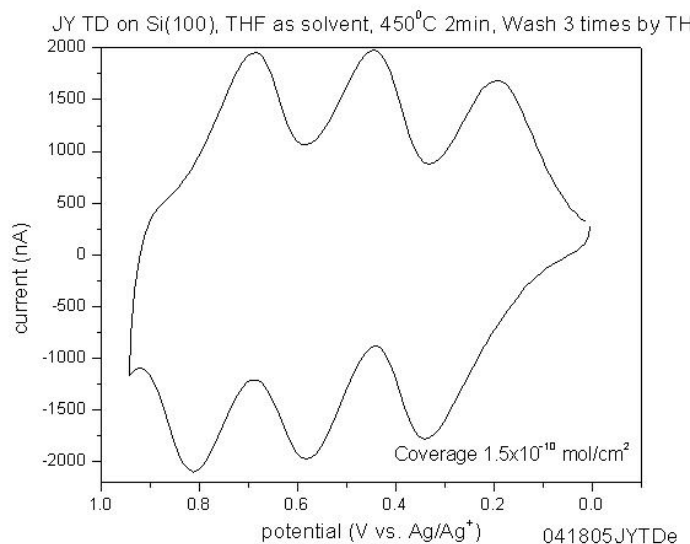


Figure 5.10. Cyclic voltammogram of compound **9** (figure courtesy of Lingyun Wei)

The instability of compound **9** can be seen in the repetition of the cyclic voltammogram experiment over thousands of cycles (Figure 5.11). Over the course of 5000

scans in the 0.0–0.9 V range, the oxidation peaks have flattened out. Similar studies on other electroactive species, such as ferrocene or porphyrins, have shown stable cycling over many more scans (>100,000). The relative instability of compound **9** limits its usefulness as a molecular information storage device. If atmospheric oxygen and/or moisture are involved in the degradation phenomena, then it is possible that experiments conducted in an inert atmosphere might provide different results.

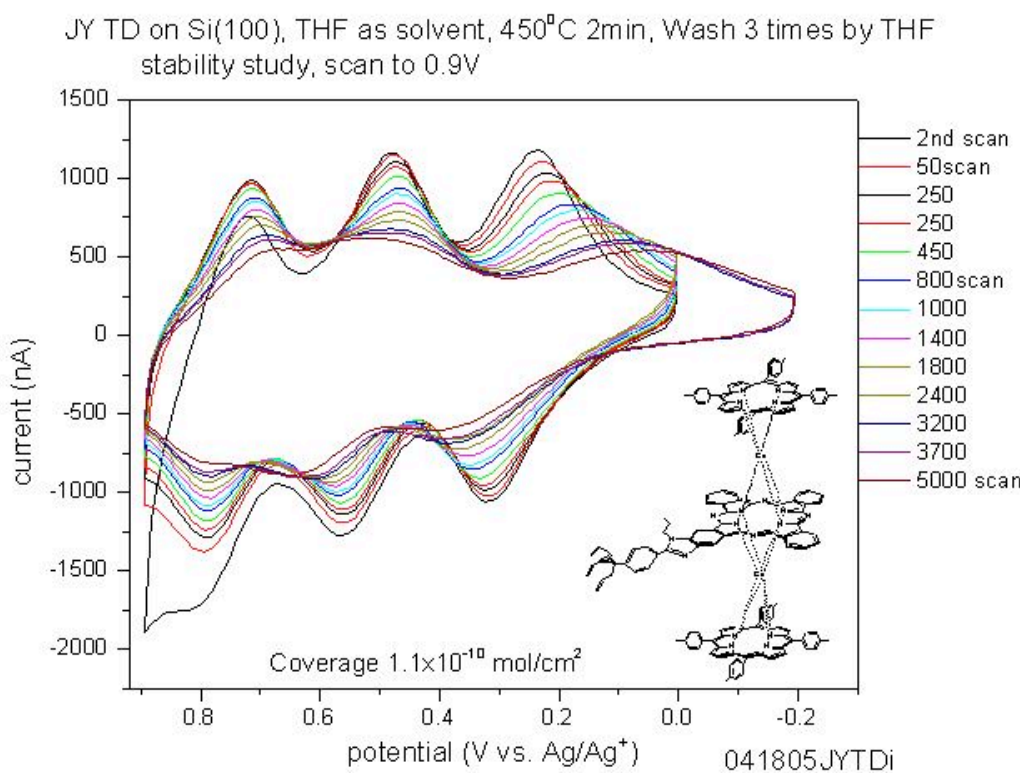


Figure 5.11. A longevity study of compound **9** composed of many voltage cycles (figure courtesy of Lingyun Wei).

Electrochemical studies of **H<sub>2</sub>-7** gave no response from the compound. Cyclic voltammetry of electrodes treated with **H<sub>2</sub>-7** was attempted, as well as square wave voltammetry of a solution of **H<sub>2</sub>-7** in CH<sub>2</sub>Cl<sub>2</sub>, without result in either experiment. Aggregation of the compound may have prevented its measurement in solution, or the oxidation potentials of the free base phthalocyanine may be beyond the window of measurement (>1.3 V vs. Ag/Ag<sup>+</sup>).

#### D. Outlook.

The architecture of the axially substituted phthalocyanine is shown in Figure 5.12. Attachment of the tether to the central ligand of the triple deckers, using the new phthalocyanine substitution pattern, affords an axially symmetric triple decker. The resulting triple decker no longer has a camshaft rotation and gave a small molecular footprint and, thus, a higher charge density upon attachment to an electroactive surface. A similar architecture would be available in a type-b triple decker via attachment to the central porphyrin, but rational methods for synthesis of type-b triple deckers are not yet available. The present strategy provides the first route wherein a triple decker is centrally disposed with respect to a linking substituent, which in this case is the all-carbon tripod for surface attachment. Although, this strategy has been shown to be successful in decreasing the footprint of the triple decker, the compound appears to be unstable to the electrochemical experiment. The cause of the instability of the compound is not currently known.

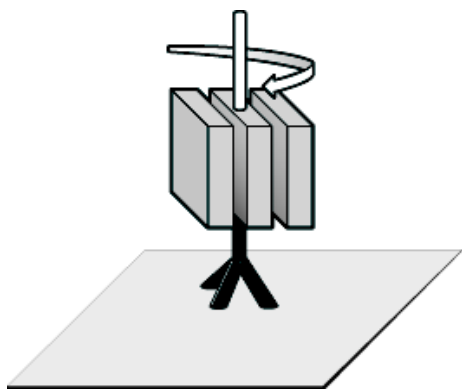


Figure 5.12. Representation of the type-a triple decker bearing the compact all-carbon tether. The tripod is attached to the (central) phthalocyanine ligand and aligned along one of the N-N axes of the phthalocyanine.

## E. Experimental Section.

**General.**  $^1\text{H}$  (400 MHz) and  $^{13}\text{C}$  (100 MHz) NMR spectra were obtained in  $\text{CDCl}_3$  unless noted otherwise. Silica gel (40  $\mu\text{m}$  average particle size) was used for column chromatography. Purified acetone was prepared from reagent grade acetone by distillation over potassium permanganate and the distillate was stored over anhydrous  $\text{K}_2\text{CO}_3$  prior to use. Other solvents used as received commercially include *N*-methyl pyrrolidinone (NMP = 1-methyl-2-pyrrolidinone, anhydrous), DMAE (redistilled grade), and MeOH (anhydrous). NaOMe was employed as a 25 wt% solution in MeOH. All other chemicals were reagent grade and were used as received. Absorption and emission data were measured in THF. The fluorescence quantum yield of **H<sub>2</sub>-7** was measured by comparison to tetra-*tert*-butylphthalocyanine, which was itself measured in both THF and  $\text{CHCl}_3$  set at  $\Phi_f = 0.70$  in THF (by comparison to the reported  $\Phi_f$  of 0.77 for tetra-*tert*-butylphthalocyanine in  $\text{CHCl}_3$  with correction for the indices of refraction of the different samples).<sup>25</sup>

**Electrode preparation:** Electrode wafers were coated with monolayers of compounds **H<sub>2</sub>-7** and **9** by heating a solution of THF containing a given compound at 400 or 450 °C under an argon atmosphere. Each cleaned wafer was kept in a septum-capped vial that had been purged with argon. A sample (2  $\mu\text{L}$  of a THF solution) of **H<sub>2</sub>-7** or **9** was introduced with a microliter syringe and placed as a drop onto the wafer. The vial was then placed on a hot plate set to the desired temperature, and allowed to heat for 2 minutes. The wafer was then cleaned with fresh THF (three times), dried under a stream of argon, and removed from the vial for electrochemical studies.

**Noncommercial Compounds:** Compounds **1**,<sup>12</sup> **2**,<sup>13</sup> **6**,<sup>22</sup> and **8**<sup>24</sup> were prepared according to the literature.

**2-(4-(4-Allylhepta-1,6-dien-4-yl)phenyl)-5,6-dicyanobenzimidazole (3).** Following a reported procedure,<sup>12</sup> a solution of **1** (198 mg, 1.25 mmol) in NMP (2.5 mL) and a solution of **2** (300 mg, 1.25 mmol) in NMP (3.5 mL) were combined in a flask fitted with a Hickman still. The mixture was heated at 120 °C and stirred for 2 h. Then FeCl<sub>3</sub>·6H<sub>2</sub>O (17 mg, 63 µmol) was added and oxygen was bubbled through the mixture with continued heating and stirring for 20 h. The cooled reaction mixture was diluted with ethyl acetate. The organic solution was washed with water and brine. The organic layer was dried (Na<sub>2</sub>SO<sub>4</sub>), filtered, concentrated, and chromatographed (silica, CH<sub>2</sub>Cl<sub>2</sub> w/ethyl acetate gradient of 0-5%). Fractions containing the desired compound were concentrated to give a reddish solid, which was chromatographed over a short plug of alumina (CH<sub>2</sub>Cl<sub>2</sub> w/ethyl acetate gradient of 10-100%) yielding a colorless solid (268 mg, 57%): mp 264–266 °C; <sup>1</sup>H NMR (d<sub>6</sub>-acetone) δ 2.57 (d, *J* = 7.2 Hz, 6H), 4.88–5.11 (m, 6H), 5.56–5.69 (m, 3H), 7.65 (d, *J* = 8.8 Hz, 2H), 8.26 (d, *J* = 8.8 Hz, 2H), 12.89 (brs, 1H); <sup>13</sup>C NMR (d<sub>6</sub>-acetone) δ 41.6, 44.0, 108.2, 116.9, 117.7, 126.4, 127.3, 128.0, 134.4, 150.2; FABMS obsd 379.1909, calcd 379.1923 (C<sub>25</sub>H<sub>22</sub>N<sub>4</sub>).

Note: Chromatography of the reaction mixture is aided by the strong blue fluorescence of the product that is visible when illuminating the column with a hand-held long wave UV lamp.

**2-(4-(4-Allylhepta-1,6-dien-4-yl)phenyl)-5,6-dicyano-1-propylbenzimidazole (4).** Following a reported procedure,<sup>12</sup> a sample of **3** (265 mg, 0.70 mmol) in NMP (2.5 mL) was heated to 120 °C and treated with DBU (105 µL, 0.70 mmol). After stirring for 2 min, iodopropane (105 µL, 0.70 mmol) was added and the mixture was stirred for 15 min. A second dose of DBU (68 µL, 0.70 mmol), followed by iodopropane (68 µL, 0.70 mmol), was

added, and 15 min later, a third identical round of DBU and iodopropane was again added. After the mixture was stirred for 15 min, the reaction mixture was allowed to cool and was diluted with ethyl acetate. The organic solution was washed with water and brine. The organic layer was dried ( $\text{Na}_2\text{SO}_4$ ), filtered, concentrated, and chromatographed (silica,  $\text{CH}_2\text{Cl}_2$  w/ethyl acetate gradient of 0-5%). Some starting material was recovered (83 mg, 31%), and fractions containing the product were concentrated to give a colorless solid (183 mg, 62%): mp 132–134 °C;  $^1\text{H}$  NMR  $\delta$  0.92 (t,  $J$  = 8.0 Hz, 3H), 1.82–1.93 (m, 2H), 2.52 (d,  $J$  = 8.8 Hz, 6H), 4.31 (t,  $J$  = 7.6 Hz, 2H), 4.98–5.09 (m, 6H), 5.50–5.63 (3H), 7.53 (d,  $J$  = 8.4 Hz, 2H), 7.70 (d,  $J$  = 8.4 Hz, 2H), 7.88 (s, 1H), 8.19 (s, 1H);  $^{13}\text{C}$  NMR  $\delta$  11.4, 23.5, 41.9, 44.1, 47.3, 108.5, 109.0, 116.7, 116.8, 118.5, 126.1, 126.4, 127.9, 129.2, 134.0, 137.9, 145.4, 149.9, 159.4; Anal. Calcd for  $\text{C}_{28}\text{H}_{28}\text{N}_4$ : C, 79.97; H, 6.71; N, 13.32; Found: C, 79.93; H, 6.73; N, 13.35.

**2-(4-(4-Allylhepta-1,6-dien-4-yl)phenyl)-1-propylimidazo[4,5-*f*]isoindole-5,7(1*H,6H*)-diimine (5).** Following a reported procedure,<sup>21</sup> a sample of **4** (105 mg, 0.25 mmol) in anhydrous MeOH (4 mL) under an argon atmosphere was heated at 70 °C. When the mixture became homogeneous, NaOMe (6  $\mu\text{L}$  of a 25 wt% solution in MeOH, 25  $\mu\text{mol}$ ) was added, the argon line was removed from the apparatus, and ammonia gas was bubbled through the mixture while the mixture refluxed for 3.5 h. During this time, additional MeOH (0.5 mL) was added at each half hour interval to prevent the reaction mixture from evaporating to dryness. The reaction flask was allowed to cool to room temperature under an atmosphere of ammonia, and then ammonia flow was stopped. The mixture was allowed to stand overnight under a slowly flowing stream of argon, whereupon most of the solvent evaporated and a white powder formed in the vessel. The mixture was taken up by pipette

and filtered. The filtered material was washed with anhydrous MeOH and dried in vacuo (53 mg, 48%): mp 230–232 °C (upon which the sample melted and turned deep green). Due to the presence of tautomeric forms of the product, the NH signals do not all integrate to integers:  $^1\text{H}$  NMR ( $\text{d}_8$ -THF)  $\delta$  0.88 (t,  $J$  = 7.2 Hz, 3H), 1.82–1.96 (m, 2H), 2.56 (d,  $J$  = 7.2 Hz, 6H), 4.38 (t,  $J$  = 7.6 Hz, 2H), 4.97–5.10 (m, 6H), 5.57–5.70 (m, 3), 7.57 (d,  $J$  = 8.0 Hz, 2H), 7.80 (d,  $J$  = 8.0 Hz, 2H), 7.84–8.40 (m, 4H);  $^{13}\text{C}$  NMR ( $\text{d}_8$ -THF)  $\delta$  10.6, 23.2, 41.8, 43.7, 46.4, 117.3, 127.2, 129.1, 134.5, 147.8; IR (film): 3397, 3276, 3200, 2958, 2927, 1536, 1432, 1149, 1121, 1077, 915.2; Anal. Calcd for  $\text{C}_{28}\text{H}_{31}\text{N}_5$ : C, 76.85; H, 7.14; N, 16.00; Found: C, 76.63; H, 7.21; N, 16.09.

Note: The title compound does not entirely precipitate from the cooled reaction mixture. The recovery is aided by gently concentrating the mixture under a stream of argon until only a small quantity of liquid remains. Once precipitated, **5** does not readily redissolve in dry methanol, but a more soluble yellow byproduct is observed that redissolved even in preparations wherein the reaction mixture had been evaporated fully to dryness. Analysis of this byproduct (obtained from the methanolic filtrate after separating the product) by  $^1\text{H}$  NMR spectroscopy confirmed that it was not **5**, but its identity was not determined.

**Tribenzo[*g,l,q*]-(*2*-{4-(4-Allylhepta-1,6-dien-4-yl)phenyl}-1-propylbenzimidazo[5,6-*b*])porphyrazine (H<sub>2</sub>-7).** A 20 mL reaction vial was charged with **5** (43 mg, 98  $\mu\text{mol}$ ), **6** (169 mg, 392  $\mu\text{mol}$ , 4 equiv), DMAE (5 mL), and a magnetic stirring bar. The vial was capped and heated in an oil bath maintained at 100 °C. Periodically, a few microliters of the reaction mixture were removed, diluted into THF, and analyzed by UV-Vis spectroscopy. After 8 h, **5** was not observed in the UV-Vis spectrum. The reaction was then cooled to room temperature and diluted with MeOH (15 mL) and allowed to stand overnight.

The mixture was centrifuged and the supernatant was removed. MeOH (20 mL) was added to the pellet and the mixture was sonicated and centrifuged again. After a third MeOH treatment and centrifugation, the pellet was dried in vacuo. The solid residue was suspended in THF (250 mL), sonicated, and filtered through celite. The filtrate was set aside. The celite was then added to a Soxhlet thimble and extracted with CH<sub>2</sub>Cl<sub>2</sub> overnight. The CH<sub>2</sub>Cl<sub>2</sub> and THF filtrates were combined and concentrated to dryness. The solid residue was redissolved in a minimum of THF and chromatographed over a column of Bio-Beads SX-3 in THF. The desired compound was recovered from the column as a dark blue-green band that was closely followed by a blue band (unsubstituted phthalocyanine) and a faint pink band (remaining **6**). The fractions containing the desired compound were concentrated and rechromatographed over Bio-Beads SX-3 in THF a second time to remove all pigment impurities. The sample was then chromatographed (silica, CH<sub>2</sub>Cl<sub>2</sub>, 1% isopropanol, 5% THF, 5% ethyl acetate). Fractions containing the desired compound were concentrated to give a blue solid (25 mg, 32%): IR (KBr pellet): 2918, 1638, 1610, 1518, 1426, 1330, 1115, 1001, 912, 740; <sup>1</sup>H NMR (d<sub>8</sub>-THF) δ -3.56 (brs, 2H), 1.16 (t, *J* = 8.0 Hz, 3H), 2.12–2.24 (m, 2H), 2.75 (d, *J* = Hz, 6H), 4.53 (t, *J* = 8.0 Hz, 2H), 5.15–5.28 (m, 6H), 5.78–5.91 (m, 3H), 7.61 (t, *J* = 7.2 Hz, 1H), 7.71 (t, *J* = Hz, 1H), 7.76–7.89 (m, 4H), 7.80 (d, *J* = 8.4 Hz, 2H), 8.09 (s, 1H), 8.13 (d, *J* = 8.4 Hz, 2H), 8.20 (d, *J* = 6.8 Hz, 1H), 8.47–9.53 (m, 2H), 8.57 (s, 1H), 8.63–8.72 (m, 3H); LD-MS obsd, 807.0; FABMS obsd 807.3717, calcd 807.3672 [(M+H)<sup>+</sup>; M = C<sub>52</sub>H<sub>42</sub>N<sub>10</sub>]; λ<sub>abs</sub> (nm) 336, 651, 669, 695; λ<sub>em</sub> (nm) 700, 714; Φ<sub>f</sub> = 0.56.

**(Li<sub>2</sub>-7).** A sample of Li ribbon (19 mg, 2.9 mmol) was added to pentanol (14.5 mL) and the mixture was refluxed until the Li was fully consumed (overnight). The mixture was cooled to room temperature and filtered through a pipette that was plugged with glass fiber

filter paper. The filtrate was not titrated but was assumed to be ~0.2 M. Next a sample of **H<sub>2</sub>-7** (25 mg, 31 μmol) was added to pentanol (9.0 mL) and briefly refluxed to dissolve all solid. Then the sample was cooled to room temperature and the lithium pentoxide solution (1.0 mL) was added. The vessel was capped with a septum and placed in an oil bath at 140 °C. As the mixture was refluxed, samples (~2 μL) were taken periodically, diluted into freshly dried THF (3 mL) and analyzed by UV-Vis spectroscopy to monitor the progress of the reaction. After 15 min from the start of refluxing, the UV-Vis spectrum of the removed sample had altered from the spectrum of the starting pigment (*vide supra*) to a new species having a more narrow Q band. The mixture was kept refluxing for a total of 90 min, although no further change was observed in the UV-Vis absorbance of the removed samples. The reaction mixture was cooled to room temperature and concentrated to dryness on a high-vacuum rotary evaporator. The residue was taken up in dry acetone and added to a thimble in a Soxhlet apparatus. The residue was extracted with dry acetone until no further color appeared from the thimble. The filtrate from the extraction was concentrated to dryness. The residue was dissolved in a minimum of dry acetone and decanted to a vial, taking care not to transfer any insoluble **H<sub>2</sub>-7** that may have formed during the extraction. The dark blue solution was then concentrated to dryness to give the product **Li<sub>2</sub>-7** as a blue solid (10 mg, 39%). Due to the sensitivity of the product to moisture, **Li<sub>2</sub>-7** was directly used in subsequent synthesis without characterization. The solids left behind in the evaporation flask and the Soxhlet thimble were combined to recover the starting material **H<sub>2</sub>-7** (15 mg, 60%):  $\lambda_{\text{abs}}$  602, 663, 671.

**(TTP)Ce(7)Ce(TTP) (9).** Following a reported procedure,<sup>15</sup> a 250 mL Schlenk flask was charged with a magnetic stirring bar and introduced into an argon glove box. Cerium

iodide (51 mg, 98  $\mu$ mol) was added and the flask was sealed with a septum and removed from the glove box. The flask was connected to an argon source, and the septum was vented with a needle to allow the outflow of argon gas. The flask was then placed in an ice bath and bis(2-methoxyethyl) ether (3.0 mL, freshly sparged with argon) was added. Then LiN(SiMe<sub>3</sub>)<sub>2</sub> (312  $\mu$ L of a 0.608 M solution freshly prepared in dry THF and sparged with argon) was added, and the mixture was stirred for 20 min, after which the flask was removed from the ice bath and stirring was continued while the mixture warmed to room temperature over 40 min. The mixture was then refluxed for 1 h by placing the flask in an oil bath at 170 °C. The flask was then removed from the oil bath long enough for refluxing to subside, briefly opened to allow the addition of **8 (H<sub>2</sub>TTP)** (16 mg, 24  $\mu$ mol), and closed again and returned to the bath to reflux for 3 h. Then the vessel was again allowed to cool and opened to remove a small sample for UV-Vis analysis. The sample was confirmed as the cerium-porphyrin half-sandwich, so **Li<sub>2</sub>-7** (10 mg, 12  $\mu$ mol) was added as a slurry in bis(2-methoxyethyl) ether (1.0 mL) and the resulting mixture was refluxed for 10 h under argon. Then the mixture was allowed to cool to room temperature and concentrated on a high vacuum rotary evaporator. The residue was triturated with MeOH, centrifuged, and the supernatant was discarded. The residue was chromatographed (silica, neat CH<sub>2</sub>Cl<sub>2</sub>, then CH<sub>2</sub>Cl<sub>2</sub> w/ 1% iPrOH, 5% THF, 5% ethyl acetate). The first band was collected and rechromatographed [silica, hexanes/CH<sub>2</sub>Cl<sub>2</sub>, (1:2)], and fractions containing the product were concentrated to give a green-black solid (9.0 mg, 30%): IR (KBr pellet): 2918, 1638, 1610, 1518, 1451, 1404, 1328, 1182, 1070, 986, 797, 740, 722; <sup>1</sup>H NMR  $\delta$  (-2.45)–(-1.30) (m, 20H), 0.75–0.85 (m, 3H), 1.13 (s, 24H), 1.73 (d, *J* = 7.2 Hz, 6H), 1.90–2.20 (m, 6H), 2.80–3.60 (m, 20H), 2.75 (d, *J* = Hz, 6H), 4.35–4.42 (m, 6H), 4.68–4.82 (m, 3H), 5.45–5.62

(m, 2H), 6.20–6.35 (m, 2H), 7.09 (s, 8H), 10.34 (s, 8H); LD-MS obsd, 2419.3; calcd 2420.74  
(C<sub>148</sub>H<sub>112</sub>Ce<sub>2</sub>N<sub>18</sub>); λ<sub>abs</sub> (nm) 359, 419, 493, 549, 608.

## F. References:

- (1) Buchler, J. W.; Ng, D. K. P. In *The Porphyrin Handbook*; Kadish, K. M., Smith, K. M., Guilard, R., Eds.; Academic Press: San Diego, CA, 2000; Vol. 3, pp 245–294.
- (2) Weiss, R.; Fischer, J. In *The Porphyrin Handbook*; Kadish, K. M., Smith, K. M., Guilard, R., Eds.; Academic Press: San Diego, CA, 2003; Vol. 16, pp 171–246.
- (3) Ng, D. K. P.; Jiang, J. *Chem. Soc. Rev.* **1997**, *26*, 433–442.
- (4) Chabach, D.; De Cian, A.; Fischer, J.; Weiss, R.; El Malouli Bibout, M. *Angew. Chem. Int. Ed. Engl.* **1996**, *35*, 898–899.
- (5) Li, J.; Gryko, D.; Dabke, R. B.; Diers, J. R.; Bocian, D. F.; Kuhr, W. G.; Lindsey, J. S. *J. Org. Chem.* **2000**, *65*, 7379–7390.
- (6) Lindsey, J. S. In *The Porphyrin Handbook*; Kadish, K. M., Smith, K. M., Guilard, R., Eds.; Academic Press: San Diego, CA, 2000; Vol. 1, pp 45–118
- (7) Gryko, D.; Li, J.; Diers, J. R.; Roth, K. M.; Bocian, D. F.; Kuhr, W. G.; Lindsey, J. S. *J. Mater. Chem.* **2001**, *11*, 1162–1180.
- (8) Schweikart, K.-H.; Malinovskii, V. L.; Diers, J. R.; Yasseri, A. A.; Bocian, D. F.; Kuhr, W. G.; Lindsey, J. S. *J. Mater. Chem.* **2002**, *12*, 808–828.
- (9) Schweikart, K.-H.; Malinovskii, V. L.; Yasseri, A. A.; Li, J.; Lysenko, A. B.; Bocian, D. F.; Lindsey, J. S. *Inorg. Chem.* **2003**, *42*, 7431–7446.
- (10) Balakumar, A.; Lysenko, A. B.; Carcel, C.; Malinovskii, V. L.; Gryko, D. T.; Schweikart, K.-H.; Loewe, R. S.; Yasseri, A. A.; Liu, Z.; Bocian, D. F.; Lindsey, J. S. *J. Org. Chem.* **2004**, *69*, 1435–1443.
- (11) Wei, L.; Padmaja, K.; Youngblood, W. J.; Lysenko, A. B.; Lindsey, J. S.; Bocian, D. F. *J. Org. Chem.* **2004**, *69*, 1461–1469.

- (12) Youngblood, W. J., This Ph.D. dissertation.
- (13) Padmaja, K.; Wei, L.; Lindsey, J. S.; Bocian, D. F. *J. Org. Chem.* **2005**, *70*, submitted.
- (14) Duchowski, J. K.; Bocian, D. F. *J. Am. Chem. Soc.* **1990**, *112*, 8807–8811.
- (15) Gross, T.; Chevalier, F.; Lindsey, J. S. *Inorg. Chem.* **2001**, *40*, 4762–4774.
- (16) Kobayashi, N.; Kondo, R.; Nakajima, S.; Osa, T. *J. Am. Chem. Soc.* **1990**, *112*, 9640–9641.
- (17) Musluoglu, E.; Gürek, A.; Ahsen, V.; Bekaroglu, Ö. *Chem. Ber.* **1992**, *125*, 2337–2339.
- (18) Sastre, A.; Torres, T.; Hanack, M. *Tetrahedron Lett.* **1995**, *36*, 8501–8504.
- (19) Weitemeyer, A.; Kliesch, H.; Wörhrle, D. *J. Org. Chem.* **1995**, *60*, 4900–4904.
- (20) Kudrevich, S. V.; Gilbert, S.; van Lier, J. E. *J. Org. Chem.* **1996**, *61*, 5706–5707.
- (21) Brach, P. J.; Grammatica, S. J.; Ossanna, O. A.; Weinberger, L. *J. Heterocyclic Chem.* **1970**, *7*, 1403–1405.
- (22) Claessens, C. G.; Gonzalez-Rodriguez, D.; del Rey, B.; Torres, T.; Mark, G.; Schuchmann, H. P.; von Sonntag, C.; MacDonald, J. G.; Nohr, R. S. *Eur. J. Org. Chem.* **2003**, *14*, 2547–2551.
- (23) Barrett, P. A.; Frye, D. A.; Linstead, R. P. *J. Chem. Soc.* **1938**, 1157–1163.
- (24) Adler, A. D.; Longo, F. R.; Finarelli, J. D.; Goldmacher, J.; Assour, J.; Korsakoff, L. *J. Org. Chem.* **1967**, *32*, 476.
- (25) Teuchner, K.; Pfarrherr, A.; Stiel, H.; Freyer, W.; Leupold, D. *Photochem. Photobiol.* **1993**, *57*, 465–471.